NUREG/CR--5402

TI89 013222

Crushed Salt Consolidation

Manuscript Completed: May 1989
Date Published: July 1989

Prepared by
S. Ouyang, J. J. K. Daemen

Department of Mining and Geological Engineering
University of Arizona
Tucson, AZ 85721

Prepared for
Division of Engineering
Office of Nuclear Regulatory Research
U.S. Nuclear Regulatory Commission
Washington, D.C. 20555
NRC FIN D1192
Under Contract No. NRC-04-86-113

ABSTRACT

The objective of this study is to investigate the time-dependent consolidation of confined crushed salt under axial loading. The crushed salt is geometrically characterized in terms of its grain size distribution and by means of particle shape determinations. Crushed salt of a selected grain size distribution is emplaced in a steel cylinder, and an axial load is applied to the salt. The deformation is monitored. The axial load is increased in steps. Results are presented as void ratio vs. time curves, for the various applied stresses. Air dried samples have a brine content of 0.2%; moistened samples have a brine content ranging from 1.75 to 8.8%. The general consolidation trend can be represented as a linear function of the logarithm of time, but with noticeable temporary accelerations. Consolidation time calculations, predicted from the results of fitted curve parameters, admittedly extrapolated far beyond the measurement range, indicate that reconsolidation of the materials as emplaced and tested here would require many centuries. It deserves emphasis that these experiments were initiated on an extremely loose crushed salt fill. Consolidation rate increases with brine content. The dependency upon applied stress remains ambiguous. The obtained void reduction rates are significantly lower than published results determined from isostatic consolidation. Given the small number of tests completed, all results and conclusions must be considered preliminary. Tests in configurations that may be more representative for expected in-situ consolidation conditions are recommended.

TABLE OF CONTENTS

TABLE OF CONTENTS--Continued

LIST OF FIGURES

LIST OF FIGURES--Continued

LIST OF FIGURES--Continued

LIST OF TABLES

PREFACE

This technical report presents experimental investigations on possible seal materials for a HLW repository in salt. The investigations were initiated prior to the adoption of the NWPAA (Nuclear Waste Policy Amendments Act). This amendments act identified the Yucca Mountain site as the first candidate for a HLW repository site. A repository at this site would be located in welded tuff. The NWPAA required that investigations on other media be terminated. As a result, the salt sealing studies reported on here were terminated before they could be completed. All results and analyses presented here were previously reported in unpublished quarterly progress reports prepared for the U.S Nuclear Regulatory Commission. The present report provides a means for putting the work permanently on record.

ACKNOWLEDGMENTS

The research reported on has been performed by the University of Arizona, Department of Mining and Geological Engineering, for the U.S. Nuclear Regulatory Commission (NRC). Project monitor for the NRC is Mr. Jacob Philip. The project is under Mr. M. Silberberg, Chief, Waste Management Branch, Division of Engineering, Office of Nuclear Regulatory Research.

Dr. Jaak J.K. Daemen, Associate Professor, Department of Mining and Geological Engineering, University of Arizona, is the Principal Investigator. Dr. James G. McCray, Acting Director, Nuclear Fuel Cycle Research Program, Department of Nuclear and Energy Engineering, University of Arizona, has provided project management assistance and nuclear waste technical assistance. Shoung Ouyang has performed the experimental work and the analysis of the results as part of his Ph.D. requirements. Dr. Kittitep Fuenkajorn reviewed parts of the report and contributed valuable improvements and suggestions, particularly with respect to research needs (Chapter 5). Experimental assistance has been provided by Teresa Lyons and Sandy Strauss. Mike Porter has typed, assembled, and produced the report.

We gratefully acknowledge Mr. Jack Hunt, Mr. Morris Worley, and Mr. Don Galbraith of Western Ag-Mineral Company for providing salt samples for testing purposes.

EXECUTIVE SUMMARY

The time-dependent consolidation of crushed salt has been investigated by means of uniaxial strain tests (confined consolidation of crushed salt emplaced in steel pipes and loaded axially). Prior to consolidation testing, the crushed salt is characterized geometrically by means of particle shape measurements and, primarily, by means of grain size distribution curves. The grain size distributions for the samples tested correspond moderately well to grain size distribution curves for salt that has been mined by machine and from which the larger grain sizes have been removed. Particle shape is a codeterminant of initial pore space and of contacts between particles, and therefore is likely to be a factor in the time-dependent deformation of crushed salt. Particle shape determinations reveal a distinct shift in dominant shape for different size ranges. Particle shape probably depends on particle preparation method, in this study on crusher, and on crushing and sieving procedure.

For consolidation testing, crushed salt of a selected grain size distribution is emplaced in a steel cylinder, an axial load is applied to the salt, and is increased stepwise in various sequences, while the axial salt deformation is monitored. Results are plotted as void ratio vs. time curves. The general trend of the consolidation curves gives a liner function of the logarithm of time. Frequent but brief accelerations of crushed salt deformation are characteristic of initial consolidation. Such accelerations decrease in frequency and amplitude with continuing consolidation.

Air-dried and moist crushed salt has been tested. Air-dried samples have a brine content of 0.2%, moistened samples have a brine content ranging from 1.75 to 8.8%. The observed consolidation rates increase with brine content. The dependency of consolidation upon applied stress remains ambiguous, probably due in part to problems associated with the experimental procedure and to inadequate or inappropriate data analysis procedures.

The void reduction rates obtained here are significantly lower than results that have been published for isostatic consolidation. This is almost certainly due to the difference in test configuration. In the test configuration reported on here, the sample is subjected to an active driving force in one direction only. During in-situ consolidation, i.e. after emplacement in a converging room, one would expect a biaxial driving displacement. In addition, during consolidation in a pipe, shear stresses develop along the salt-pipe interface, and reduce the axial load transmitted to the salt. This nonuniform load may be responsible for the nonuniform consolidation of the salt clearly observed in many of the samples.

Given the small number of tests completed, all results and conclusions must be considered preliminary. Chapter 5 of this report presents an extensive discussion of desirable follow-up work. Future research

should be aimed in particular either at obtaining a reliable mechanistic model or reliable empirical bounding estimates in order to allow making extrapolations far beyond the durations for which measurements are possible. A number of tests are proposed aimed at pursuing one or both of these approaches.

CHAPTER ONE

INTRODUCTION

Crushed salt has been proposed as backfill or sealing material for nuclear waste repositories in salt (e.g. Meyer et al., 1980; Gureghian et al., 1983; Kelsall et al., 1983; Stormont, 1984). The emplacement of crushed salt within repository excavation has a number of attractive features. It provides a method for disposal of excavated salt. Backfill reduces the ultimate deformation of the rock mass into the openings, and hence reduces surface subsidence as well as deformation of aquitards. Backfill will be recompressed if the excavations close sufficiently. If the backfill is compressed sufficiently, it may form a seal. Such a seal would have the desirable aspect, in all probability, of being geochemically and mechanically compatible with the surrounding rock mass. This compatibility should greatly reduce concerns about durability or longevity of seals. Many of the reasons invoked to recommend backfilling of repository openings with crushed rock have long been recognized in mining, explaining the widespread practice of backfilling mines, for stabilization, disposal and sealing purposes (Rausch and Stitzer, 1973; Allen and Paone, 1982; Brezovec, 1983; Brezovec and Hedges, 1986). Backfill in particular has long been used in evaporite mining (e.g. Grim, 1968, p. 228), and has been investigated extensively in this context (Miller, 1983; Mraz Project Consultants, Ltd., 1987).

The levels of performance, and especially the reliability requirements of the sealing performance are likely to be more stringent for radioactive waste repositories than for conventional mining applications. This explains the extensive investigations on crushed salt that have been performed within the context of various nuclear waste disposal programs.

Crushed salt has been considered as backfill material in the design concepts for a nuclear waste repository in salt (Giuffre et al., 1979; Kelsall et al., 1982; Christensen et al., 1983; Kelsall et al., 1983). Kelsall et al. (1985a,b,c) propose crushed salt as a major backfill component in schematic designs for penetration seals for salt repositories. Creep closure of the storage rooms, tunnels, and shafts is likely to compress the crushed salt backfill and create an impermeable monolith to retard ground water flow and radionuclide migration (Kelsall et al., 1982). The understanding of the consolidation behavior of crushed salt is thus of primary concern to a long-term assessment of the sealing performance of crushed salt backfill. Because crushed salt consolidation depends on a time-dependent interaction between the gradually closing excavation and the progressively stiffening crushed salt inclusion, the predictability of excavation closure under the increasing internal reaction forces exerted by the consolidating crushed salt is equally important.

Hansen (1976), Shor et al. (1981), Baes et al. (1983), Ratigan and Wagner (1978), Stinebaugh (1979), Holcomb and Hannum (1982), Kappei and Gessler (1984), Liedtke and Bleich (1984), IT Corporation (1987), Pfeifle (1987a), Pfeifle et al. (1987), Holcomb and Shields (1987), and Holcomb and Zeuch (1988) have studied the consolidation of crushed or granular salt in uniaxial strain or under hydrostatic compression. IT Corporation (1984) summarizes work performed prior to 1983. This report identifies a significant discrepancy between results reported by Ratigan and Wagner (1978) and those reported by Holcomb and Hannum (1982). The former indicate a relatively fast consolidation rate, such that for most locations in a repository, effective consolidation of crushed salt to a porosity of 0.6% would occur within 100 to 700 years. The latter predict a much slower rate, as did Holcomb and Zeuch (1988), such that the effective consolidation would require more than several thousands of years (Kelsall et al., 1984). The former experiments were conducted on crushed Avery Island salt from New Iberia, Louisiana, the latter on crushed Mississippi Chemical Company and WIPP salt from southeastern New Mexico.

Shor et al. (1981) first suggested that the consolidation of granular salt may be greatly enhanced by the presence of brine. Investigations by Miller (1983), Liedtke and Bleich (1984), IT Corporation (1987), Pfeifle et al. (1987), and Holcomb and Shields (1987) confirmed the increased consolidation rate upon the addition of small amounts of water. Yost and Aronson (1987) provide a phenomenological explanation, supported by analysis of experimental results for accelerated consolidation in the presence of water. One particular test result of IT Corporation (1987; also Case et al., 1987) on crushed WIPP salt (maximum particle size of 20 mm, uniformity coefficient of 5.6, moisture content of 2.3 %, maximum hydrostatic pressure of 17.25 MPa, test duration of 32 days) shows that the initial porosity of 31% was reduced to 5% and the permeability was reduced to 10^{-2} microdarcy (10^{-16} cm^2). Holcomb and Shields (1987) conducted hydrostatic consolidation tests on crushed WIPP salt (maximum particle size of 10 mm, moisture content of 0.5 to 3%, hydrostatic pressure of 0.69 to 3.44 MPa, test duration of 19 to 52 days). They conclude that adding small amounts of water to the as-mined WIPP salt results in a consolidation rate such that times required for the crushed salt to form an effective barrier to fluid flow, assuming a fractional density of 0.95, are on the order of 1 year, at stresses in the 1 MPa range. A fractional density of 0.945 was obtained in a multistage hydrostatic consolidation test for approximately 102 days with maximum pressure of 6.9 MPa.

CHAPTER TWO

CRUSHED SALT CHARACTERIZATION

2.1 Introduction

Crushed salt consolidation, compaction, and hence permeability depend on the interaction between particles. Contact forces, resulting stresses within particles, and hence particle creep, particle fracturing or crushing, and reaction forces between particles, and eventually between crushed salt and converging excavation walls, depend on the initial arrangement of the particles, as well as on the changing interactions as particle and rock mass deformations take place. For these reasons, initial geometrical characterization of crushed salt is considered potentially useful. Geometrical characterization is performed in terms of grain size distribution and of particle shape determination.

2.2 Particle Size and Size Distribution of Crushed Salt

Quasi-static compaction and creep consolidation characteristics of crushed salt have been measured by Ratigan and Wagner (1978) and by Holcomb and Hannum (1982). According to IT Corporation (1984, p. 9), Ratigan and Wagner's tests were conducted on uniformly graded Avery Island salt with a maximum particle size of about 10 mm. Holcomb and Hannum's tests were conducted on salt from WIPP and from a potash mine in New Mexico. The as-excavated material collected by IT Corporation (1984, p. 5) from WIPP was well graded with a maximum particle size of 75 mm. Only particles smaller than or equal to 19 mm were used for testing. The creep strain rates obtained by Holcomb and Hannum decrease more rapidly with time than those obtained by Ratigan and Wagner. Although differences are obvious among test conditions (such as hydrostatic compression, test duration) and dimensions of samples tested (such as sample length to diameter (L/D) ratio), the deviation in the creep rate may be due, in part, to the variations in initial average particle size and size distribution. Stinebaugh (1979) tested samples with particle size ranges of 4.7 to 9.3 mm, 1.2 to 2.3 mm, and less than 0.04 mm, and concluded that particle size had no significant impact on ultimate compressibility, although it did influence the constitution of the compacted sample (Stinebaugh, 1979, p. 35). Miller (1983) tested two size ranges, -10 mm and -2 mm, and found the differences in volumetric closure at 180 kN to be insignificant. Shor et al. (1981), as summarized by IT Corporation (1984, p. 72), and by Holcomb and Zeuch (1988, p. 6), consolidated very small salt crystals (up to 0.42 mm), and found a strong size dependency of the consolidation rate. Kappei and Gessler (1984) observed significantly faster consolidation for smaller grain sizes, but attribute the difference largely to differences in initial bulk density. Pfeifle et al. (1987) tested uniformly distributed and well-graded distributions of equal mean grain size of 1 mm. They concluded that grain size distribution has a significant impact on the bulk density ratio during total

consolidation, as well as on the compressive strength of the consolidated salt.

A 6-inch diameter broken core drilled from a salt block obtained from Western-Ag Minerals Company, Carlsbad, New Mexico, was used for preparation of crushed salt for the tests reported on here. Salt crushing procedures are described in Appendix A. The crushed salt obtained in the laboratory was well graded, with a maximum particle size of about 12.7 mm. The maximum particle size was controlled by adjusting the opening of the roller crusher. The grain size distribution is shown in Figure 2.1. Also plotted on the same figure is a typical grain size distribution for crushed salt produced by a roadheader-type continuous mining machine at the WIPP site in southeastern New Mexico (from Kelsall et al., 1984). Pfeifle (1987b, p. 26), Kappei and Geissler (1984), and Liedtke and Bleich (1984) show grain size distribution curves that include significantly larger sizes for salt cut by roadheaders. Although the crushed salt produced in the laboratory appears to be more uniform, the similarity between the two distribution curves suggests that the laboratory-prepared crushed salt may be representative of crushed salt obtained in the field.

As the consolidation rate of crushed salt (and hence the rate of the reduction in permeability) depends on the initial average particle size, it seems appropriate to set an upper bound for the grain size to be tested. Instead of choosing one specific size, a ratio of chamber diameter to the maximum size of crushed salt to be installed is employed, and is initially assigned to be 10. A small deviation from the ratio is permitted to allow for sieve availability. It is also necessary to set a lower bound for the minimum grain size, since the consolidation or compaction of crushed salt may be hindered by the entrapped air in finely powdered crushed salt (Stinebaugh, 1979). A grain size of 0.074 mm (retained by sieve #200) is assigned as the minimum irrespective of the diameter of the test chamber. Sieve analysis of crushed salt aggregates follows ASTM C136-84a standard practice (Appendix B).

2.3 Particle Shape Analysis of Crushed Salt

Shor et al. (1981) have demonstrated that the consolidation and loss of permeability of salt crystal aggregates is a function of the initial void fraction, which depends, in turn, on the particle shape and the state of packing. Zeuch et al. (1985, p. 6) point out the strong correlation between initial and final density in the data obtained by Holcomb and Hannum (1982). Miller (1983) emphasizes the importance of initial density, to the point of considering precompaction of emplaced fill as one of the most productive methods for stiffening stowed crushed salt. IT Corporation (1987, p. 22; also, Case et al., 1987) shows a clear correlation between initial and final density. Kappei and Gessler (1984) consider the initial bulk density as decisive for the course of load consolidation, and conclude that emplacement method may well override all other parameters if it can assure dense in-situ compaction. Holcomb and Zeuch (1988) repeatedly point out the complexities introduced in the interpretation of consolidation tests as a result of differences in initial density between various tests. They

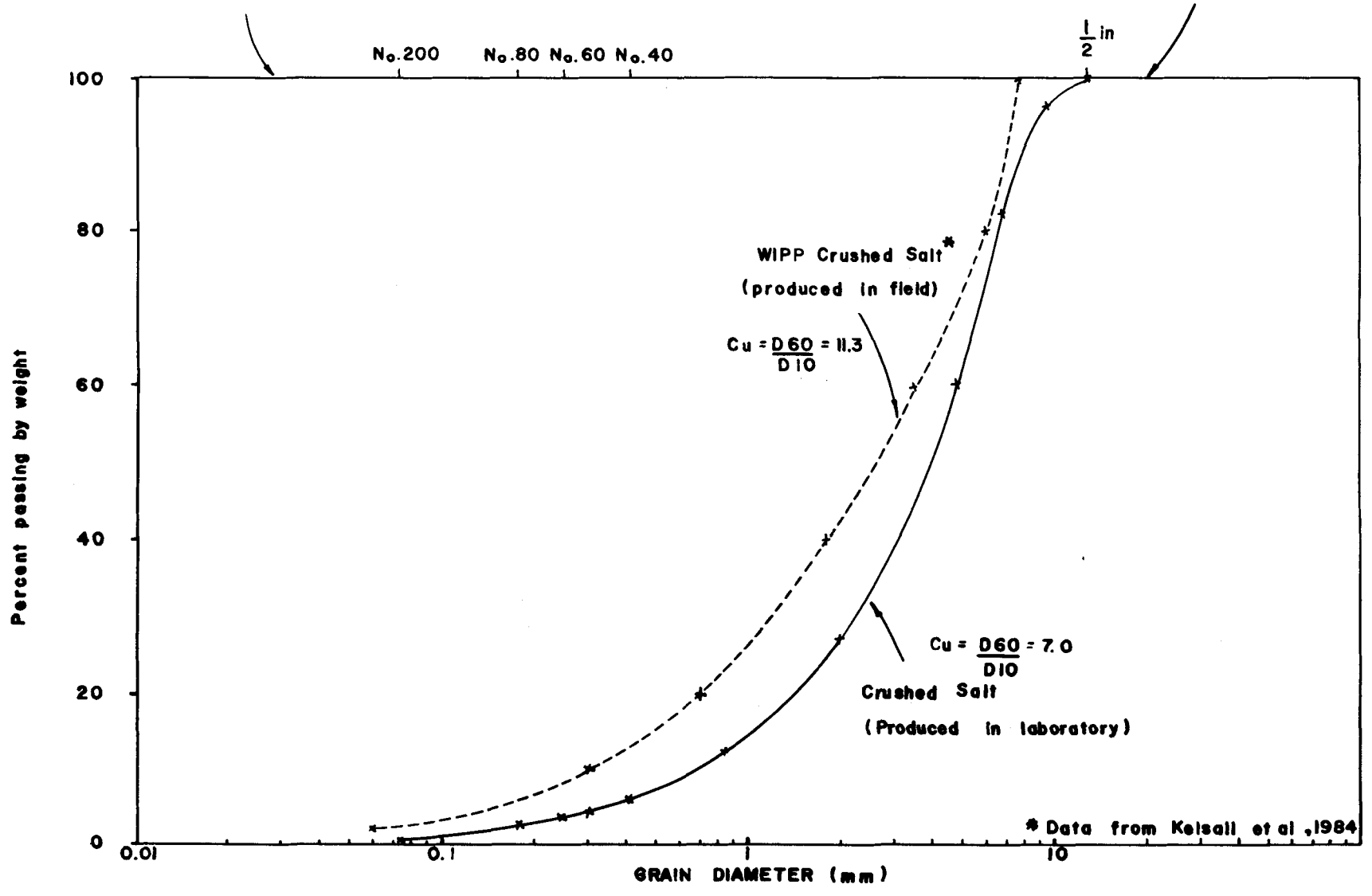

Figure 2.1 Grain size distribution of crushed salt.

show that scatter in results can be reduced greatly by a dimensionless formulation of a relative density as a preeminent independent variable.

Most workers in the field of the packing of granular materials acknowledge the importance of the shape of the particles in determining the packing state. However, very little work has been done in studying the relationship between particle shape and packing. Part of the problem in analyzing the effects lies in quantifying shape (Fowkes and Fritz, 1974). A qualitative shape determination, therefore, is usually made as part of the visual classification of granular materials. The salt particles obtained in the laboratory are angular to subangular in a range from 12.7 mm to 0.4 mm. Particles smaller than 0.4 mm appear more or less cubic in shape. The shape of crushed salt particles tends to change as the average grain size changes. A similar trend was observed by Williams and Daemen (1987) in a shape analysis of crushed basalt.

The particles used for the shape analysis were obtained from a crushed salt sample made for sieve analysis. The grain size distribution of the crushed salt sample can be seen in Figure 2.1. Five size fractions were selected for particle shape characterization: 12.70-9.42 mm (0.5-0.371 in), 9.42-6.68 mm (0.371-0.263 in), 6.68-4.75 mm (0.263-0.187 in), 4.75-1.98 mm (0.187-0.0781 in), and 1.98-0.84 mm (0.0781-0.331 in). Numbers of particles sampled from each fraction are 107, 50, 100, 150, and 99, respectively. All particles were measured individually to determine their three main dimensions, i.e. the lengths of the longest axis (a), the intermediate axis (b), and the shortest axis (c). Appendix C (Method B) describes the measurement procedures.

Ratios of b/a and c/b were calculated to provide a data base for Zingg's classification (Zingg, 1935; Winterkorn and Fang, 1975, p. 96; Williams and Daemen, 1987, Fig. 3.19). The results are shown in Figures 2.2 through 2.6. The crushed salt particles in the fraction of 12.70-9.42 mm (0.5-0.371 in) appear to be disk-shaped (Figure 2.2). As the fraction size decreases, the salt particle shape migrates and becomes more or less equiaxial (presumably cubic for crushed salt), as portrayed in Figures 2.3 through 2.5. For the size fraction of 1.98-0.84 mm (0.0781-0.0331 in), the particle shape diverges away from the cubic into disk-shaped, blade-shaped and roller-shaped (Figure 2.6).

Ratios of c/a and ac/b^2 were used by Malewski (1984) to study particle shape characteristics of crushed basalt and granite. They were employed to characterize the particle shape of crushed salt. In addition, the volume shape factor (α_v) and the surface shape factor (α_s) have been calculated (Herdan, 1960, p. 26, eqns. 3.1 and 3.2; Harr, 1977, p. 17, eqn. 1-14). The procedures for determining the volume and surface shape factors are given in Appendix C (Method C). Table 2.1 tabulates the averages and standard deviations for a, b, c, b/a, c/b, c/a, ac/b^2, α_v, and α_s. The results are plotted against the mean fraction size in Figures 2.7 through 2.10.

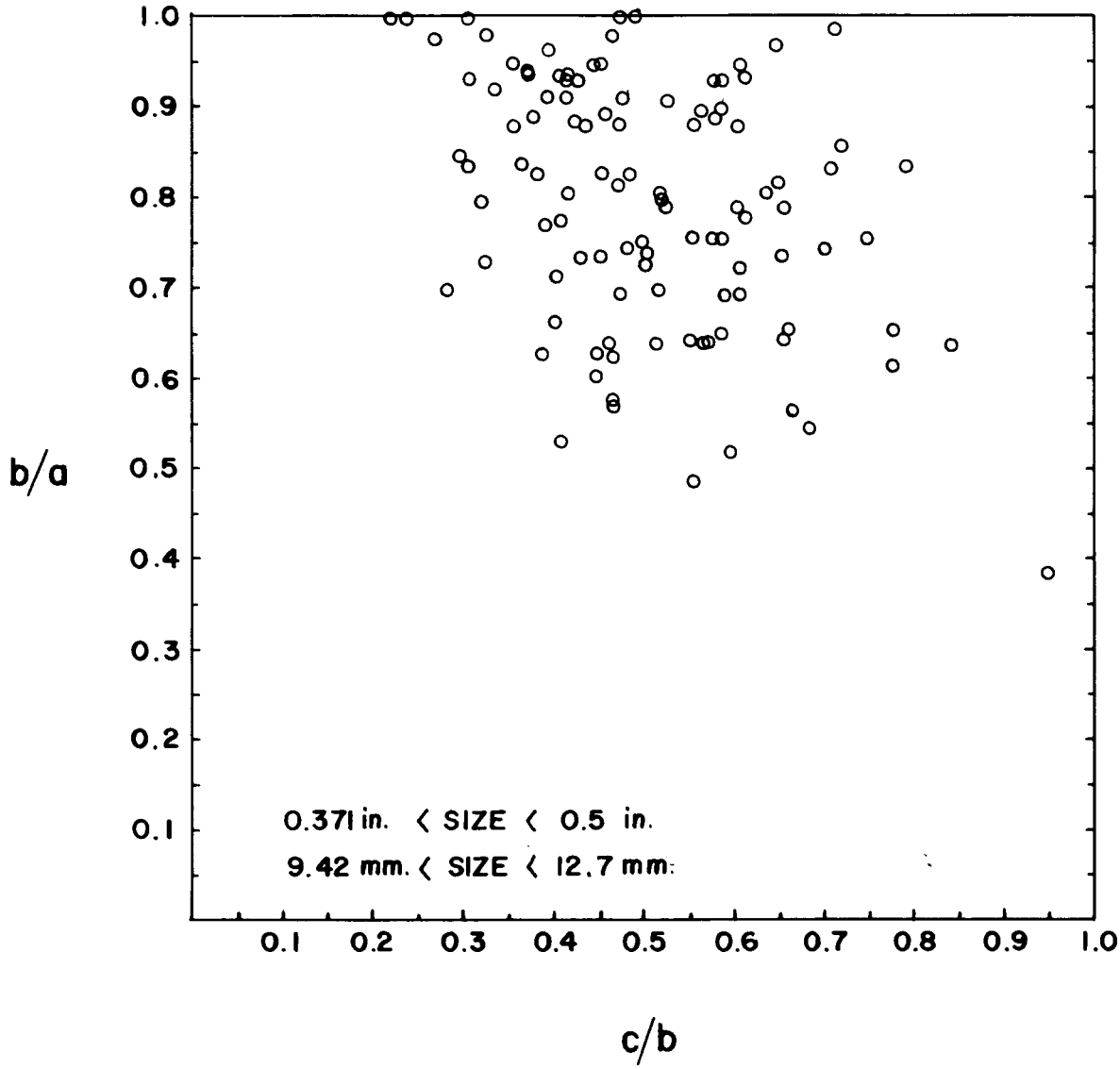

Figure 2.2 Zingg's classification for crushed salt particles in size fraction of 9.42-12.7 mm. Sample (S4-CS1-SN1).

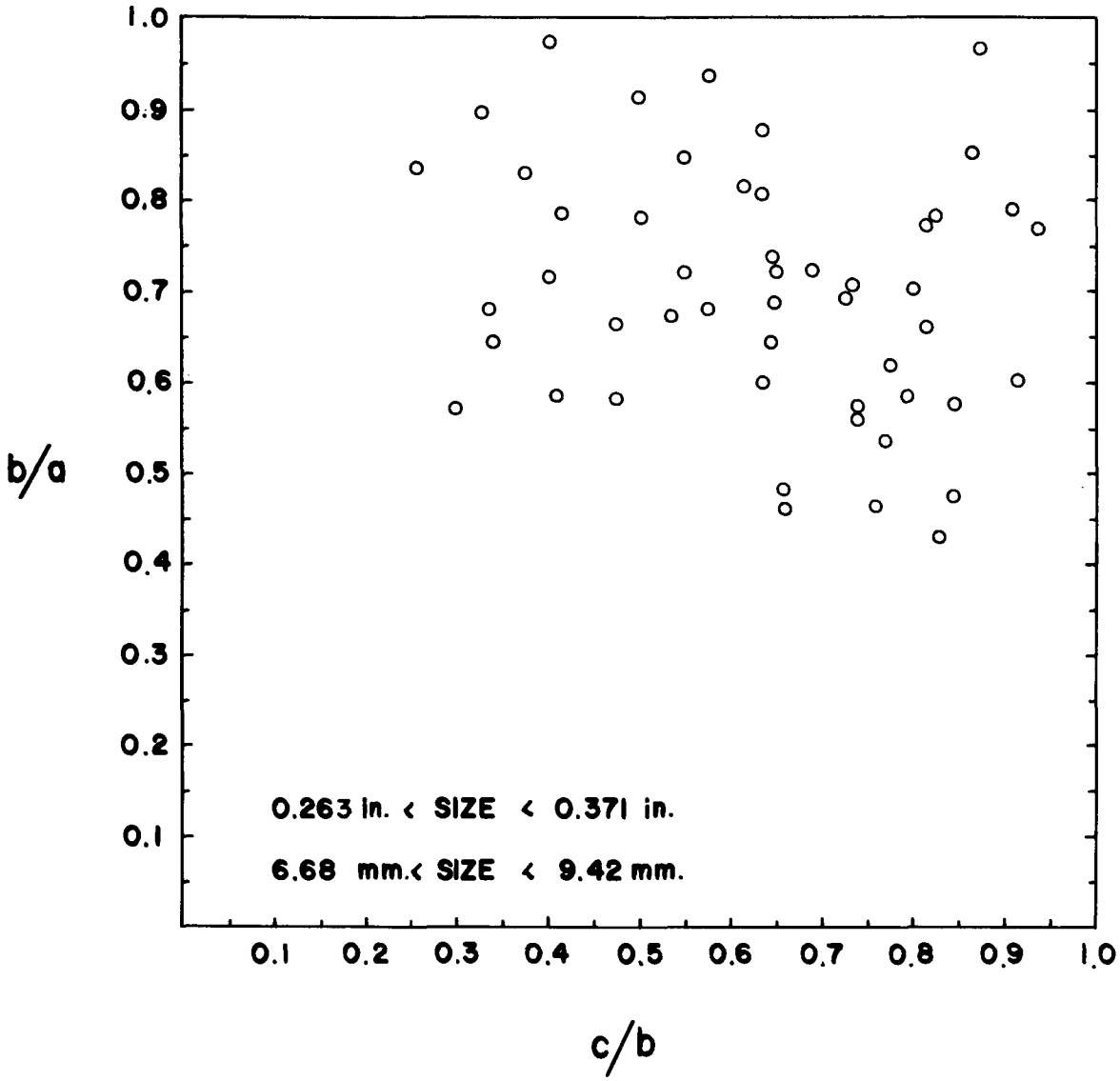

Figure 2.3 Zingg's classification for crushed salt particles in size fraction of 6.68-9.42 mm. Sample (S4-CS1-SN1).

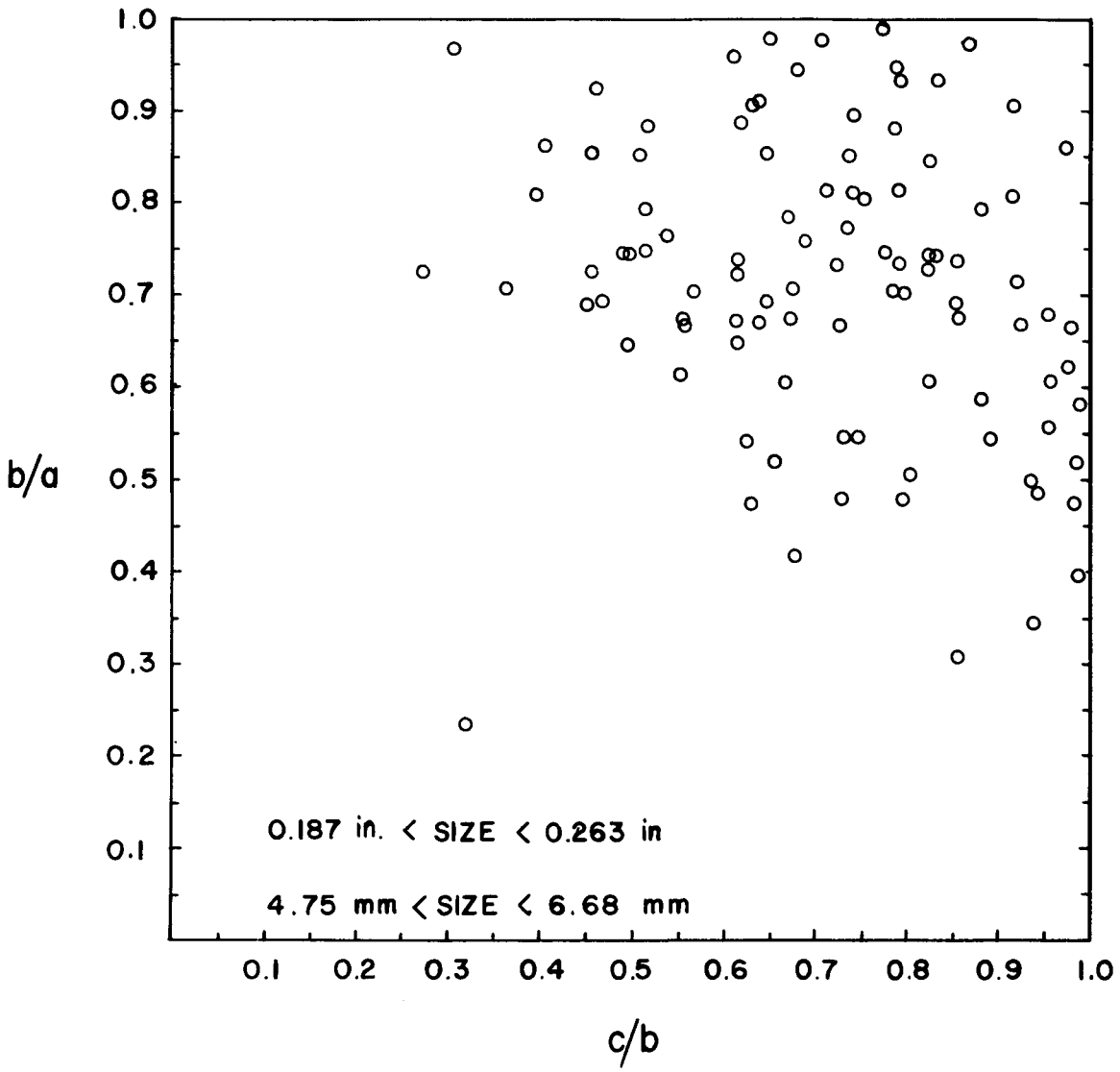

Figure 2.4 Zingg's classification for crushed salt particles in size fraction of 4.75-6.68 mm. Sample (S4-CS1-SN1).

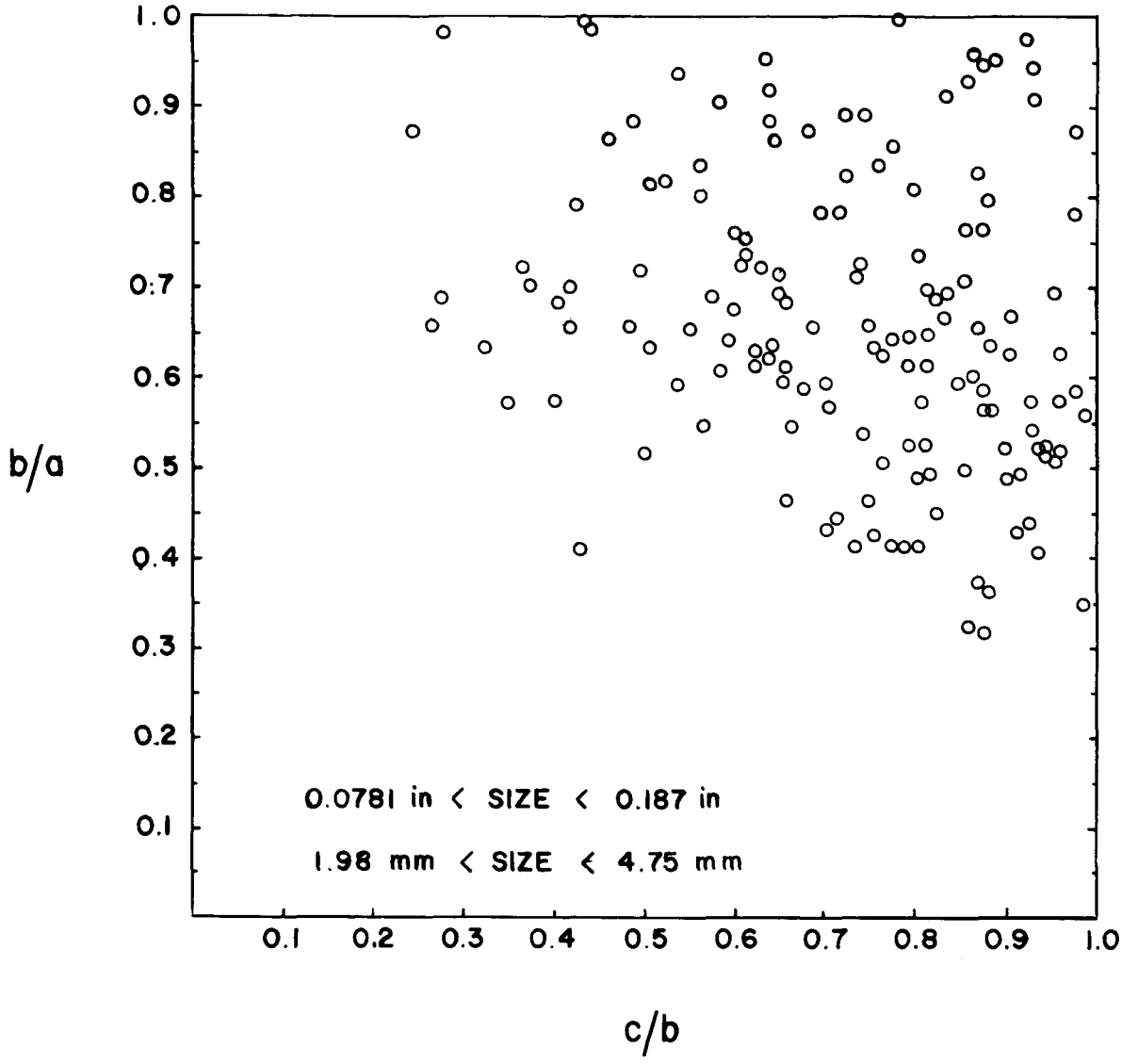

Figure 2.5 Zingg's classification for crushed salt particles in size fraction of 1.98-4.75 mm. Sample (S4-CS1-SN1).

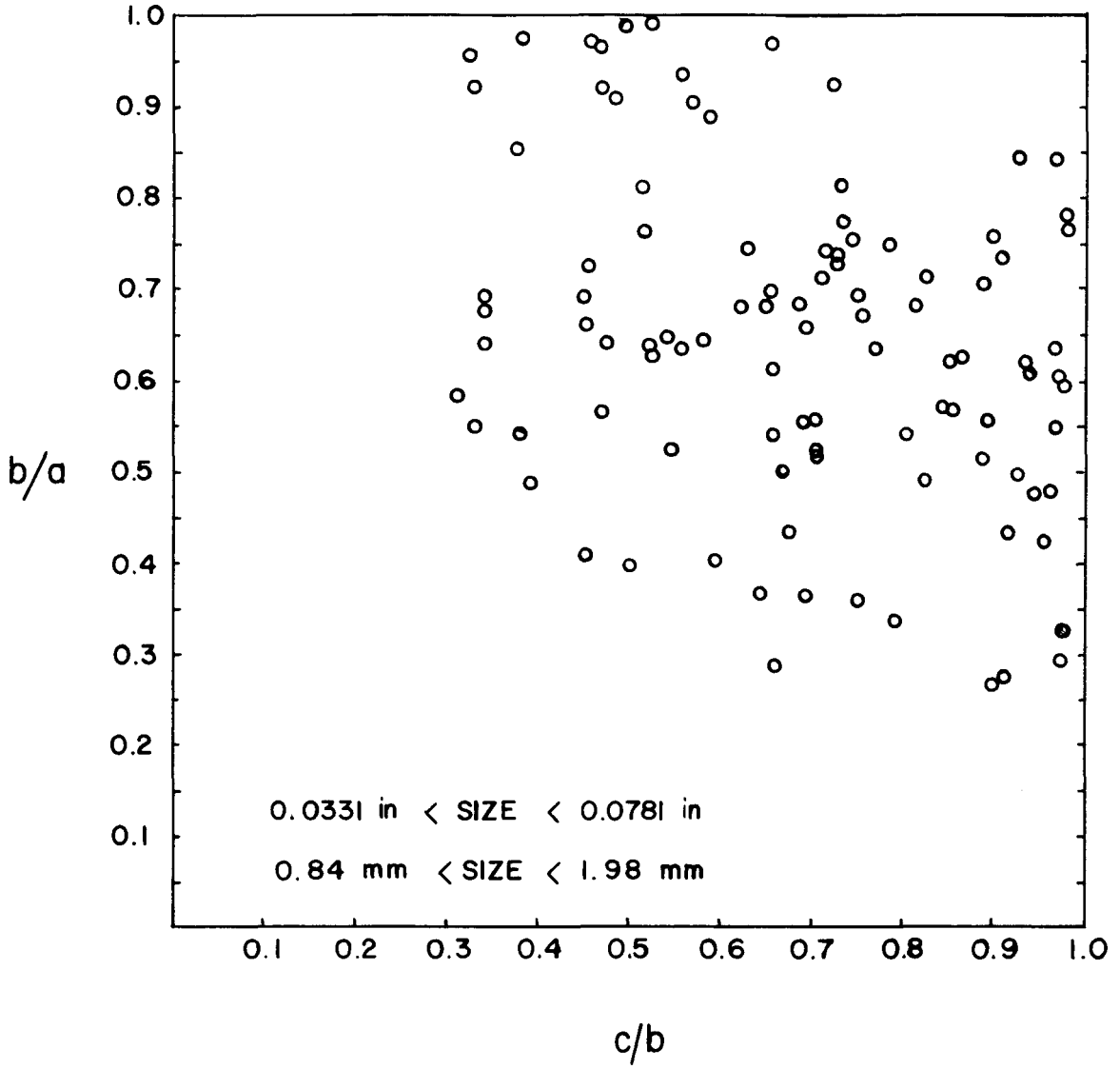

Figure 2.6 Zingg's classification for crushed salt particles in size fraction of 0.84-1.98 mm. Sample (S4-CS1-SN1).

Table 2.1 Shape Analysis for Crushed Salt. Sample (S4-CS1-SN1).

Size Fraction (mm)	a (mm)	b (mm)	c (mm)	b/a	c/b	c/a	ac/b^2	α_v	α_s
12.7-9.42	14.92 (3.02)	11.66 (1.98)	5.74 (1.10)	0.80 (0.13)	0.51 (0.14)	0.40 (0.11)	0.67 (0.29)	0.31 (0.08)	2.99 (0.36)
9.42-6.68	12.65 (2.32)	8.63 (1.11)	5.37 (1.43)	0.70 (0.14)	0.63 (0.18)	0.44 (0.14)	0.96 (0.38)	0.37 (0.11)	3.26 (0.49)
6.68-4.75	9.07 (2.38)	6.17 (0.92)	4.29 (0.91)	0.71 (0.16)	0.71 (0.18)	0.50 (0.15)	1.08 (0.47)	0.41 (0.10)	3.47 (0.46)
4.75-1.98	6.73 (1.61)	4.29 (0.87)	3.00 (0.77)	0.66 (0.16)	0.72 (0.18)	0.47 (0.15)	1.18 (0.51)	0.40 (0.10)	3.43 (0.47)
1.98-0.84	2.88 (0.68)	1.78 (0.37)	1.17 (0.33)	0.65 (0.18)	0.68 (0.20)	0.43 (0.15)	1.18 (0.64)	0.37 (0.11)	3.31 (0.50)

NOTE: a, b and c represent average lengths of the longest, the intermediate, and the shortest axes, respectively. α_v and α_s are average volume shape factor and surface shape factor. Numbers in parentheses indicate standard deviations.

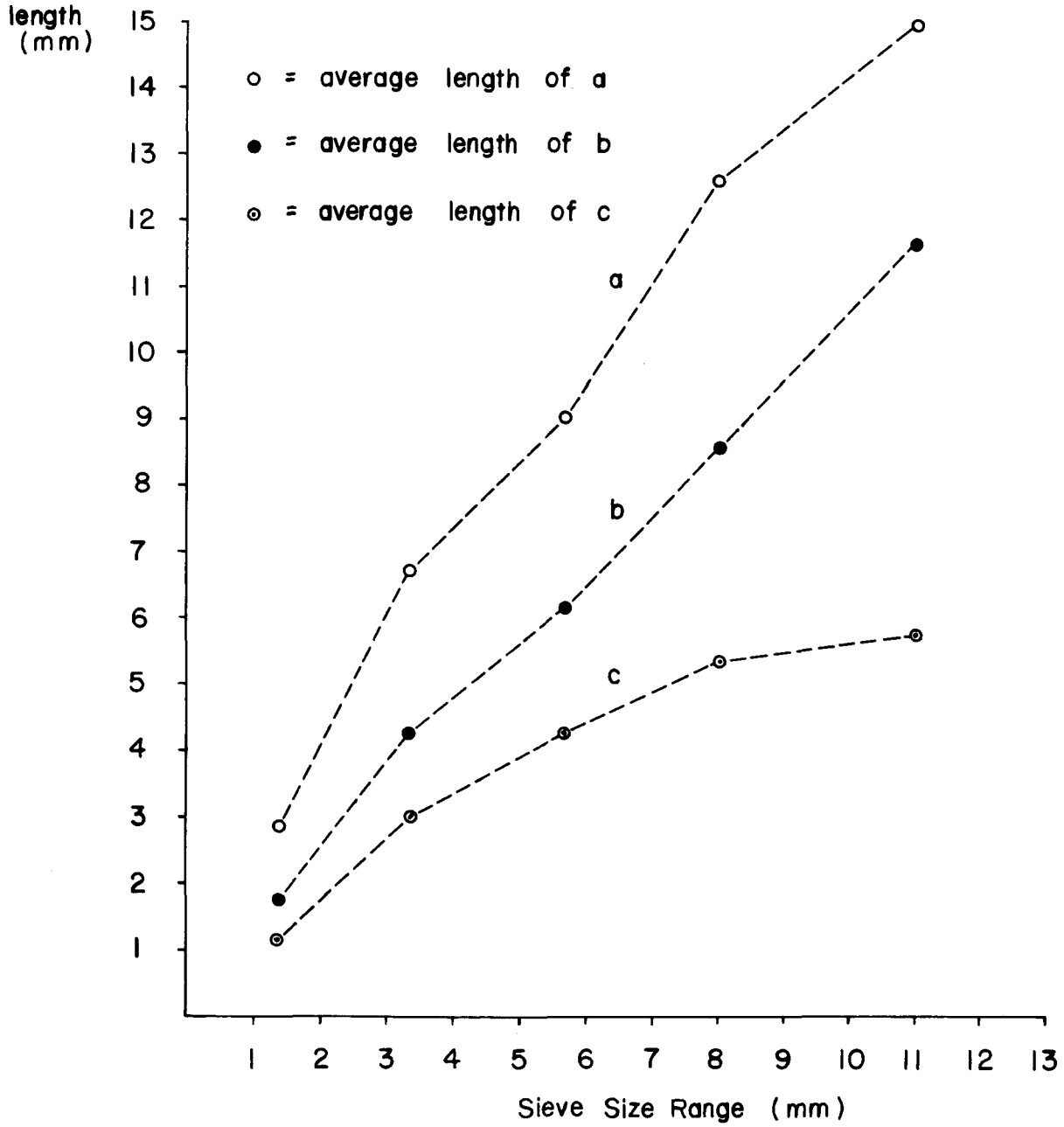

Figure 2.7 Variation of average lengths of a, b and c axes of crushed salt particles with sieve size fractions. Sample (S4-CS1-SN1).

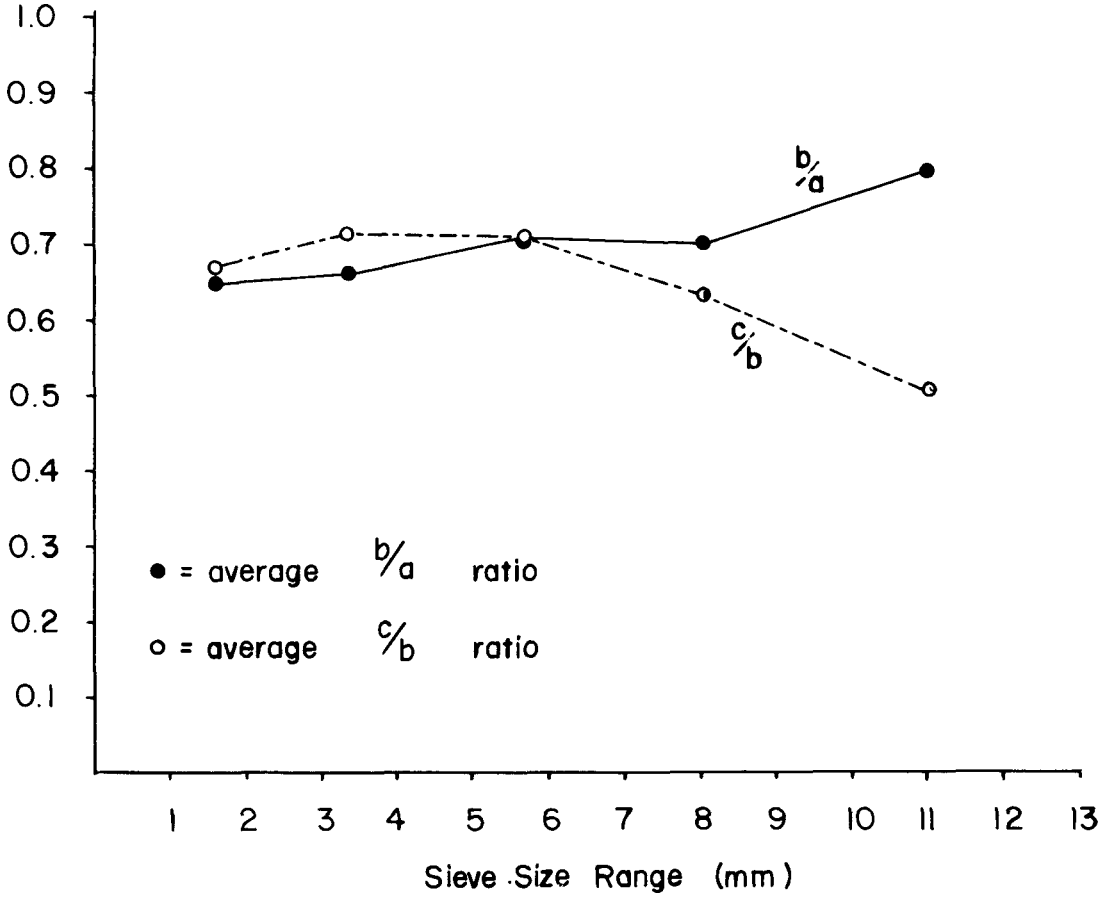

Figure 2.8 Variation of average b/a and c/b ratios of crushed salt particles with sieve size fractions. Sample (S4-CS1-SN1).

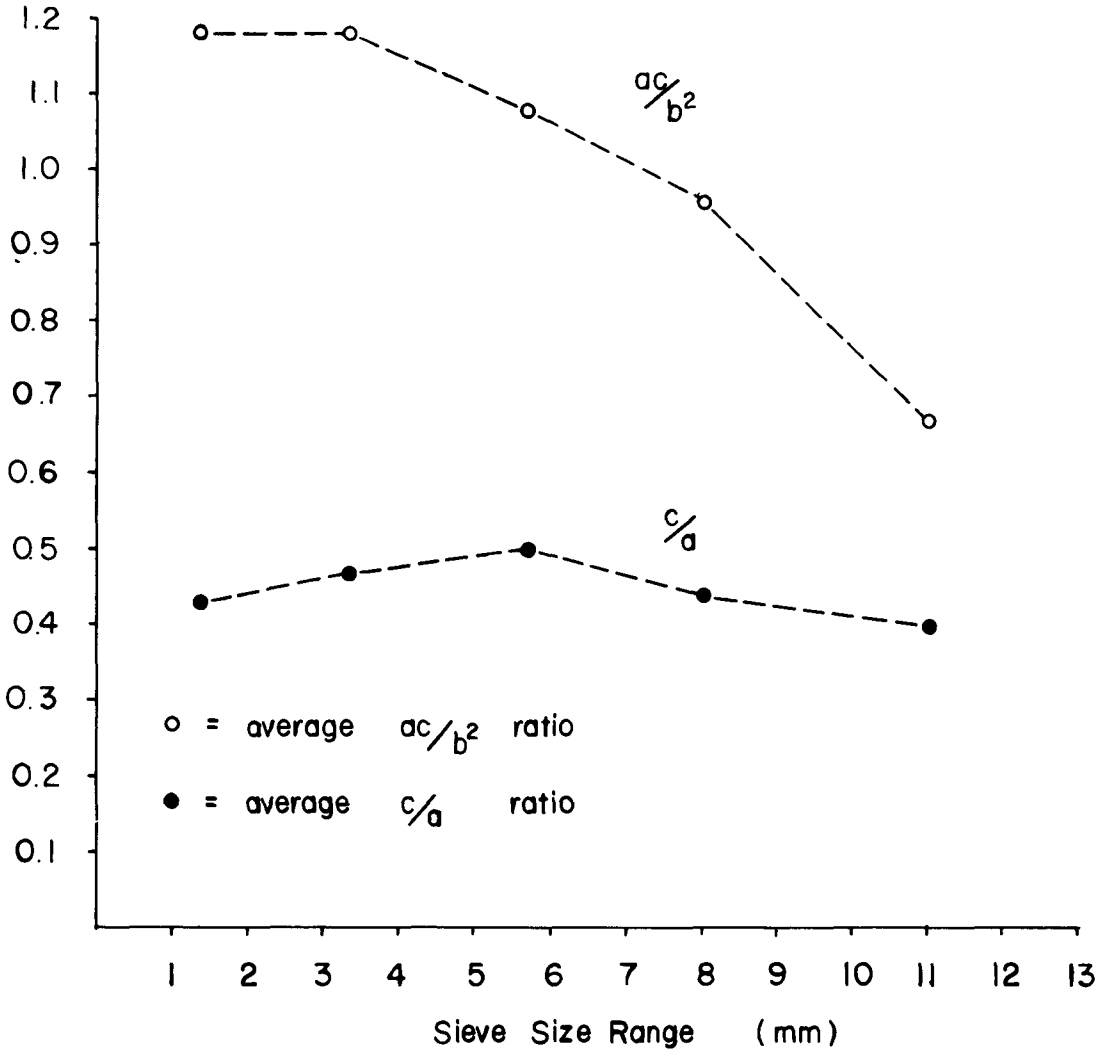

Figure 2.9 Variation of average ac/b^2 and c/a ratios of crushed salt particles with sieve size fractions. Sample (S4-CS1-SN1).

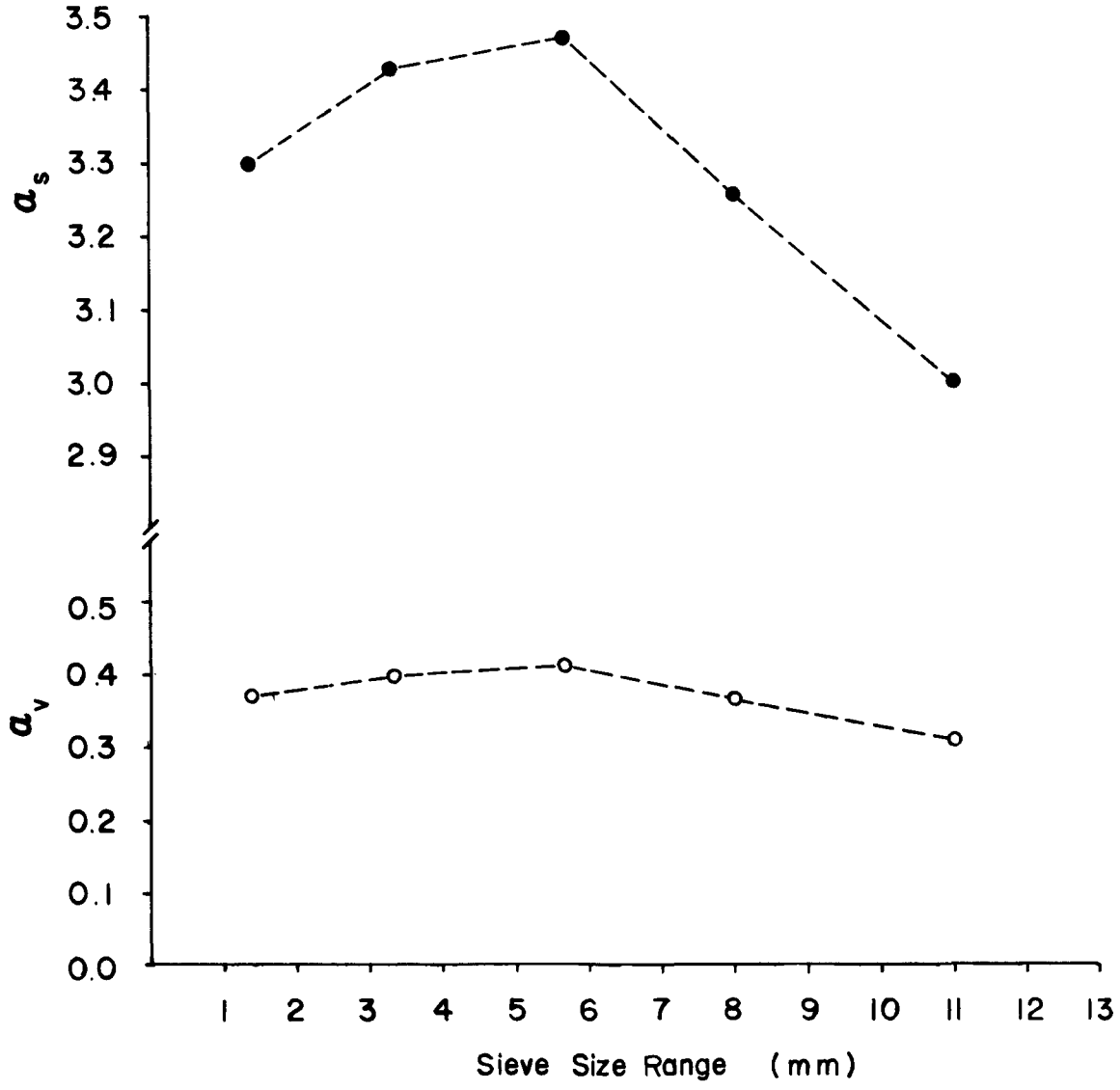

Figure 2.10 Variation of average volume-shape factor (α_v) and surface-shape factor (α_s) for crushed salt particles with sieve size fractions. Sample (S4-CS1-SN1).

Examination of the differences between a and b, as well as between b and c (Figure 2.7), suggests that there is a tendency for symmetry change of the salt particles with the fraction size. The tendency is also evident in Figure 2.8 as the b/a and c/b curves cross over. This characterization parallels the results based on Zingg's classification. The average c/a ratios for each size fraction are relatively uniform. The average ac/b^2 ratios exhibit greater variation (Figure 2.9). The volume shape factor (α_v) remains essentially uniform for different size fractions of crushed salt (Figure 2.10). However, the surface shape factor varies significantly across the size fractions, and in particular when the fraction size increases. This is contrary to the finding of a relatively constant surface shape factor reported by Martin (1928, as cited by Herdan, 1960) on granular shape analyses. Whether the discrepancy is related to or influenced by the shape migration of crushed salt is not clear.

The design and operation of crushing equipment influence sphericity of crushed particles (Blanks, 1952; Rockwood, 1948, as cited by Mather, 1955). Malewski (1984) reports a small dependence of the crushed particle shape on the original block sizes of basalt. It is clear that numerous factors influence particle shape. One needs to caution, therefore, against generalizations or extrapolations of characterizations of the particle shape of crushed salt based on one set or a limited range of fragmentation conditions.

CHAPTER THREE

CRUSHED SALT CONSOLIDATION

3.1 Introduction

Crushed salt has been proposed as backfill or sealing material for a nuclear waste repository in salt (Kelsall et al., 1984). In order to assess the possible sealing performance, studies regarding crushed salt consolidation and the decrease in permeability with consolidation and time are necessary.

This study evaluates some aspects of the consolidation of crushed salt. Particle size and grain size distribution may influence the consolidation of crushed salt (Stinebaugh, 1979; Shor et al., 1981; IT Corporation, 1984 and 1987; Pfeifle et al., 1987; Urai et al., 1986). Particle shape, orientation, and surface texture affect the behavior of a particulate system (Krumbein and Sloss, 1963; Orr, 1966; Fowkes and Fritz, 1974; Harr, 1977), and are likely to be additional factors that need to be considered in crushed salt consolidation. Due to the difficulties in measuring and quantifying particle orientation and surface texture, their characterization is not included as part of this project. It is postulated that they are secondary variables, or that they are identical (e.g. surface texture) for the experiments performed. Appendices C and B give the procedures used for characterizing particle shape and particle size of crushed salt, respectively. Particle size analysis is essential for the characterization of crushed salt to be used for plugs or backfill. Particle shape analysis is deemed important for basic investigations of consolidation, even though it is, for most cases, extremely laborious and time-consuming. A particle shape analysis may be beneficial because the shape-related parameters, such as specific surface and angularity factor, can be used in Kozeny's equation (Kozeny, 1927), the Kozeny-Carman equation (Carman, 1939), or the empirical formula proposed by Loudon (1952) to estimate the permeability of a consolidated crushed salt plug. Moreover, particle shape is likely to have an influence on salt consolidation, because it influences contact stress distributions, particle stresses, and hence particle creep and interparticle healing or crystal growth.

Shor et al. (1981) studied the consolidation of salt aggregates in Monel and glass tubes under constant axial load and concluded that the consolidation rate increased with increasing stress and decreased with increasing particle size. They also observed that the consolidation rate was markedly increased by adding a small amount of water to the sample. Quasi-hydrostatic consolidation of crushed salt performed by IT Corporation (1987) and RE/SPEC, Inc. (Pfeifle et al., 1987) confirmed an increased consolidation rate resulting from introducing extra moisture to crushed salt. Liedtke and Bleich (1984) found oedometer type consolidation tests to be very sensitive to initial brine content, but virtually independent of stress for a stress range from 5 to 17 MPa.

Holcomb and Zeuch (1988) discuss pressure and time dependency in more fundamental phenomenological terms. Their experiments demonstrate pressure sensitivity, and their analysis and discussion explains why such sensitivities are easily missed unless experiments are designed and interpreted correctly.

The strategy of emplacing nuclear waste in an underground salt repository includes backfilling the storage rooms and the access tunnels (Yost and Aronson, 1987). Creep closure of the storage rooms and tunnels is likely to compress the crushed salt backfill and create an impermeable monolith to retard ground water flow and radionuclide migration (Kelsall et al., 1982).

In this chapter, mechanisms controlling crushed salt consolidation and its influencing variables are discussed. Also reported are consolidation results and unconfined compressive strength of consolidated crushed salt samples.

3.2 Mechanisms of Crushed-Salt Consolidation

The consolidation of a soil sample (or a particulate system in general) usually involves the following three mechanisms: (1) deformation of grains, (2) compression of air and fluids in the voids, and (3) squeezing out of air and fluids from the voids (Holtz and Kovacs, 1981, p. 286). The primary reduction in volume in consolidating a saturated clay sample is due to fluids flowing out of the voids. The consolidation rate is then controlled by the permeability of the clay sample. Figure 3.1a shows a typical consolidation curve for saturated clay. Crushed salt consolidation behaves differently, as shown in Figure 3.1b. This is because during most of the consolidation the permeability of a crushed salt sample is so large that the pore pressure can never build up. The pore pressure dissipates virtually instantaneously upon the application of loading. The consolidation of crushed salt thus is controlled by the deformations of its structure and constituent salt particles. Whether or not such venting will occur in situ may be a significant variable in predicting salt consolidation.

Mechanisms such as grain re-orientation, grain breakage (crushing), plastic deformation (intragranular gliding or dislocation), and possibly dissolution-reprecipitation are involved in the natural consolidation of sediments (De Boer, 1977). However, deformations caused by grain re-orientation, grain breakage, and dislocation are not nearly large enough to explain the observed level of natural consolidation (Lowry, 1956; Waldschmidt, 1941; as cited by De Boer, 1977). A diffusion type process called "pressure solution" is proposed to account for the much lower porosities observed in natural sediments. During this process the material at or near the grain contacts (highly stressed surfaces) is gradually removed due to the enhanced solubility and transported through diffusion to reprecipitate in less stressed surfaces. As a result, the neighboring grains slowly interpenetrate and the porosity is reduced (Weyl, 1959; De Boer, 1977). This process is extremely slow in a dry condition because of the diffusion step, but it can be accelerated in the presence of fluids or moisture, especially if the material is an ionic solid (e.g. sodium chloride).

Studies on the consolidation of crushed and granulated salt have shown that the presence of brine markedly accelerates the creep consolidation (Shor et al., 1981; Pfeifle et al., 1987; IT Corporation, 1987). This phenomenon may be accounted for by enhanced pressure solutioning. There is evidence that the Joffe effect may also be responsible for the increased consolidation rate (Varo and Passaris, 1977; Stokes et al., 1960; Jenyon, 1986). The Joffe effect, as defined by Stokes et al. (1960), describes an increased plastic behavior due to the change in fracture behavior of solids brought about by the elimination of surface defects in a solvent. Stokes et al. (1960) also reported that water immersion leads to an enhancement of ductility of a sodium chloride crystal which is retained indefinitely in dry air only if the crystal is dried without leaving a surface precipitate. Yost and Aronson (1987) have proposed three mechanisms to explain the Joffe effect, namely (1) dissolution of pre-existing surface cracks, (2) facilitation of glissile dislocation nucleation at salt surfaces, and (3) removal by dissolution of surface obstacles to dislocation egress.

Shor et al. (1981) suggested that the consolidation of crushed salt involves recrystallization and crystal growth, a process analogous to the sintering of metal or ceramic powders. Consolidation of crushed salt, as indicated by reduction in permeability, was found to be most rapid in brine and least rapid in air, suggesting that mechanical deformation was not an important mechanism in the consolidation of crushed salt. Holcomb and Zeuch (1988, p. 19) argue that crushed salt compaction more closely resembles isostatic hot-pressing, and have developed and experimentally evaluated corresponding theories in considerable detail (Zeuch et al., 1985; Zeuch, 1989).

In summary, grain re-orientation, grain breakage, intergranular gliding, and intragranular dislocation are primary controlling mechanisms for the consolidation behavior of dry crushed salt. In the presence of brine or moisture, consolidation is accelerated by the enhanced mechanisms of dislocation, pressure solution and the Joffe effect.

3.3 Variables Influencing Crushed-Salt Consolidation

Several investigators (Hansen, 1976; Ratigan and Wagner, 1978; Stinebaugh, 1979; Shor et al., 1981; Holcomb and Hannum, 1982; Kappei and Gessler, 1984; Liedtke and Bleich, 1984) have studied the consolidation behavior of crushed salt in laboratory experiments. A summary (IT Corporation, 1984) of some of these studies suggests that crushed-salt consolidation is affected by a number of variables, including salt impurities, grain size, grain size distribution, initial porosity, moisture content, stress state, load path, temperature, and time. Calculations and experiments also indicate that initial density greatly affects the time required for consolidation (Hunter, 1980; Kelsall et al., 1982; Kappei and Gessler, 1984; Holcolmb and Zeuch, 1988). It was originally intended, for this investigation, to study all the aforementioned variables except salt impurities. It is assumed that salt impurities are relatively uniform for the salt used for testing. A comprehensive study of the effects of the variables on crushed-salt consolidation requires a large number of tests. Priority

has been given to testing crushed salt samples which contain 2 to 4% brine by weight. In addition to uniform-graded samples, crushed salt samples of a grain size distribution similar to that of the "fine" WIPP crushed salt have been tested.

3.4 Experimental Scheme

The consolidation of crushed salt is a complex process. Although a theoretical model for crushed-salt consolidation is desirable, a complete one may not be attainable in the near future. However, it is postulated that if the relationship between the crushed-salt consolidation and the major influencing variables can be identified, an empirical model may be constructed. Given the need to extrapolate any consolidation predictions for time periods exceeding measurement periods by orders of magnitude, it is clear that fundamental behavior laws should be integrated within semi-empirical formulations to the greatest extent possible. A test matrix is outlined to examine variables that significantly affect the consolidation of crushed salt.

In a typical consolidation curve of crushed salt (Figure 3.1b), three types of consolidation have been identified, namely (1) instantaneous consolidation, (2) transient creep consolidation, and (3) steady-state creep consolidation (the terminology is derived from conventional practice for describing time-dependent rock deformation, Jaeger and Cook, 1979, Ch. 11). There is evidence indicating that the so-called steady-state creep consolidation may actually change with time (Crawford et al., 1971, for consolidation of saturated clay; Nelson and Kelsall, 1984, for salt creep). Therefore, it is appropriate to replace "transient creep" with "primary creep", and "steady-state creep" with "secondary creep" to avoid ambiguity. This uncertainty may be resolved by performing long-term consolidation on crushed salt, or possibly more efficiently by the bounding strategy developed by Wawersik (1983).

Conceptually, for the proposed studies of the consolidation of crushed salt in a pipe, the axial pressure is incremented in steps of 3.45 MPa (500 psi) until the maximum allowable pressure is reached. Table 3.1 gives the maximum allowable pressure and factor of safety of the pipe flow permeameters. The proposed test matrix is best explained through the following example (also see Table 3.2). For a given grain size distribution, temperature, and moisture content, four crushed salt samples are tested in 101.6 mm pipe flow permeameters. The first sample is loaded to 3.45 MPa (500 psi) for 15 days and then at 6.9 MPa (1000 psi) for another 15 days. The load is incremented until the maximum allowable pressure of 13.8 MPa is reached. The second sample is loaded at an initial pressure of 6.9 MPa (1000 psi) for 20 days, then at 10.35 MPa (1500 psi) for another 20 days and so on. The third sample is first loaded to 10.35 MPa (1500 psi) for 30 days and then at 13.8 MPa (2000 psi) for an additional 30 days. The fourth sample is loaded at 13.8 MPa (2000 psi) for 60 days. This test matrix is advantageous for studying changes of the instantaneous consolidation and secondary creep consolidation with respect to load path and time.

(a) Saturated Clay

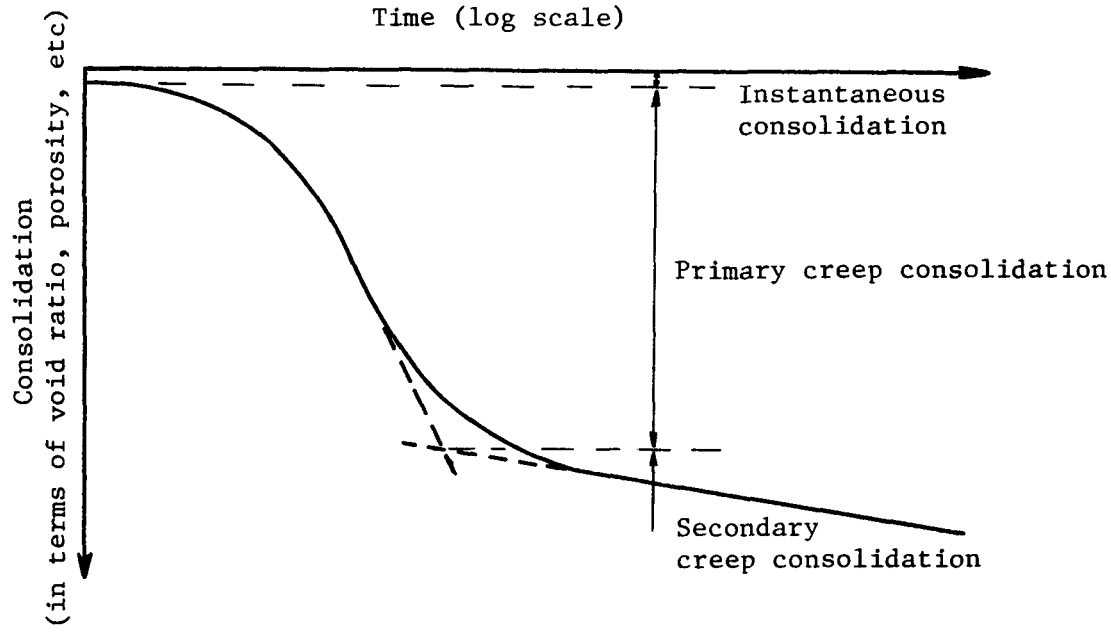

(b) Crushed Salt

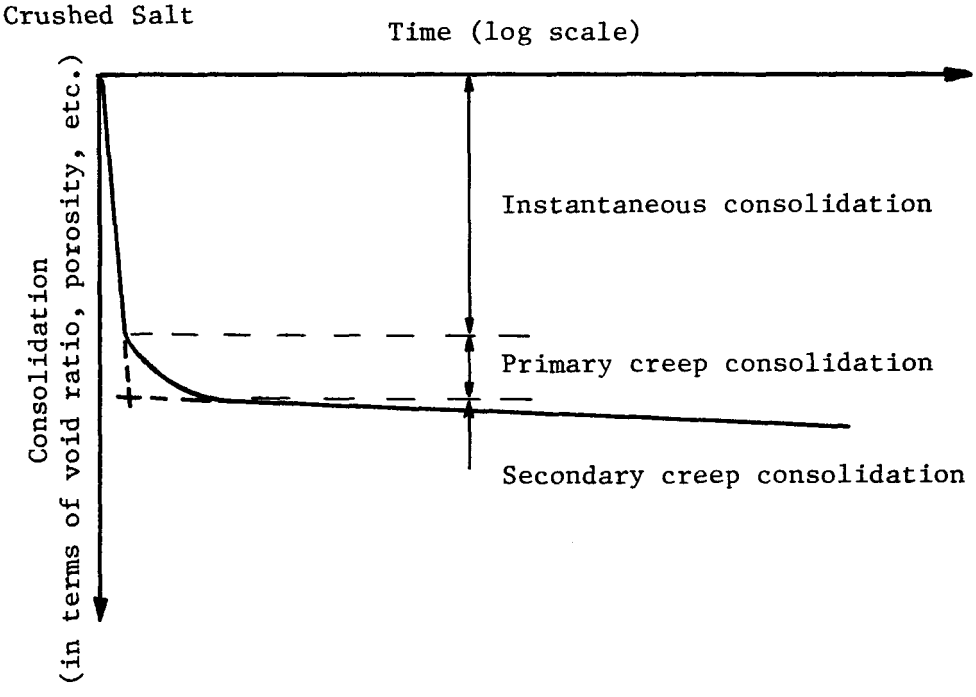

Figure 3.1 Typical consolidation curves for (a) saturated clay and (b) crushed salt.

Table 3.1 Maximum Allowable Axial Pressures and Factors of Safety for Pipe Flow Permeameters

Pipe Diameter (mm)	Maximum Allowable Axial Pressure (MPa)	Factor of Safety for Pipe*	Factor of Safety for Bolts**
203.2 (8 in)	10.34 (1500 psi)	2.27	1.95[@], 6 1.27 mm (1/2") bolts
101.6 (4 in)	13.79 (2000 psi)	2.44	5.86, 6 1.27 mm (1/2") bolts
25.4 (1 in)	17.24 (2500 psi)	3.50	14.64, 3 7.94 mm (5/16") bolts

*The yield stress for pipes of 203.2, 101.6, and 25.4 mm in diameter are 300 MPa (43,500 psi), 286.9 MPa (41,600 psi), and 275.9 MPa (40,000 psi, an assumed strength), respectively.

**The yield stress of steel bolts is 862 MPa (125,000 psi).

[@]Additional bolts can be added to raise the factor of safety at least up to 2.0.

Table 3.2 Conceptual Test Matrix for Consolidation of 101.6 mm (4 in) Crushed Salt Samples (P_{max} = 13.79 MPa, P_{incr} = 3.45 MPa)

Sample Number	Initial Axial Pressure (MPa)	Number of Pressure Increments	Test Duration for Each Increment (days)
1	3.45 (500 psi)	3	15
2	6.90 (1000 psi)	2	20
3	10.34 (1500 psi)	1	30
4	13.79 (2000 psi)	0	60

Ten crushed-salt consolidation tests have been performed. The tests are grouped into Series A, Series B, and an initial 20-cm diameter test. The results are described in Sections 3.5, 3.6, and 3.7. The purpose of the Series A tests is to examine the effects of grain size, grain size distribution, and brine content on consolidation. Series B tests are designed to study changes of the instantaneous and secondary consolidation with respect to load path and time.

3.5 Quasi-Static Confined Consolidation of a 20 cm Diameter Crushed Salt Sample

A 20 cm (8 in) pipe permeameter is used to consolidate crushed salt with grain sizes from 12.7 to 0.075 mm (0.5 in to 0.0029 in), an average grain size of 5.04 mm (0.2 in), based on a weight average (Table 3.3). The grain size distribution of this sample 1 (Figure 3.2) exhibits a characteristic gap-graded distribution (Harr, 1977, p. 12). Subsequent sieve analyses on samples from the same population show a similar distribution. One follow-up sieving result is shown in Figure 3.2 for comparison (sample 2). Salt crushing follows the procedure in Appendix A. The original salt block (after removal of cored samples) was heavily hammered and chiseled. Pieces of various sizes of rock salt were collected for crushing in a jaw crusher. The gap-graded size distribution might have resulted from the way in which the salt block was fragmented (Malewski, 1984; Mather, 1955).

The emplacement of air-dried crushed salt follows the procedure given in Appendix D. Minimal kneading efforts were exerted during installation. Upon completion of the permeameter assemblage, an air pressure of about 0.35 MPa (50 psi) was applied to assure a close contact between the piston and the top porous stone. The crushed salt sample weighs 8259 g and has an initial length of 189.89 mm. The bulk sample occupies 6195.8 cm^3 prior to consolidation. The volume of salt solids is calculated as 3823.6 cm^3, based on an average density of 2.16 g/cm^3 (135 lb/ft^3) (Fuenkajorn and Daemen, 1988, Table L.1). This gives an initial void ratio of 0.62. The average moisture content of the sample was about 0.2% by weight, as determined by weighing and oven-drying of three randomly selected samples of approximately 90 grams each.

The crushed salt sample was initially incrementally loaded in the following order (in gage pressure): 0.86 MPa (125 psi), 1.72 MPa (250 psi), 3.45 MPa (500 psi), 5.17 MPa (750 psi), and up to 6.48 MPa (940 psi). Durations for each increment were approximately 66, 48, 37, 23, and 42 hours (Figure 3.3). The longitudinal (axial) displacement was monitored by a dial gage (to 0.01 mm). The applied pressure was reduced to zero 216 hours after the test started. The sample rebound was then monitored for 48 hours. The results in Figures 3.3 and 3.4 include consolidation data up to the pressure of 6.48 MPa (940 psi), in the form of void ratio vs. time. The test was continued upon receiving a high-pressure gas regulator and 15 cm (6-inch) piston rod. Figure 3.5 shows the complete consolidation curve up to 10.34 MPa.

Table 3.3 Median Sizes and Normalized Weight Frequencies for Crushed Salt Sample S4-CS2-SN1.

Size Fraction (mm)	Median Size, x_i (mm)	Normalized Frequency by Weight (%), $f(x_i)$
12.70 - 9.42	11.060	15.67
9.42 - 6.68	8.050	15.60
6.68 - 4.75	5.715	15.95
4.75 - 2.00	3.375	25.92
2.00 - 0.84	1.420	15.35
0.84 - 0.42	0.630	5.93
0.42 - 0.25	0.335	2.77
0.25 - 0.18	0.215	1.24
0.18 - 0.11	0.145	0.38
0.11 - 0.07	0.090	1.19

The weight average particle size = $\sum x_i f(x_i)/100 = 5.04$ mm

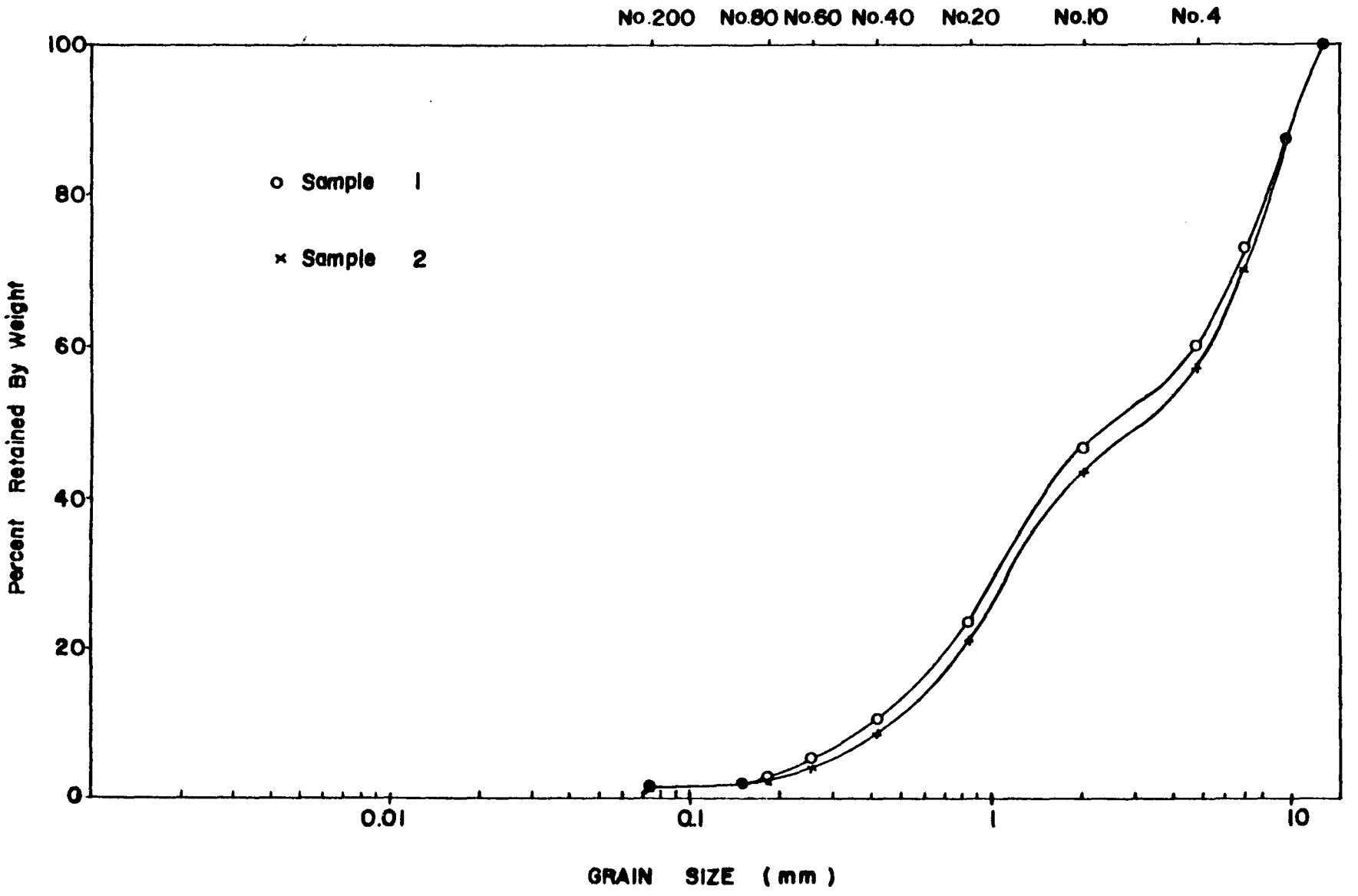

Figure 3.2 Grain size distributions of crushed salt. Sample 1 (S4-CS2-SN1) is used for the consolidation test. Sample 2 (S4-CS2-SN2) is a grain size distribution control sample.

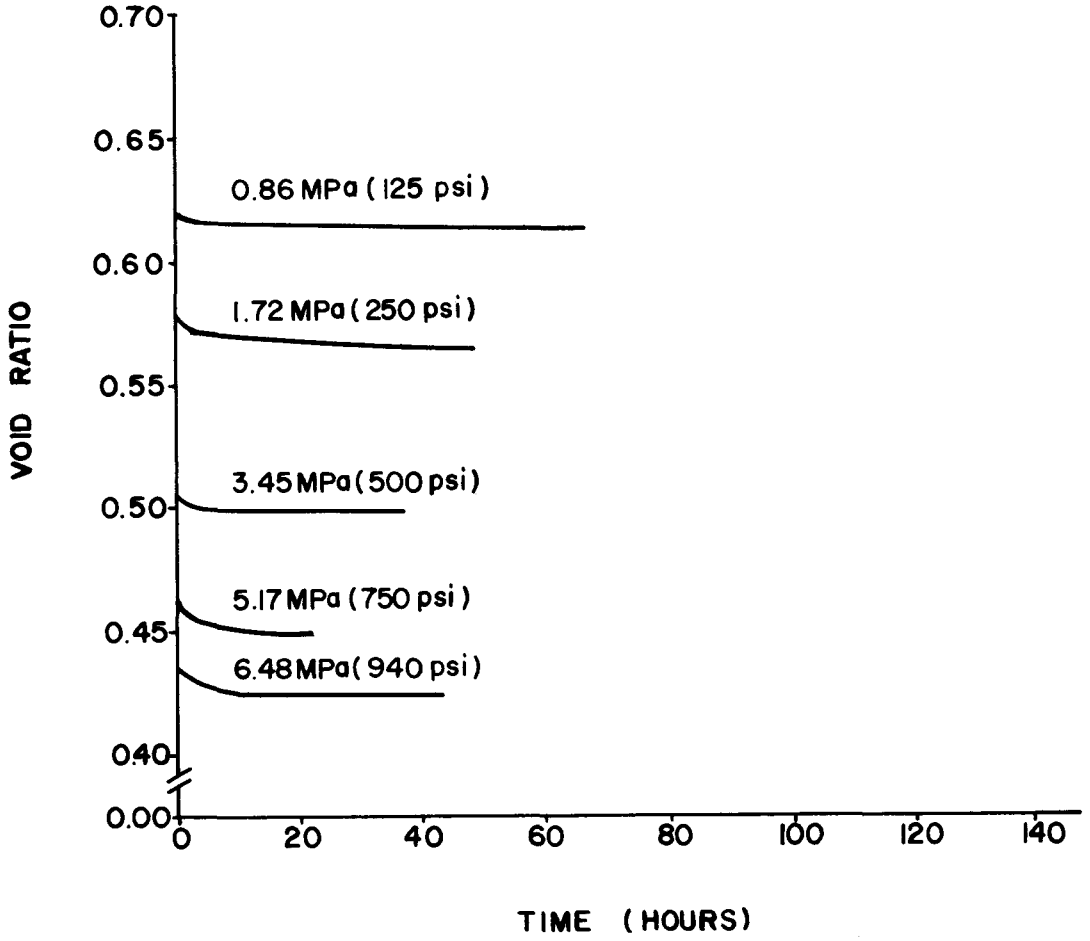

Figure 3.3 Quasi-static consolidation of 20 cm diameter crushed salt sample. The time scale is re-initialized for each consolidation increment. Numbers along each curve indicate the corresponding quasi-static applied uniaxial stress. Sample S4-CS2-SN1-8-CD1.

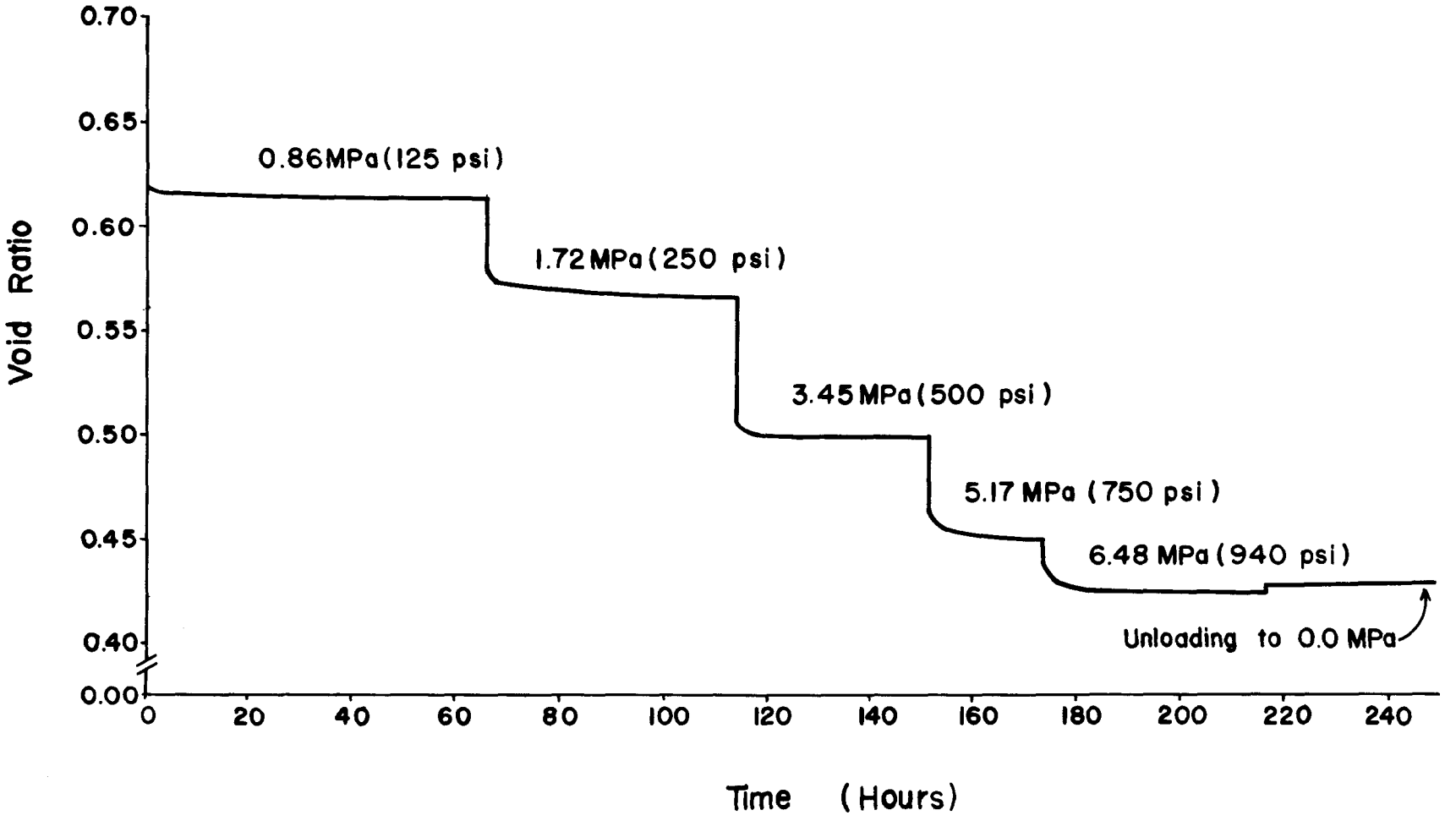

Figure 3.4 Quasi-static consolidation of 20 cm diameter crushed salt sample S4-CS2-SN1-8-CD1 for 5 increments of the applied axial stress.

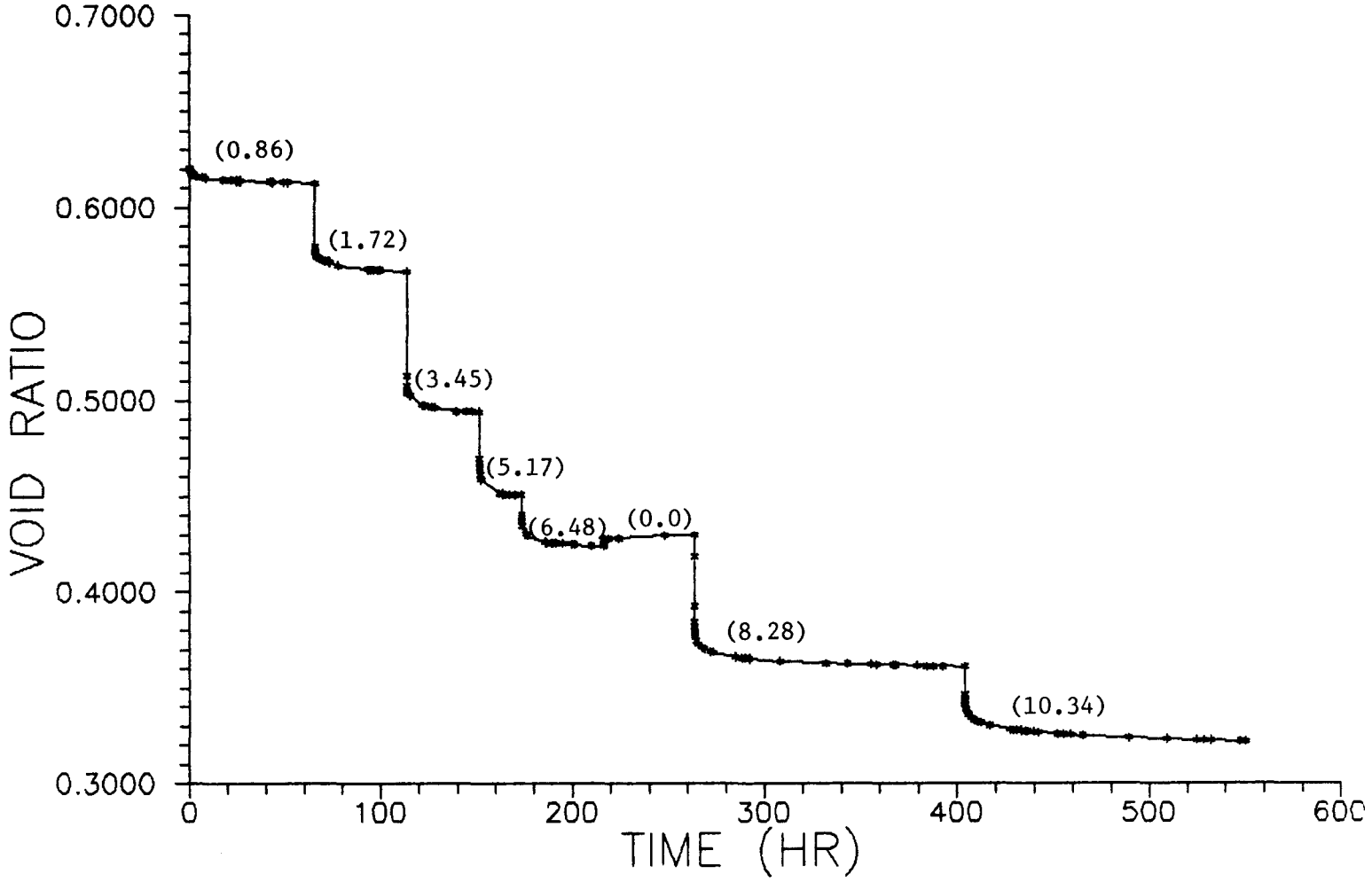

Figure 3.5 Uniaxial strain quasi-static consolidation of well-graded crushed salt. Sample S4-CS2-SN2-WG-8-CD-1-D (203.2 mm in diameter, air-dried). Numbers in parentheses indicate the applied quasi-static axial stress in MPa.

The deformation of rock salt may be accounted for by mechanisms such as particle fragmentation (crushing), intergranular and/or intragranular slip/shear (Le Comte, 1965; Lindner and Brady, 1984). It is believed that the particle crushing and the intergranular slip/shear are major mechanisms in consolidation of crushed salt. Crushing may play an important role in the early stage when the pressure is being incremented, as suggested by the accompanying noises. The intragranular gliding may be postulated to be insignificant within the range of applied pressures (Lindner and Brady, 1984), based on the applied external pressures. However, this could be an oversimplification which does not adequately recognize the local effects, e.g. the high stress concentrations at contact points. Moreover, strong arguments have been presented to consider crushed salt consolidation, even physically, i.e. not only for descriptive modeling purposes, as equivalent to hot-pressing (Zeuch et al., 1985; Holcomb and Zeuch, 1988).

About 12% reduction in the sample length has occurred. The void ratio decreased from 0.620 to 0.424, based on a simplified calculation, neglecting lateral steel cylinder expansion, approximately a 32% reduction. The corresponding porosities are 38.3% and 29.8%. A total sample rebound of 0.66 mm was measured. This may be the elastic or viscoelastic rebound of the crushed salt sample (if any) and/or the rebound of the stainless steel pipe upon depressurization.

3.6 Quasi-Static Confined Consolidation of Crushed Salt: Series A Tests

Four quasi-static consolidation tests have been performed to study the effects of initial particle size and brine content. Samples were installed in pipes (pipe flow permeameters) and loaded axially. No (or minimal) lateral deformation was allowed. The lateral restraint and the associated friction along the sides of the sample makes it difficult to interpret the complete stress conditions during consolidation. It may correspond to actual in-situ installation, in which axial load is a dominant consolidation driving force (e.g. for backfill in a vertical shaft?).

The maximum particle size is kept to less than one-tenth of the pipe diameter in order to avoid arching (Appendix D). A smaller ratio (possibly 1/50 to 1/100) may be desirable to ensure a uniform flow across the plugs during permeability testing (Schwartz and Smith, 1953; Orr, 1966, p. 183).

Sample installation follows the procedure for pipe flow testing (Appendix F). Testing follows the pipe flow testing procedure (Appendix F), with omission of steps for sample saturation and permeability testing. Two sets of tests were conducted in pipes of 25.4 and 101.6 mm diameter each. The axial stress paths were kept the same for each set of experiments by using a single shared pressurization system.

Table 3.4 gives sample number, dimensions, characteristics, and sample number designation details. Table 3.5 summarizes the results. Graphical representations are shown in Figures 3.6 through 3.8 and 3.10 through 3.12.

Table 3.4 Crushed Salt Consolidation Sample Dimensions and Particle Characteristics: Test Series A

Sample Number*	Sample Diameter (mm)	Initial Sample Length (mm)	Initial Average Particle Size D_{50} (mm)**	Uniformity Coefficient C_u***	Particle Size Range (mm)
S4-CS2-SN2-WG-8-CD-1-D	203.2 (8 in)	189.89	2.51	12.2	12.70-0.075
S4-CS2-SN4-UG-1-CD-1-D	25.4 (1 in)	85.93	-	1.1	2.36-2.00
S4-CS2-SN4-UG-1-CD-2-D	25.4 (1 in)	85.17	-	1.4	0.841-0.419
S4-CS2-SN3-WG-4-CD-1-D	101.6 (4 in)	90.17	2.0	9.5	6.68-0.075
S4-CS2-SN3-WG-4-CD-2-W	101.6 (4 in)	98.55	2.0	9.5	6.68-0.075

*Sample number designation contains the following information: number of salt block used for crushing, crushing operation number, sieve analysis operation number, particle grading (WG - well graded; UG - uniform graded), size of plug (inches), type of experiment (CD - consolidation), test number of the experiment, and the moisture condition of the sample (D - air dried; W - wet).

** D_{50} = grain size (mm) corresponding to 50% passing by weight.

*** $C_u = D_{60}/D_{10}$, where D_{60} and D_{10} are grain sizes (mm) corresponding to 60% and 10% passing weight.

Table 3.5 Summary of Results of Crushed Salt Consolidation: Test Series A

Sample No.	Brine Content (%)	Porosity* (%)	Void Ratio*	Fractional Density*,#	Maximum Axial Pressure (MPa)	Test Duration (hr)	Room Temperature (^{o}C)	Room Relative Humidity Range (%)
S4-CS2-SN2-WG-8-DC-1-D	0.2 (air-dried)	38.3/24.3	0.62/0.32	0.62/0.76	10.3	550.3	26 ± 1	40-36
S4-CS2-SN4-UG-1-CD-1-D	0.2 (air-dried)	49.9/32.6	0.99/0.48	0.50/0.67	17.2	456.5	21 ± 1	68-38
S4-CS2-SN4-UG-1-CD-2-D	0.2 (air-dried)	48.9/34.7	0.96/0.53	0.51/0.65	17.2	456.5	21 ± 1	68-38
S4-CS2-SN3-WG-4-CD-1-D	0.2 (air-dried)	37.2/21.3	0.59/0.27	0.63/0.79	10.3	334.5	21 ± 1	68-38
S4-CS2-SN3-WG-4-CD-2-W	1.75 (wet)	37.5/21.7	0.60/0.28	0.62/0.78	10.3	334.5	21 ± 1	68-38

*The first number indicates the initial value. The second number indicates the final value, at the end of testing.

#The fractional density is the ratio of the calculated density of the consolidated crushed salt to that of salt particles. Density of salt is assumed to be 2.16 g/cm^{3} (Fuenkajorn and Daemen, 1988, Appendix L).

Three types of consolidation are identified from the consolidation curves of crushed salt, namely (1) the instantaneous consolidation due to initial compression, (2) the transient creep or primary consolidation, and (3) the steady-state or secondary creep consolidation. The crushed salt consolidation parallels the creep behavior of rock described by Jaeger and Cook (1979, Ch. 11), except that the instantaneous consolidation is irreversible. The elastic deformation of crushed salt during the consolidation comprises only a small fraction of the total deformation as is shown by the rebound after unloading (e.g. Figure 3.5). The instantaneous consolidation increases with axial stress and decreases with reduced void ratio. When the axial stress increment is larger (e.g. 3.45 MPa), the instantaneous consolidation is progressively reduced as the uniaxial quasi-static consolidation proceeds (Figures 3.6, 3.7, 3.10 and 3.11). It is postulated that adjustments of particle orientation and the packing state may occur during unloading. This may result in enhanced instantaneous consolidation upon reloading as shown in the latter part of the consolidation curve in Figure 3.5.

Figures 3.6 and 3.7 depict the consolidation curves of two air-dried, 25.4-mm diameter samples of different uniform particle size (2.36-2.00 mm and 0.841-0.419 mm, respectively). The two curves are plotted on the same graph to facilitate comparison in Figure 3.8. The sample with larger particle size consolidates more rapidly than the sample of smaller particle size. This is contrary to the finding by Shor et al. (1981). The conclusion by Shor et al. (1981) is based on tests of crushed salt consolidated in brine. Stinebaugh (1979) studied the compressibility of granulated rock salt (presumably air-dried) and found that material size has little effect on compressibility. This suggests that the dependency of crushed salt consolidation on particle size may not be significant if the test sample is dry. Urai et al. (1986) observed higher strain rates for finer grained compacted and annealed wet synthetic salt. The considerable remaining uncertainties with regard to the influence of particle size are discussed briefly in Section 2.2. The uncertainty with regard to grain size effects indicates the need for additional testing.

Two crushed salt samples with the same grain size distribution (Figure 3.9) were installed in pipes of 101.6 mm diameter to study the effect of brine content. The grain size distribution for the two plugs follows closely the distribution of the "Fine Sample" obtained from the WIPP site (IT Corporation, 1984, p. 6, Figure 2-1). Sample S4-CS2-SN3-WG-4-CD-1-D consists of air-dried crushed salt particles, the brine content of which has been determined to be 0.2%. Sample S4-CS2-SN3-WG-4-CD-2-W consists of moistened crushed salt with a 1.75% brine content. Figures 3.10 and 3.11 show the consolidation curves. Figure 3.12 depicts both curves. At the beginning of the test, the wet sample consolidates faster than the dry sample. The consolidation rate of the wet sample decreases with consolidation and time. The tests were conducted in a vented condition. The moisture was removed through evaporation. As a result of the moisture loss, crystallization formed solid bridges between particles, and hence the crushed salt became stiffer. This probably accounts for the reduction of the consolidation rate. The sample rebound upon unloading is much more conspicuous for

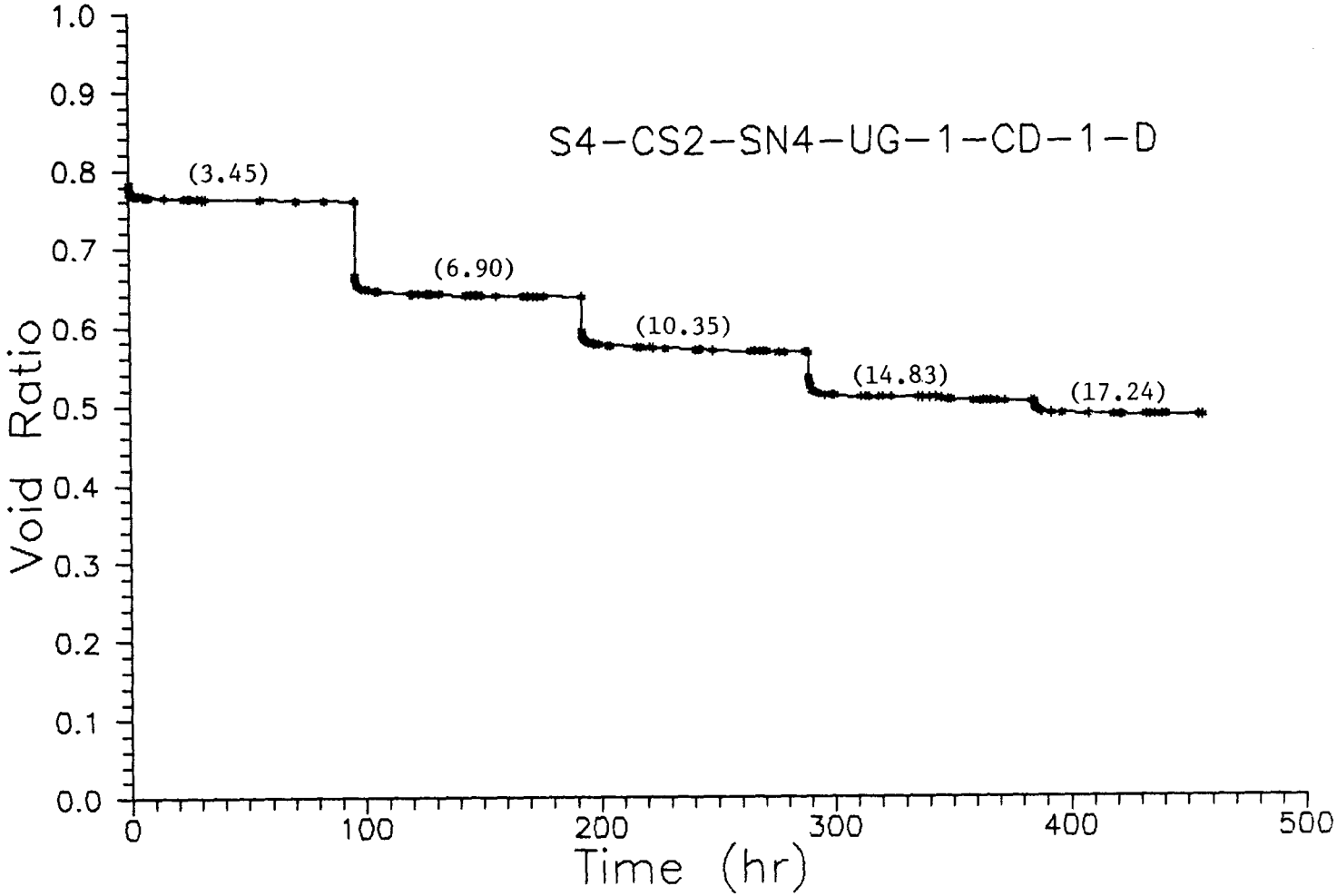

Figure 3.6 Uniaxial strain quasi-static consolidation of uniform-graded crushed salt. Sample S4-CS2-SN4-UG-1-CD-1-D. Particle sizes range from 2.36 to 2.00 mm, air-dried. Numbers in parentheses indicate the applied quasi-static axial stress in MPa.

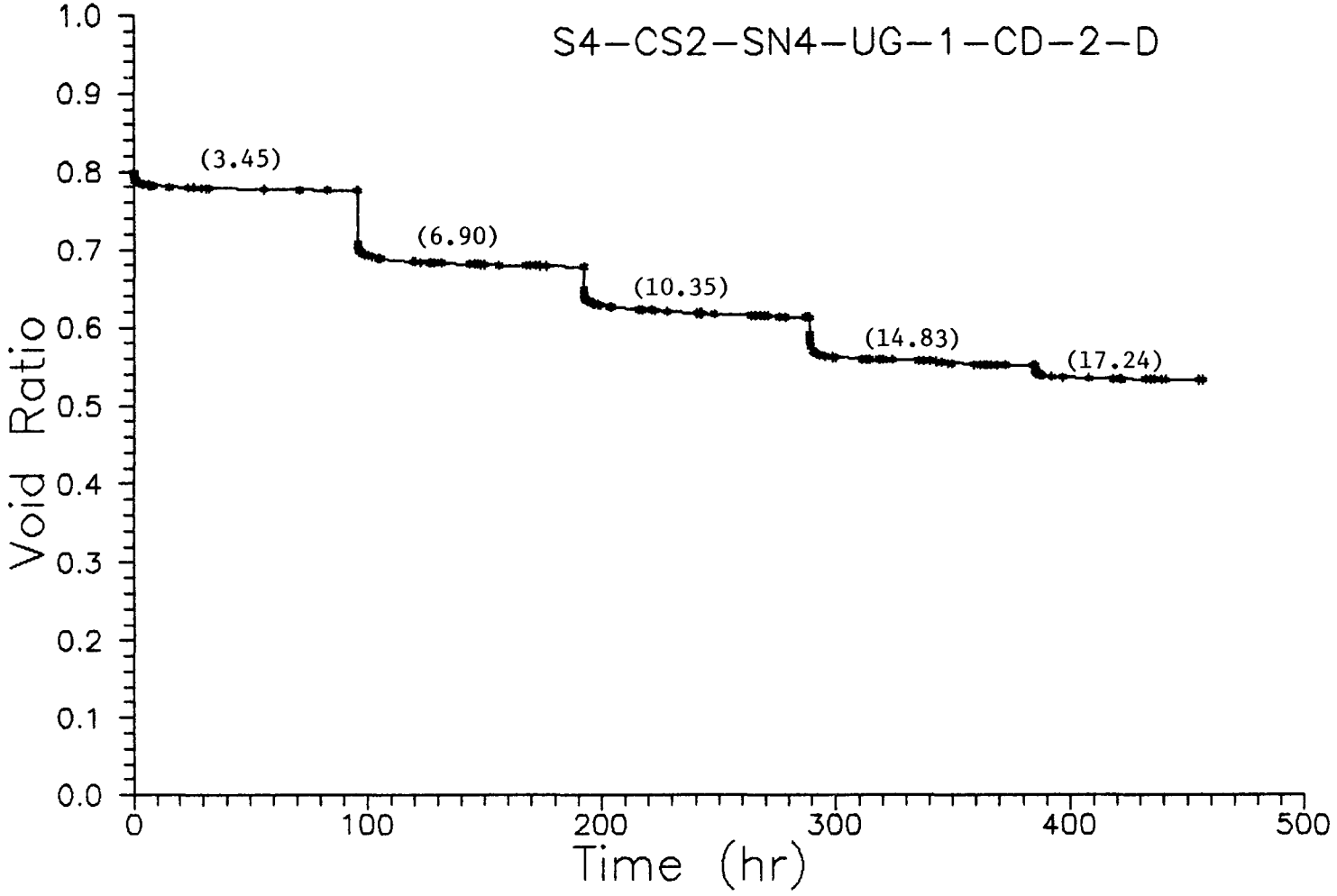

Figure 3.7 Uniaxial strain quasi-static consolidation of uniform-graded crushed salt. Sample S4-CS2-SN4-UG-1-CD-2-D. Particle sizes range from 0.841 to 0.419 mm, air-dried. Numbers in parentheses indicate the applied quasi-static axial stress in MPa.

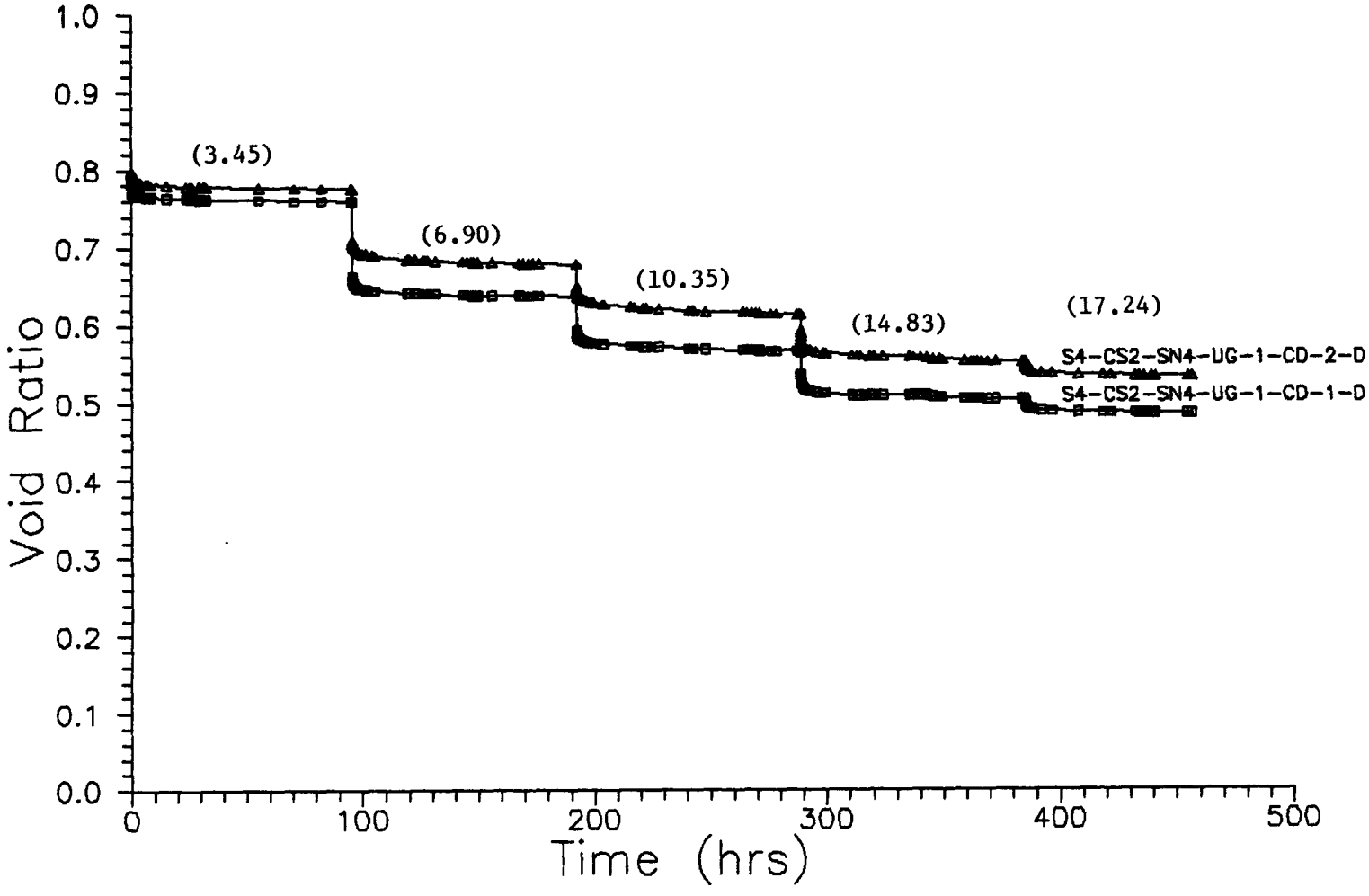

Figure 3.8 Uniaxial strain quasi-static consolidation of uniform-graded crushed salt. Samples S4-CS2-SN4-UG-1-CD-1-D and S4-CS2-SN4-UG-1-CD-2-D. The former has particle sizes ranging from 2.36 to 2.00 mm, the latter from 0.841 to 0.419 mm, air-dried. Numbers in parentheses indicate the applied quasi-static axial stress in MPa.

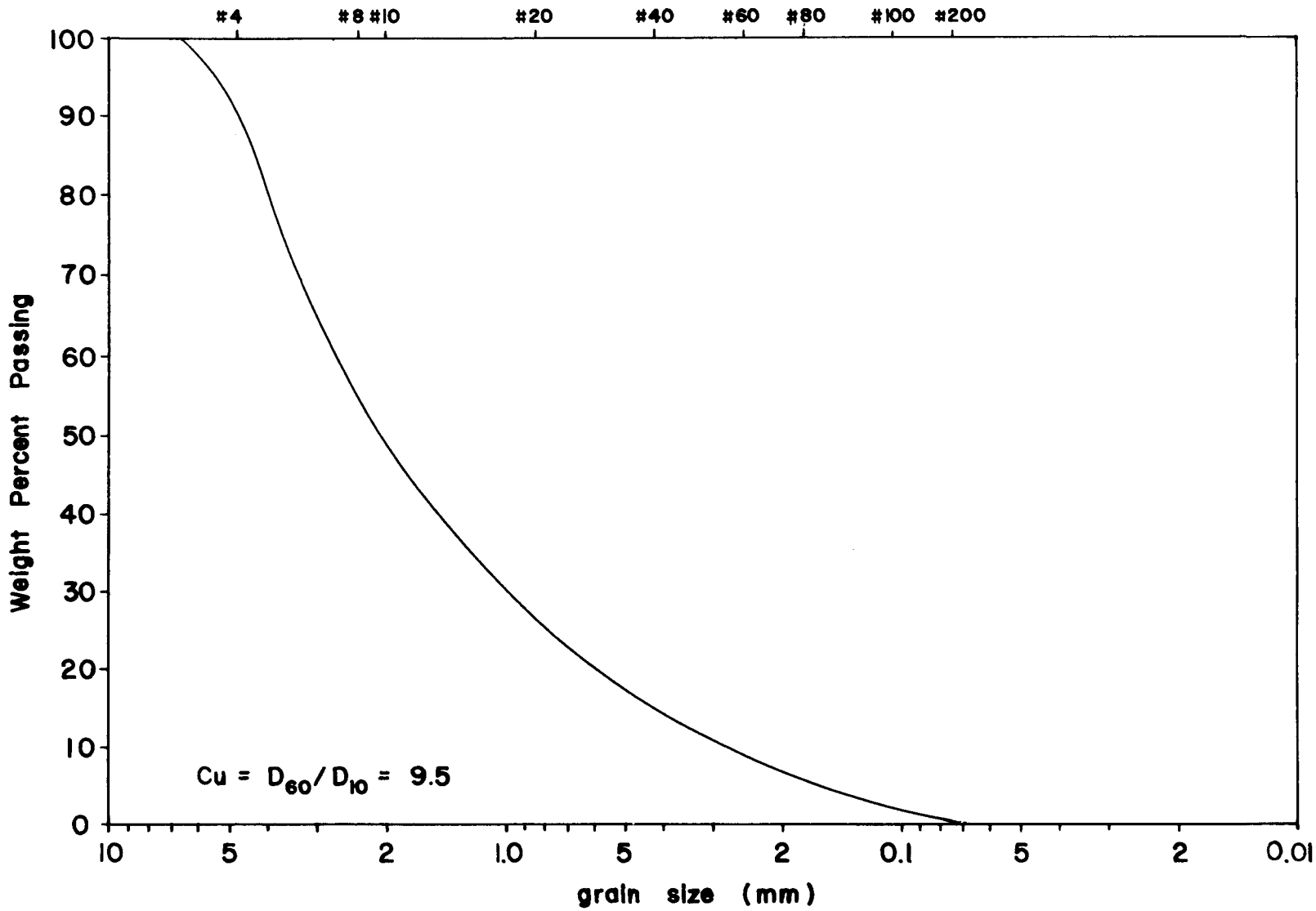

Figure 3.9 Grain size distribution of crushed salt samples S4-CS2-SN3-WG-4-CD-1-D and S4-CS2-SN3-WG-4-CD-2-W. This distribution is similar to that of the "Fine Sample" obtained from the WIPP site (IT Corporation, 1984, Fig. 2-1).

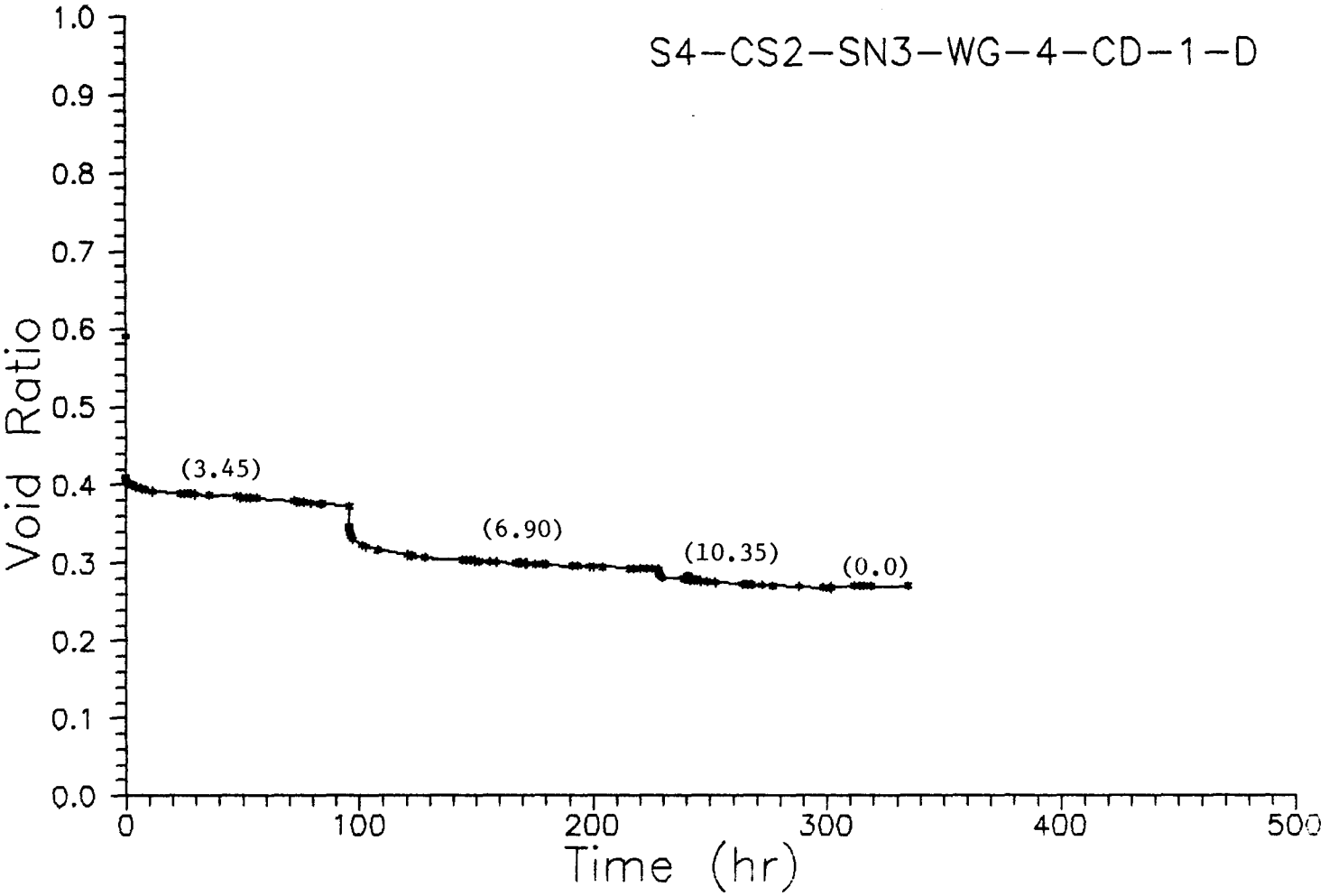

Figure 3.10 Uniaxial strain quasi-static consolidation of well-graded crushed salt sample S4-CS2-SN3-WG-4-CD-1-D (101.6 mm in diameter), with 0.2% brine content. Numbers in parentheses indicate the applied quasi-static axial stress in MPa.

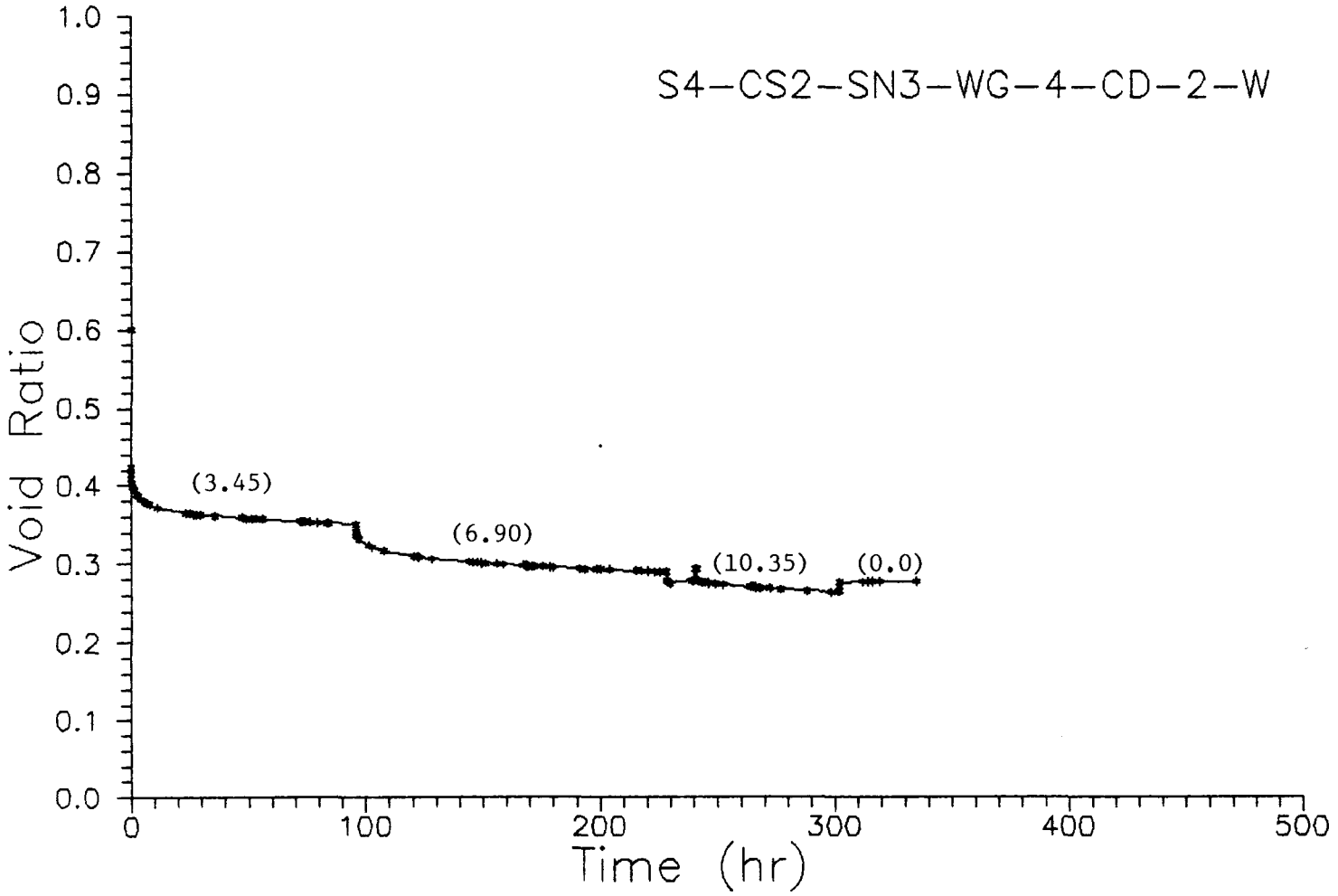

Figure 3.11 Uniaxial strain quasi-static consolidation of well-graded crushed salt sample S4-CS2-SN3-WG-4-CD-2-W (101.6 mm in diameter), with 1.75% brine content. Numbers in parentheses indicate the applied quasi-static axial stress in MPa.

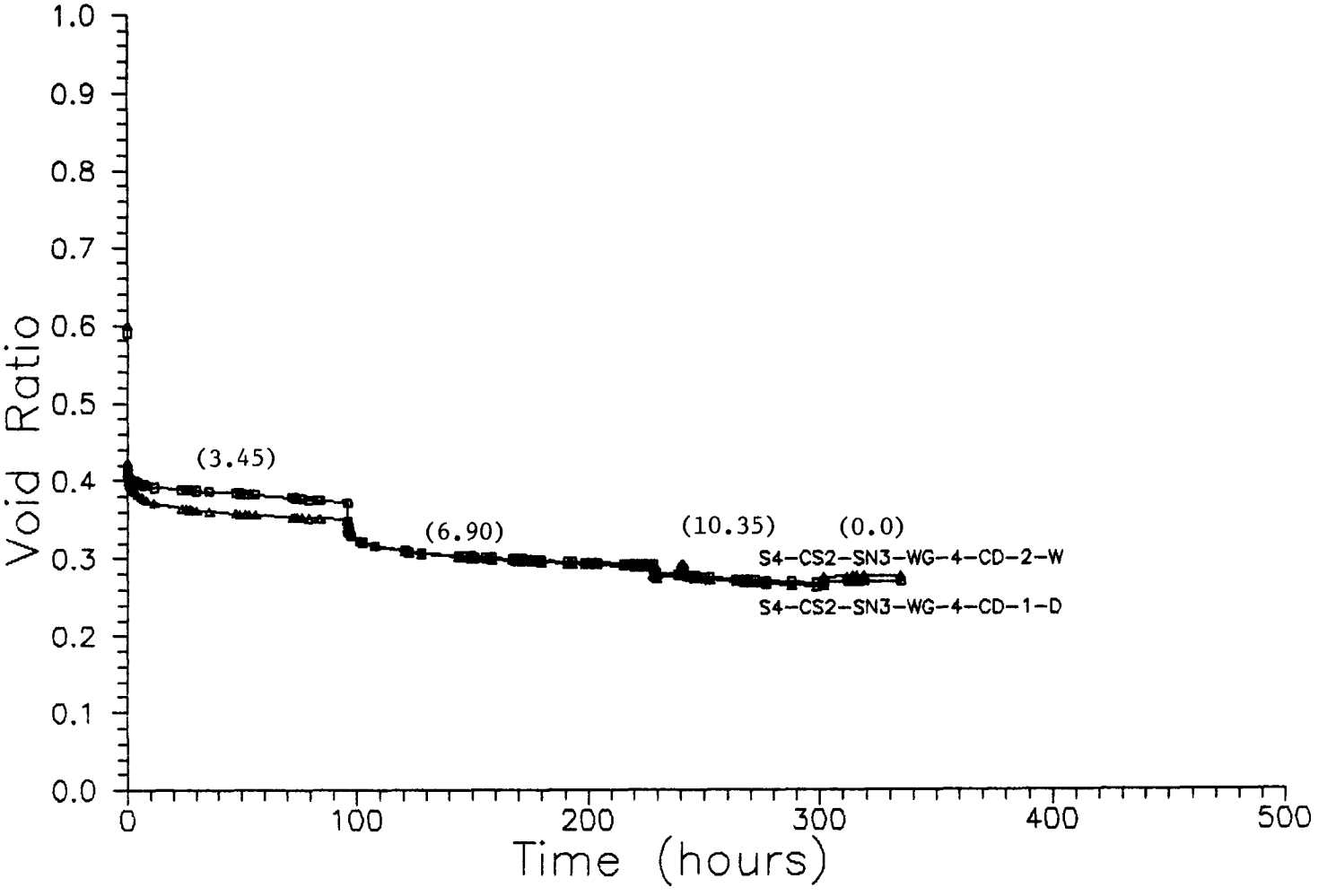

Figure 3.12 Uniaxial strain quasi-static consolidation of well-graded crushed salt samples S4-CS2-SN3-WG-4-CD-1-D and S4-CS2-SN3-WG-4-CD-2-W. Numbers in parentheses indicate the applied quasi-static axial stress in MPa.

the wet sample than for the dry one (Figures 3.10 and 3.11). Both samples remain a solid mass after having been pushed out from the pipes. The consolidated wet sample appears more uniform and homogeneous than the consolidated dry sample and appears to be stronger.

Samples S4-CS2-SN4-UG-1-CD-1-D and S4-CS2-SN4-UG-1-CD-2-D have been pushed out of their containment pipes (25.4 mm in diameter) from the bottom end at the completion of consolidation testing. Contrary to what was expected, neither sample formed an intact mass (Figure 3.13). Very little consolidation occurred in the lower portions of the samples. This was because a ridge had been left on the inner pipe wall when the section within which the piston travels was machined out. The inner surface of the pipes had been smoothed to an extremely fine finish down to 76.2 mm (3 in). This leaves an internal diameter change of approximately 1 mm at a depth of 76.2 mm. The appearance of the two consolidated samples can be interpreted as a result of stress relaxation when the samples were pushed out of the pipes from the bottom end. The cones in the middle and bottom portions most likely indicate that the relatively small pipe wall edge caused considerable disturbance of the consolidation of the salt below the ridge. If this were true, it would suggest that a local stiff inclusion could have a surprisingly significant influence on crushed salt consolidation. The asperity has been removed prior to subsequent testing.

3.7 Quasi-Static Confined Consolidation of Crushed Salt: Series B Tests

Five multistage uniaxial strain consolidation tests were performed on samples with the same initial grain size distribution. The first three tests study the effect of brine content on consolidation. The last two tests examine effects of stress path as well as of the initial void ratio. The results include consolidation curves for each test, in the form of void ratio vs. time. Also reported are the estimated consolidation rates and the extrapolated times to a void ratio of 0.06, at which the consolidated crushed salt is assumed to form an effective barrier to brine and radionuclide migration. Lastly, the results are compared with hydrostatic consolidation results obtained by Holcomb and Shields (1987), and the differences are discussed.

3.7.1 Sample Preparation

Five samples have been constructed using salt crushed from block no. 3 after cores had been drilled from the block. Salt crushing has followed the procedure in Appendix A. All five samples have a designed grain size distribution, with particle size ranging from 0.075 to 6.68 mm and a uniformity coefficient (C_u) of 9.5. This grain size distribution closely follows the distribution of the "Fine Sample" obtained from the WIPP site (IT Corporation, 1984, p. 6, Figure 2-1; Figure 3.9 of this report).

Crushed salt amounts from each size fraction were measured to achieve the designated grain size distribution. The crushed salt was then thoroughly mixed in a plastic pan. A predetermined amount of saturated

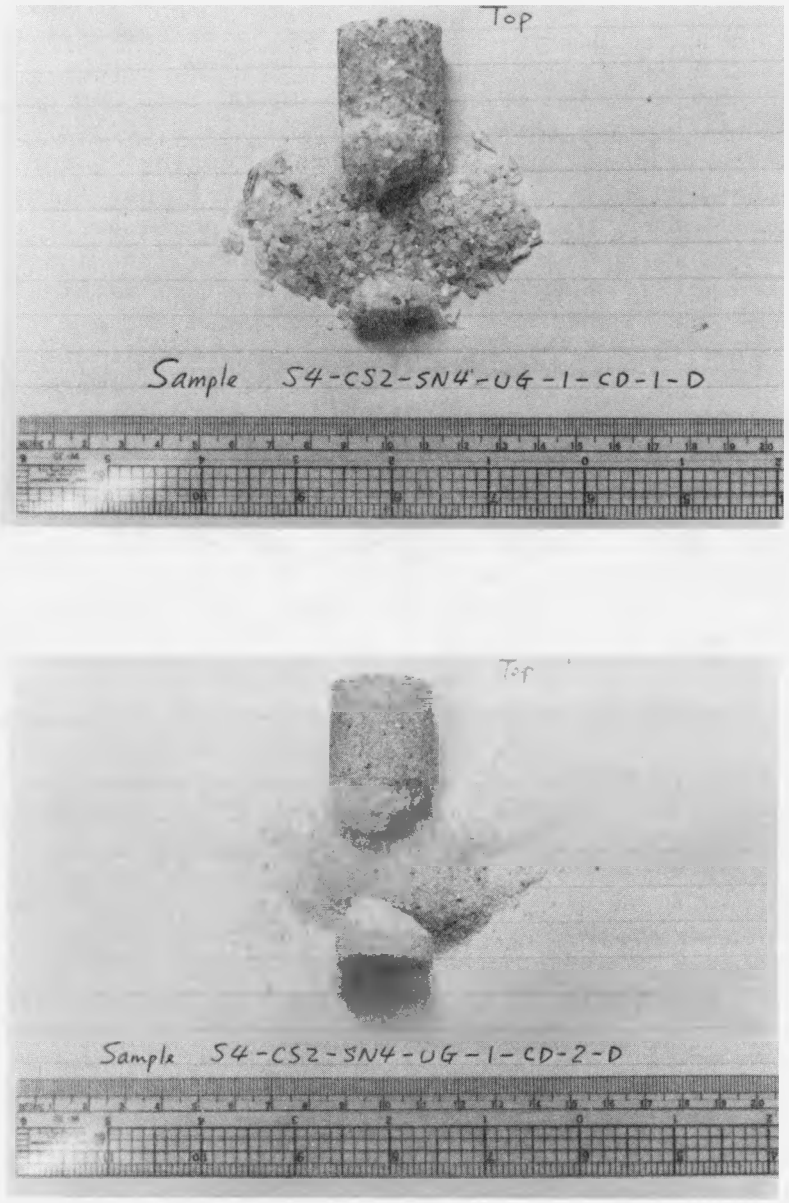

Figure 3.13 Salt samples pushed out of pipe in which they were "consolidated". Influence of peripheral interface pipe diameter change on consolidation is obvious. The cone shapes may indicate a distortion of the samples due to the stress distribution caused by the asperity. Consolidation below pipe diameter decrease was minimal, at best. Both samples are uniform-graded, and 25.4 mm in diameter. Particle size ranges: 2.00-2.36 mm (top), 0.419-0.841 mm (bottom).

brine was sprayed evenly on the crushed salt in three to four applications, each application followed by mixing. The wet crushed salt was transferred into a test chamber using a small shovel. The sample installation follows the method given in the pipe flow testing procedure (Appendix F). As a result of mixing with brine, small salt particles tend to adhere to large particles and the particle segregation effect common during pouring is markedly reduced. Some kneading efforts were applied during installations of samples 4 and 5. The crushed salt prepared for sample construction generally had an excess of 200 to 400 g. The remaining crushed salt was used for the determination of brine content.

Table 3.6 gives sample number, dimensions, brine content, and initial void ratio. Sample number designation for Test Series B contains the following information: number of salt block from which testing material is obtained (S3 - salt block no. 3), material characteristics (CS - crushed salt), sample diameter (inches), type of experiment (CD - consolidation), and test number of the experiment. The test number will be used for identification purposes.

3.7.2 Test Procedures

The multistage uniaxial strain consolidation testing follows the pipe flow test procedure (Appendix F) with omission of steps for sample saturation and permeability testing, except for sample 3, which was saturated. All five tests were performed under drained conditions.

In consolidating wet crushed salt in pipes under drained conditions, prevention of loss of moisture to the atmosphere is crucial. Consolidating a wet sample in a closed system [i.e. undrained condition, or unvented (Holcomb and Hannum, 1982)] would be an obvious solution. However, in undrained consolidation testing, the compressed air leak (if any) from the pneumatic loading system may cause a build-up of pore pressure within a crushed salt sample and complicate its consolidation behavior. Even in a leakproof system, this may be the explanation for the observation by Holcomb and Hannum (1982, p. 13) that samples consolidated unvented showed considerably higher compressibilty and did not form a coherent mass. Drained consolidation is therefore performed. It is recognized that unvented testing may be equally representative, necessary and productive, depending on the conditions subsequent to emplacement in repository excavations. To minimize the loss of sample moisture, a U-shaped tygon tubing, the horizontal portion of which was filled with 2 to 4 cc saturated brine, was connected to the bottom outlet of the sample holder. A small amount of hydraulic oil was injected into the tubing to protect the saturated brine from direct contact with the atmosphere. The liquids (oil and brine) in this buffer zone can move inside the tubing to make room for the air expelled from the pore space due to consolidation. This expelled air volume can be measured and compared to the pore volume reduction of a sample. The moisture state of the crushed salt sample under consolidation should be protected from evaporation by the buffer zone and remain relatively constant throughout the test. Upon the application of axial pressure, the displacement of the crushed salt sample was recorded with time.

Table 3.6 Crushed Salt Consolidation Sample Dimensions and Characteristics: Test Series B

Sample Number	Sample Diameter (mm)	Initial Sample Length (mm)	Brine Content[a] (percent by weight %)	Initial Void Ratio
S3-CS-4-CD-1	102.87	97.79	2.10 (2.16)	0.735
S3-CS-4-CD-2	102.87	97.18	3.47 (4.01)	0.775
S3-CS-4-CD-3	102.87	98.04	8.79[b]	0.773
S3-CS-4-CD-4	102.41	121.08	2.69 (3.06)	0.613
S3-CS-4-CD-5	102.46	121.08	2.91 (3.06)	0.620

[a]Determination of the brine content of crushed salt samples follows the procedure given in Appendix E. The calculated moisture content was translated into brine content, assuming that the solubility of salt in water at the testing temperature of 21°C is 40%. The number in parentheses indicates the brine content calculated based on the amount of brine (weight) sprayed during sample preparation.

[b]This sample was initially brine-saturated. Upon loading, water evaporated due to gas leakage through the piston seal.

All five tests were conducted in the same room, at a mean temperature of 20.5°C ± 1.5°C. The relative humidity of the room air varied from 47 to 58%, typically around 50%. Each axial pressure was maintained through a regulating valve. The "constant" pressure fluctuates by about 7%. This variation is likely due to friction of the piston seal (South and Daemen, 1986, p. 88), or lack of sensitivity of the pressure regulator, or changes in temperature. The number of pressure steps, axial pressure and duration can be found in Table 3.7.

3.7.3 Results

Results of the five consolidation tests on wet crushed salt samples are summarized in Table 3.7. The changes of void ratio with time are depicted in Figures 3.14 through 3.23. They are expressed in two forms: void ratio vs. time (in hours) and void ratio vs. the logarithm of time (in minutes). The consolidation under each pressure step is treated as an individual subtest and is therefore presented as a separate curve. The creep consolidation of the crushed salt generally gives a linear relation between void ratio and the logarithm of time over the first two logarithmic cycles of time. Deviations from this linear relationship become apparent as time increases (Figures 3.15, 3.17, 3.19 3.21 and 3.23). Around the fourth logarithmic cycle of time, the linear relation appears re-established. This may indicate that the logarithmic creep behavior is confined to certain time intervals, suggesting that the combined effect of the changing stresses at grain contacts and the corresponding deformational responses renders a linear relation between void ratio and the logarithm of time. Similar observations have been reported in the creep behavior of Cretaceous claystone (Feda, 1982, p. 337). Sudden changes in the consolidation rate can be seen in the plots. This behavior is more conspicuous when the vertical scale (i.e. void ratio) is enlarged (Figure 3.24). Similar results have been observed during observed during creep consolidation of clay and chalk (Lo, 1961; Suklje, 1969, as referred to in Feda, 1982). This phenomenon may be attributable to structure collapses of a particulate system under constant loading (Feda, 1982, p. 337-338).

A compressed air leak along the piston of the pneumatic loading system has been detected for the first three tests. One immediate result was that initially saturated sample 3 dried out, at least partially. The tests were continued by continuously supplying compressed nitrogen air. A severe leak was observed for sample 3 when the axial pressure was incremented from the initial 2.07 MPa to 4.14 MPa. This test was discontinued approximately 9 hours later due to a large pressure drop in the source tank. The brine content of this sample was subsequently determined to be 8.79%.

Constitutive models for crushed salt consolidation have been developed by Ratigan and Wagner (1978), Zeuch et al. (1985, the hot-pressing model), and Shor et al. (1981, the sintering model). These models are often found inapplicable to other experimental results (Sjaardema and Krieg, 1987, for the first two models and Baes et al., 1983, for the third model). The simple, linear relation between void ratio (or volume strain) and the logarithm of time, as well recognized in soil

Table 3.7 Results of the Multistage Uniaxial Consolidation Tests on Wet Crushed Salt Samples: Test Series B

Sample Number	Brine Content (%)	Pressure Step	Consolidation Pressure (MPa)	Duration (hours)	Void Ratio[a]	Fractional Density[a]
S3-CS-4-CD-1	2.10	1	2-2.14	404.9	0.7352-0.4522	0.5763-0.6886
		2	4-4.17	365.8	0.4522-0.4054	0.6886-0.7116
		3	6.03-7.17	473.8	0.4054-0.3547	0.7116-0.7382
S3-CS-4-CD-2	3.47	1	2-2.14	404.9	0.7748-0.4484	0.5634-0.6904
		2	4-4.17	365.8	0.4484-0.3958	0.6904-0.7165
		3	6.03-7.17	473.8	0.3958-0.3329	0.7165-0.7502
S3-CS-4-CD-3	8.79	1	2-2.14	404.9	0.7727-0.3363	0.5641-0.7483
		2	4-4.14	8.9[b]	0.3363-0.3301	0.7483-0.7519
S3-CS-4-CD-4	2.69	1	6.79-7.31	353.5	0.6127-0.3047	0.6201-0.7665
			9.97-10.38	409.4	0.3047-0.2790	0.7665-0.7819
S3-CS-4-CD-5	2.91	1	3.31-3.83	354.8	0.6196-0.3792	0.6174-0.7251
		2	6.45-7.41	410.4	0.3792-0.3369	0.7251-0.7480

[a]The first number indicates the starting value (void ratio or fractional density), the second number indicates the ending value. Fractional density is defined as the ratio between the sample density and the salt density (2.16 g/cc).

[b]A significant compressed air leak was caused by a failure of the piston rod seal. The experiment was discontinued.

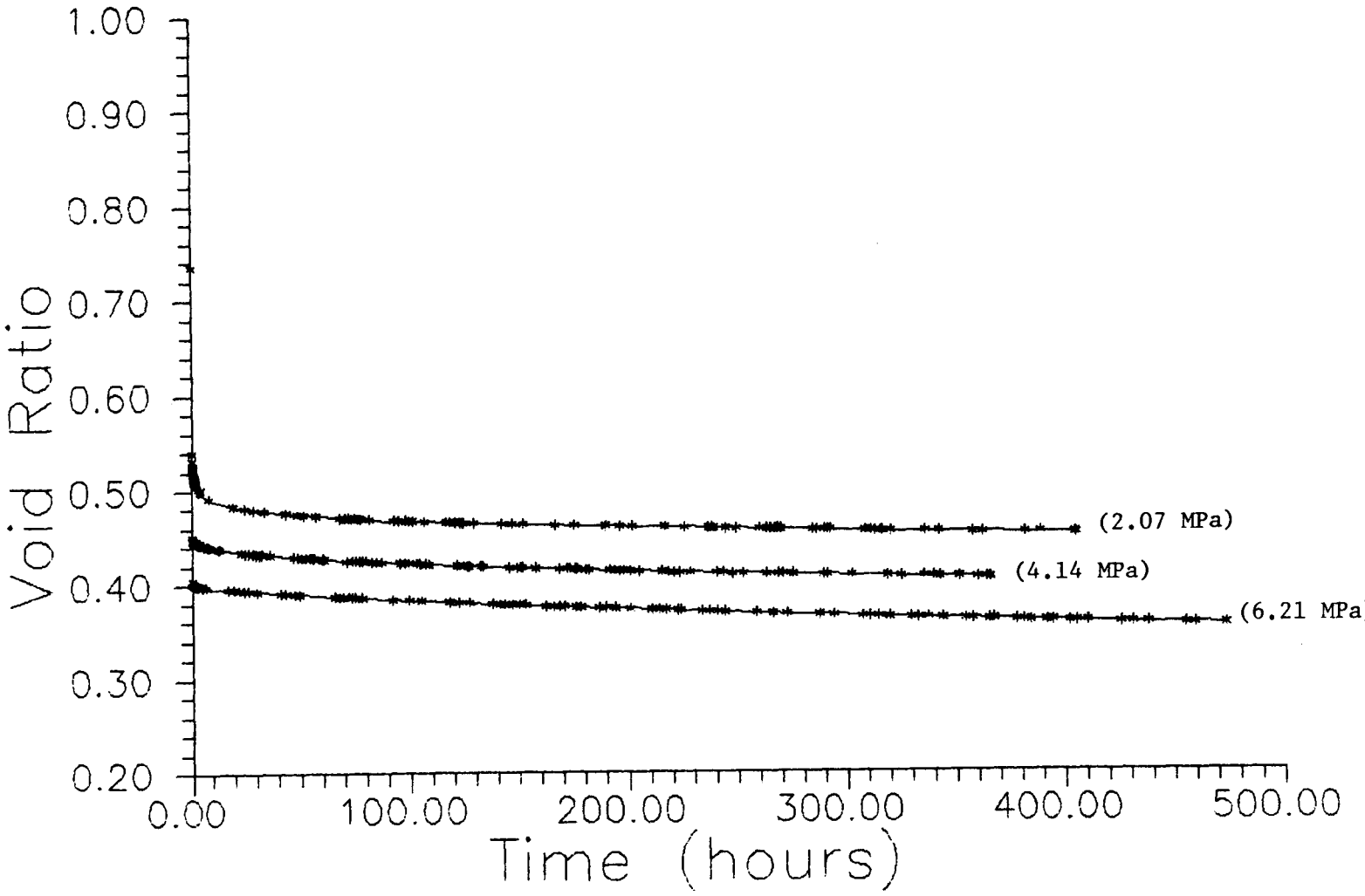

Figure 3.14 Sample S3-CS-4-CD-1 void ratio as a function of time.

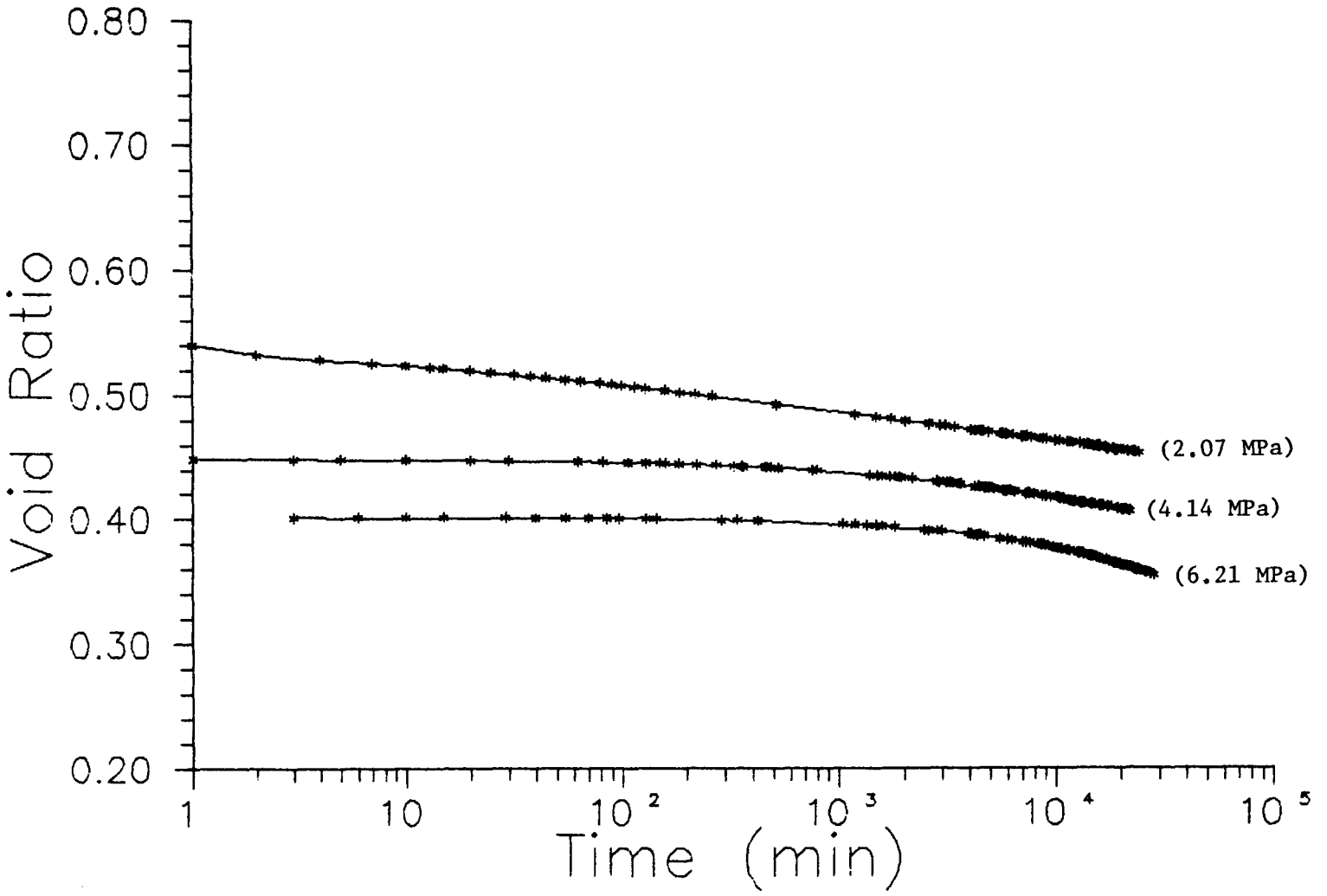

Figure 3.15 Sample S3-CS-4-CD-1 void ratio as a function of the logarithm of time.

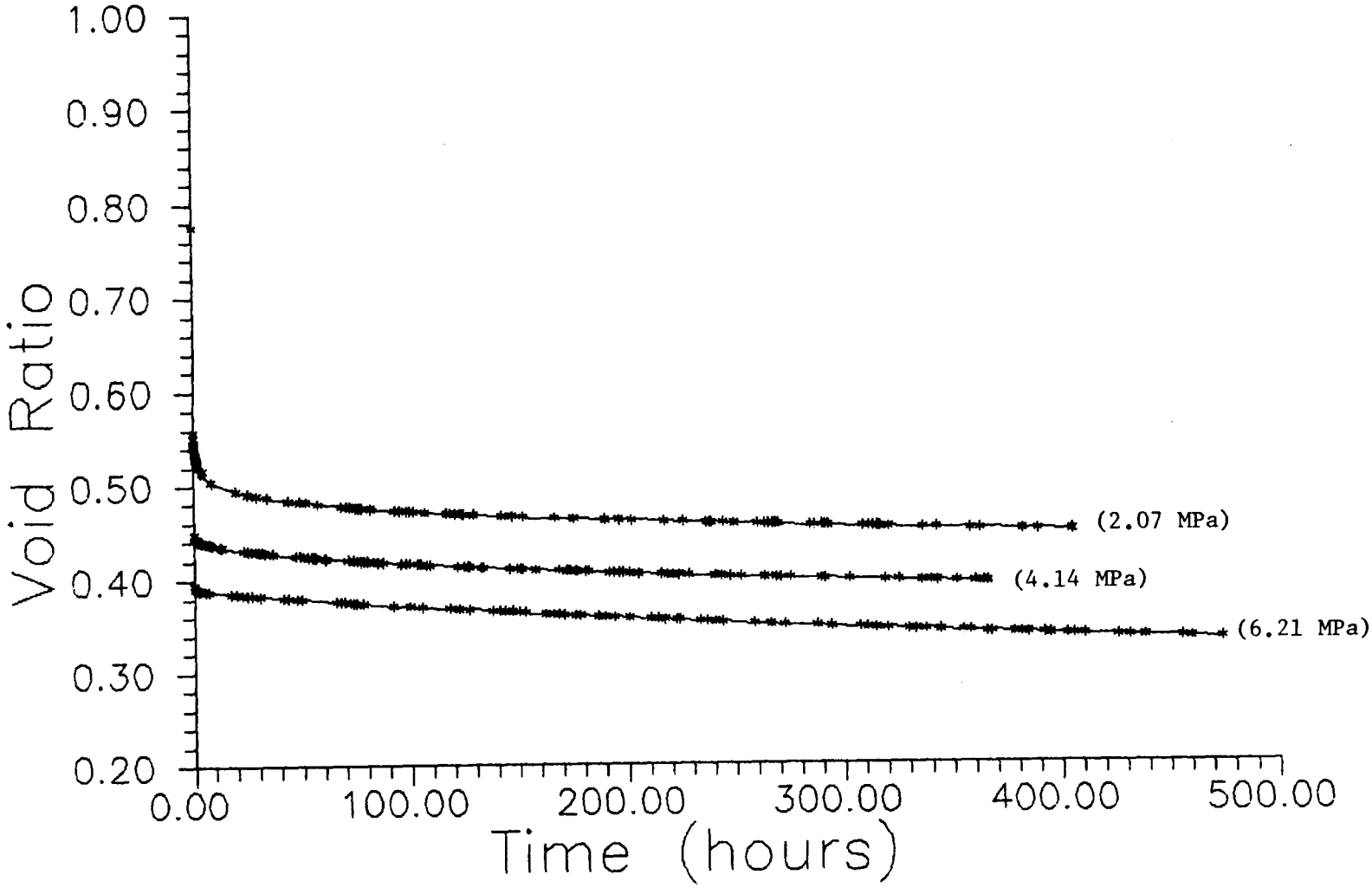

Figure 3.16 Sample S3-CS-4-CD-2 void ratio as a function of time.

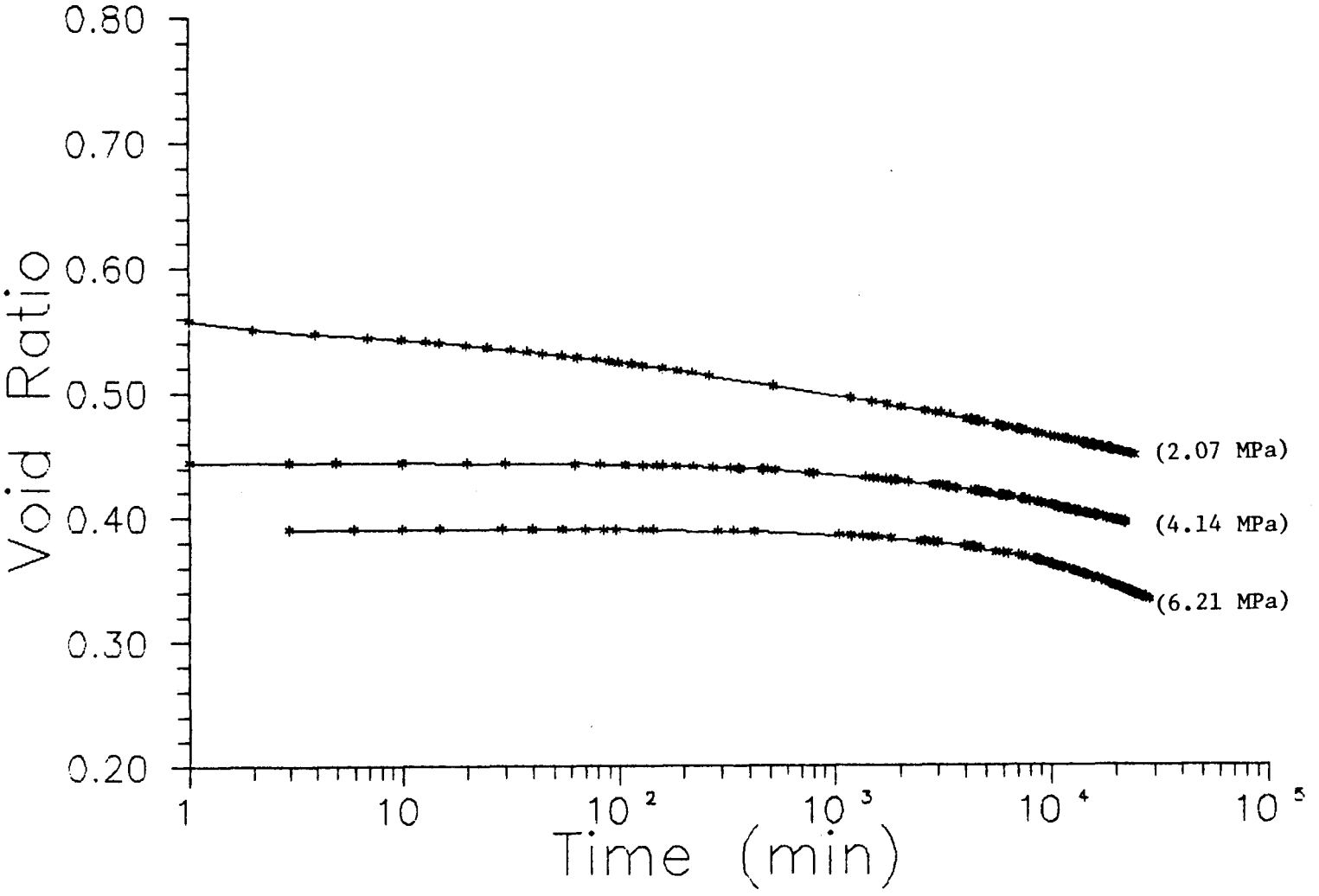

Figure 3.17 Sample S3-CS-4-CD-2 void ratio as a function of the logarithm of time.

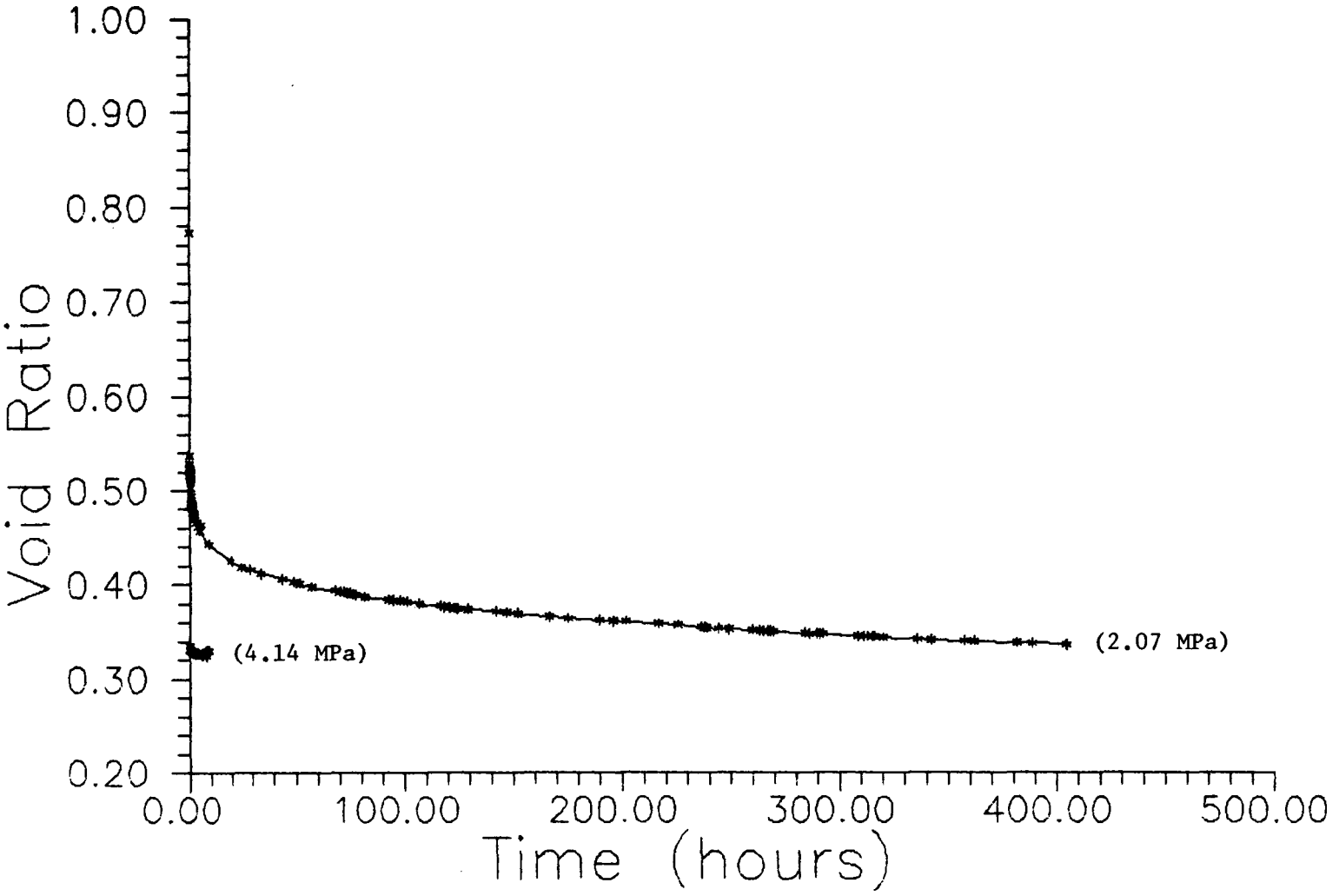

Figure 3.18 Sample S3-CS-4-CD-3 void ratio as a function of time.

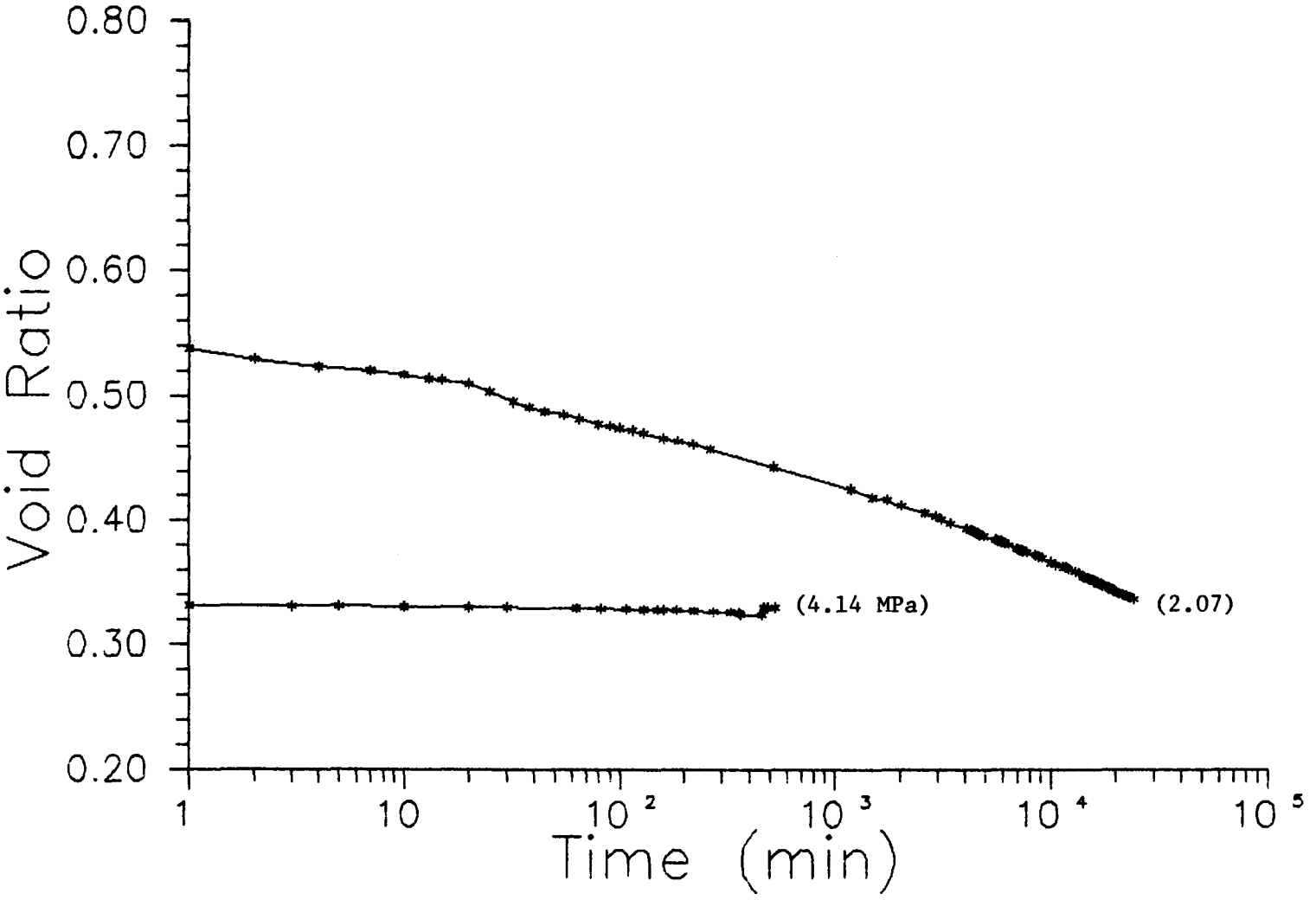

Figure 3.19 Sample S3-CS-4-CD-3 void ratio as a function of the logarithm of time.

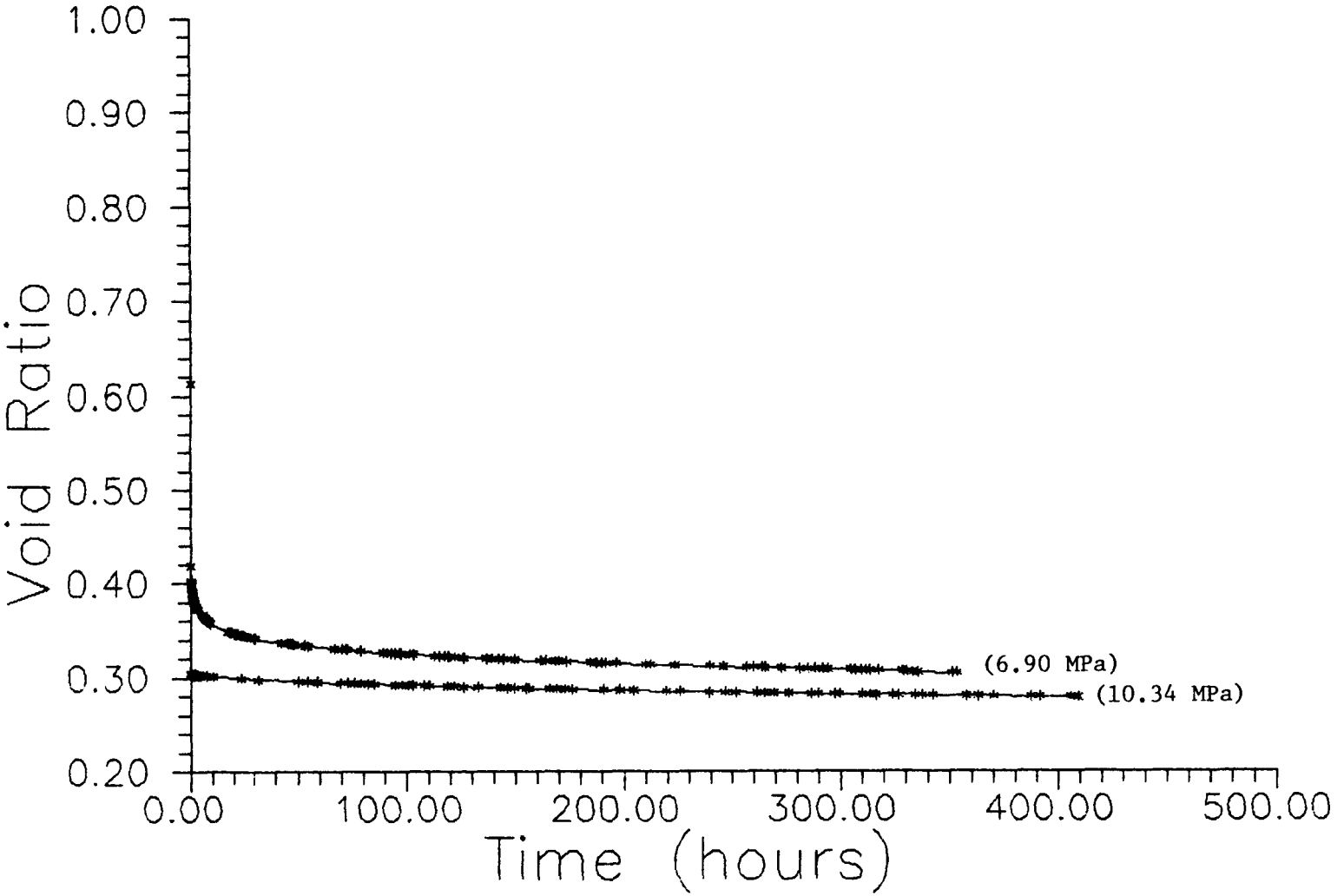

Figure 3.20 Sample S3-CS-4-CD-4 void ratio as a function of time.

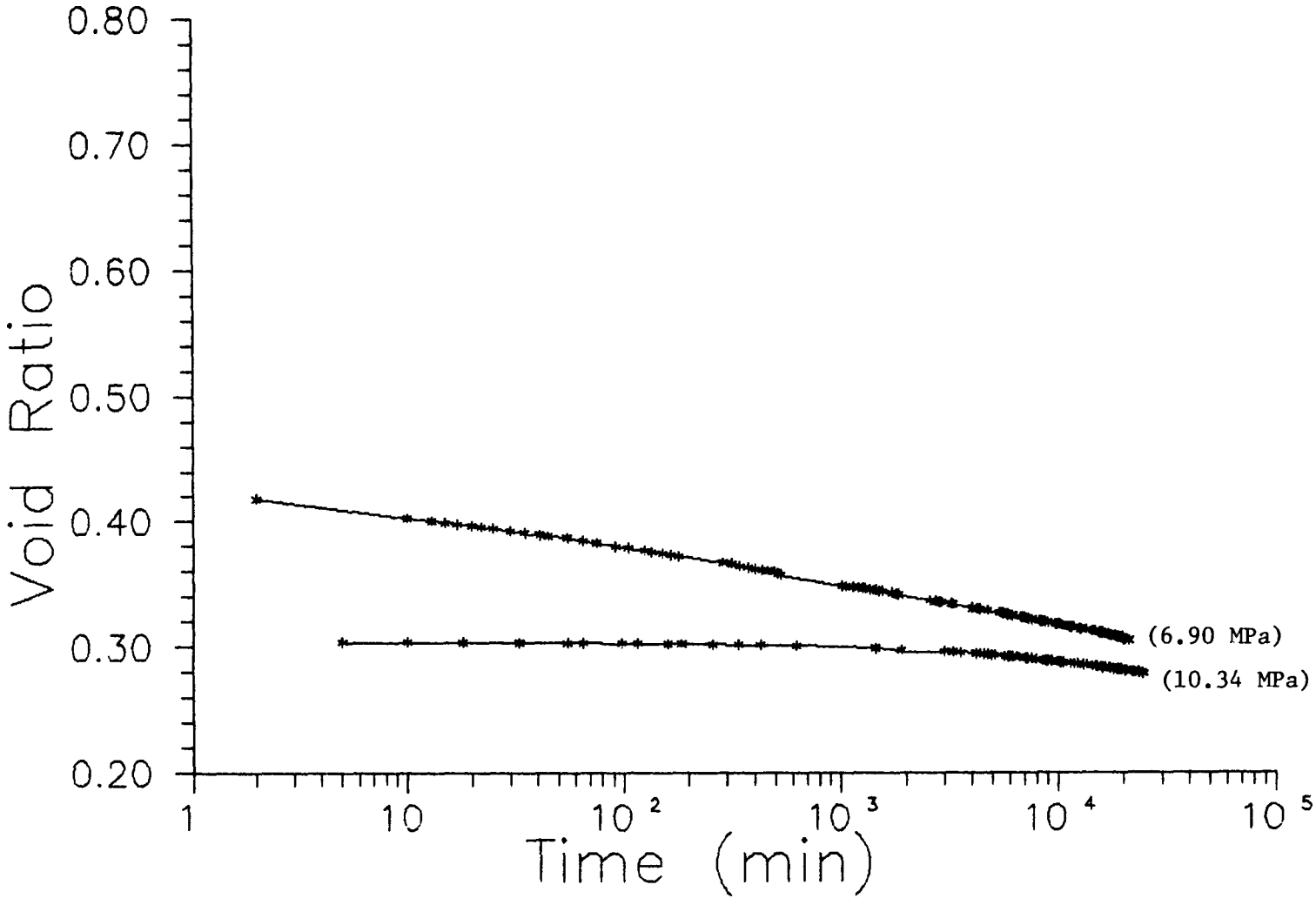

Figure 3.21 Sample S3-CS-4-CD-4 void ratio as a function of the logarithm of time.

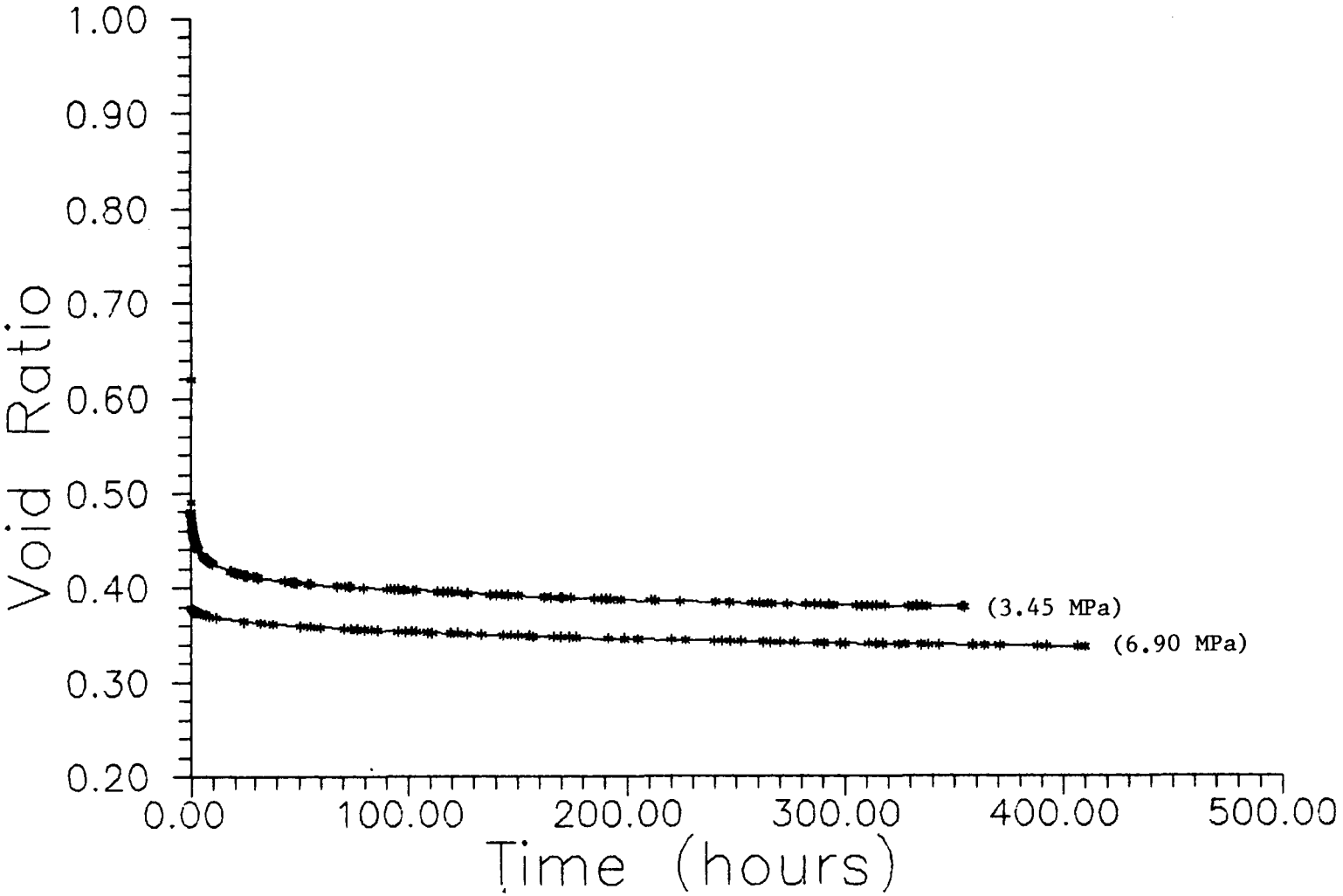

Figure 3.22 Sample S3-CS-4-CD-5 void ratio as a function of time.

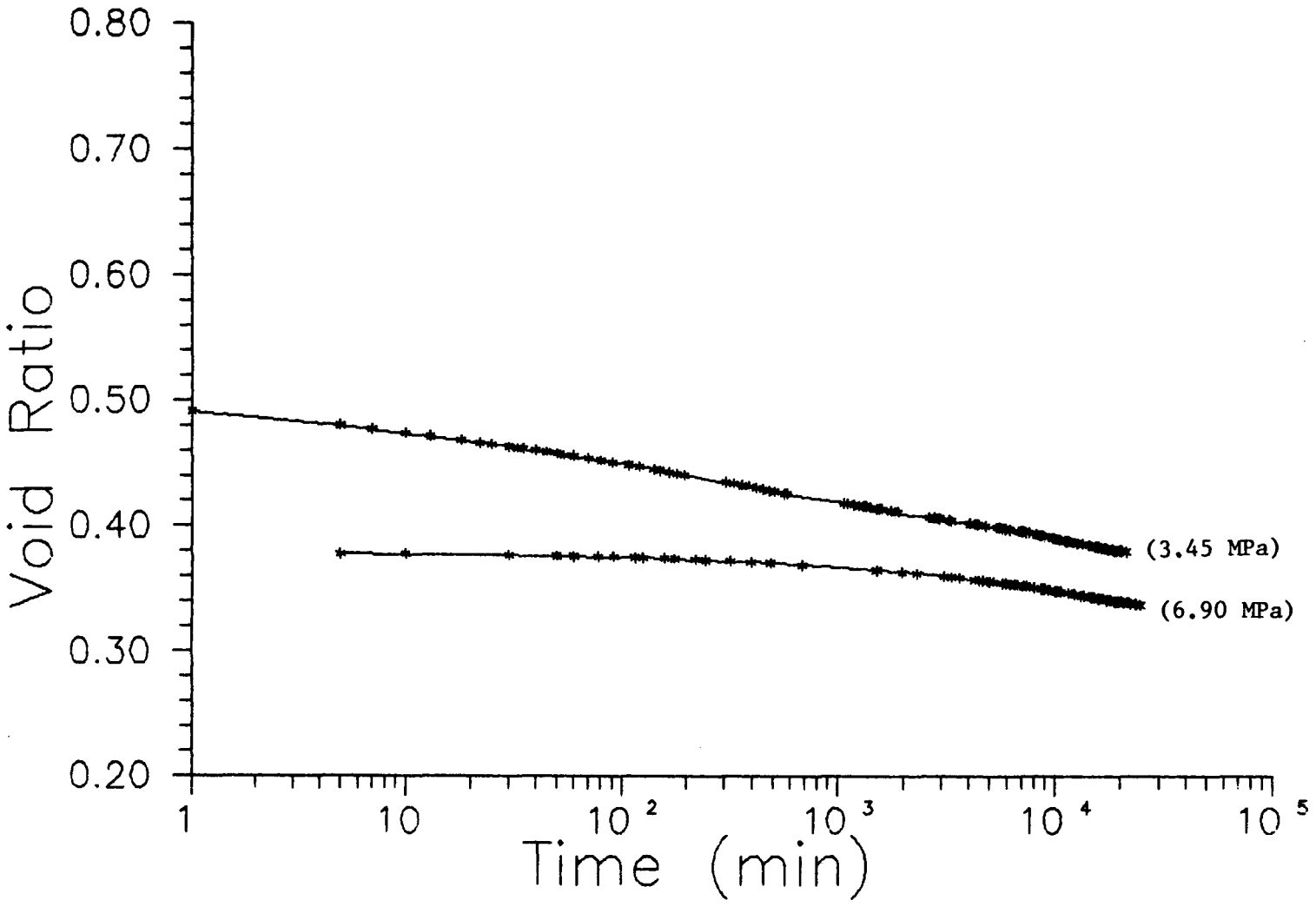

Figure 3.23 Sample S3-CS-4-CD-5 void ratio as a function of the logarithm of time.

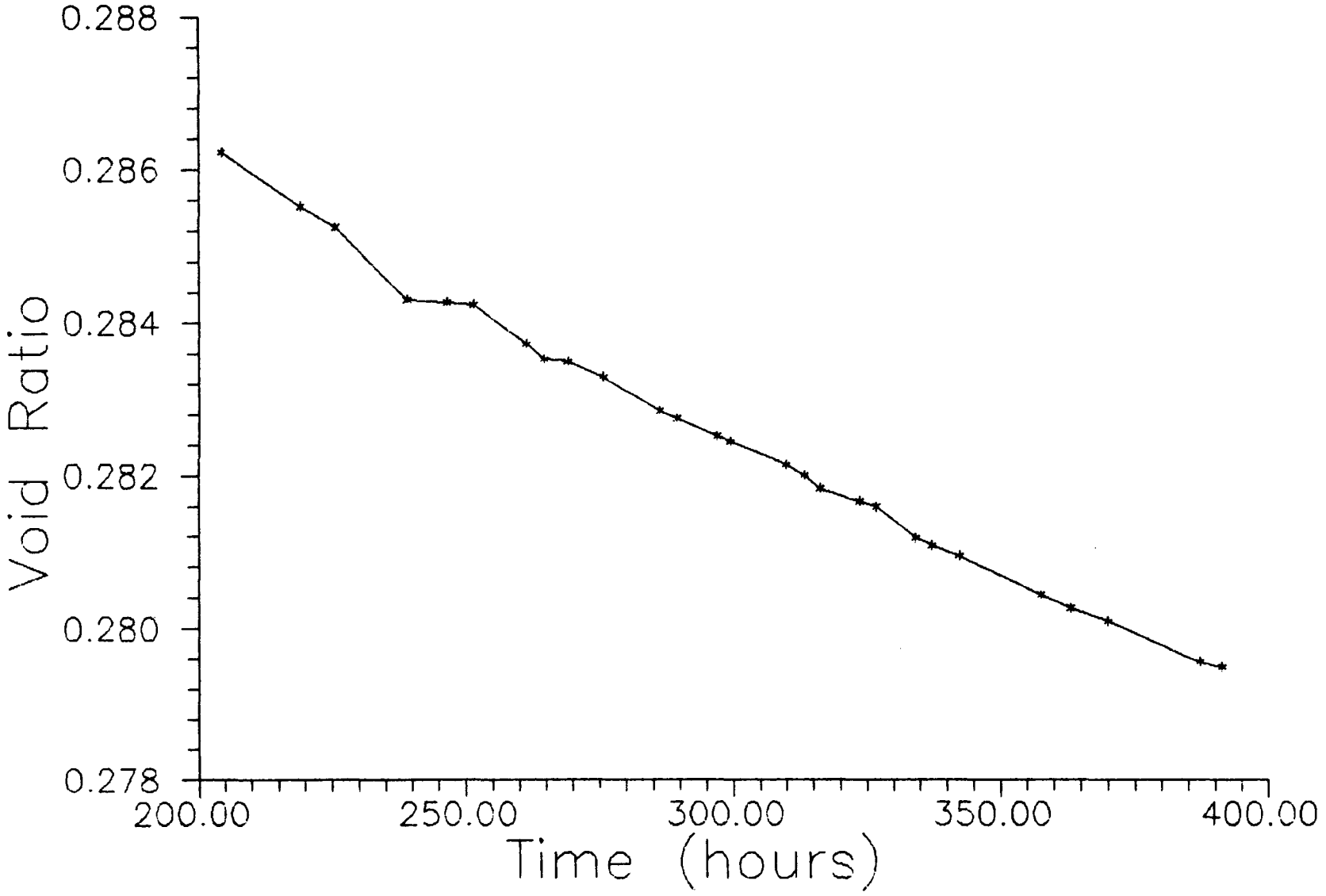

Figure 3.24 Enlarged view of void ratio reduction with time for part of the consolidation test of sample S3-CS-4-CD-4.

and rock consolidation studies (Ladd et al., 1977; Feda, 1982, p. 336), has been used to describe crushed salt consolidation (Holcomb and Hannum, 1982; Holcomb and Shields, 1987; Yost and Aronson, 1987; Sjaardema and Krieg, 1987; Holcomb and Zeuch, 1988; also Shor et al., 1981). This empirical relation generally fits the crushed salt consolidation results very well when the early time data is excluded (Holcomb and Hannum, 1982; Holcomb and Shields, 1987). It also is confirmed by a time exponent of virtually -1 obtained by Liedtke and Bleich (1984) by fitting strain rate data. The same approach was adopted here, since the main interest is the long-term crushed salt consolidation. The empirical equation has the form: $e(t) = a - b \log(t)$, where t is time in hours and e(t) is the void ratio at time t. For each axial pressure, five fits were performed on the data sets of the consolidation results after 0, 24, 120, 240 and 300 hours. The fitted values of a and b, and the corresponding coefficient of correlation (R) are presented in Table 3.8. Also given in the table are the extrapolated times (in hours) to e = 0.06, a realistic void ratio for intact rock salt (Kelsall et al., 1984). As shown in Table 3.8, the void ratio prediction generally is good after 120 hours. Considering only those fits with correlation coefficients greater than 0.995, the extrapolated time to e = 0.06 ranges from 9.7×10^{5} to 3×10^{21} hours (110 to 3.4×10^{17} years), typically from 3×10^{6} to 6×10^{13} hours (340 to 6.85 billion years). It indicates that at least a few hundred years may be required for the crushed salt to reconsolidate to an intact state.

The parameter a corresponds to the fitted void ratio at t = 1 hour. Taking the derivative of the empirical equation with respect to time gives the void ratio reduction rate $de/dt = -0.434\ b/t$. The void ratio reduction rate is thus predicted to decrease with time. Parameter b is a measure of the rate. To study the effect of brine content on the consolidation rate, the fitted b values (for data after 120 hours) are plotted against the brine content for the first three tests. Brine content is the only major difference among the three samples. The consolidation rate appears to increase as brine content increases (Figure 3.25). Figure 3.26 shows consolidation rate as a function of axial stress. For samples 1 and 2, the creep rate increases as the axial stress increases. For samples 4 and 5, the creep rate decreases as the pressure increases. Samples 4 and 5 were subjected to initial pressures of 6.9 and 3.445 MPa, respectively, followed by an increment of 3.45 MP. Samples 1 and 2 were subjected to an initial pressure of 2.07 MPa, followed by an increment of 2.07 MPa. It is postulated that the differences in initial loading and in subsequent pressure increments might have led to different sample structures (e.g. grain size, grain size distribution, grain-to-grain contact) or packing states. Different creep responses have been reported for kaoline clay samples having different fabric structures (Krizek et al., 1977). It is believed that the difference is real, rather than an experimental error. The consolidation rates (b values) for Tests 1, 2, 4 and 5 have been plotted against the void ratio range from which the consolidation rate was obtained (Figure 3.27). There seems to exist a transition void ratio above which the consolidation rate increases as the pressure increases and below which the effect diminishes drastically. Similar

Table 3.8 Results of Curve Fitting and Extrapolated Times to Reach e = 0.06

ID Number[a]	Data Used for Curve Fitting	a	b	Coefficient of Correlation (R)	Extrapolated Time (hours)	Extrapolated Time (Years)
1-1	> 0 (hours)	0.50878	0.02091	0.9963	2.89×10^{21}	3.3×10^{17}
	> 24	0.51552	0.02408	0.9991	8.30×10^{18}	9.5×10^{14}
	> 120	0.51920	0.02560	0.9978	8.66×10^{17}	9.9×10^{13}
	> 240	0.52249	0.02694	0.9917	1.47×10^{17}	1.7×10^{13}
	> 300	0.51421	0.02369	0.9818	1.48×10^{19}	1.7×10^{15}
1-2	> 0 (hours)	0.44626	0.01304	0.9279	4.22×10^{29}	4.2×10^{29}
	> 24	0.47311	0.02584	0.9946	9.74×10^{15}	1.1×10^{12}
	> 120	0.48383	0.03045	0.9984	8.31×10^{13}	8.3×10^{13}
	> 240	0.48748	0.03189	0.9958	2.53×10^{13}	2.9×10^{9}
	> 300	0.49980	0.03675	0.9818	9.28×10^{11}	1.1×10^{8}
1-3	> 0 (hours)	0.40282	0.01356	0.8952	1.94×10^{25}	2.2×10^{21}
	> 24	0.44834	0.03355	0.9773	3.77×10^{11}	4.3×10^{7}
	> 120	0.47778	0.04563	0.9963	1.43×10^{9}	1.6×10^{5}
	> 240	0.49406	0.05204	0.9994	2.19×10^{8}	2.5×10^{4}
	> 300	0.49392	0.05199	0.9985	2.22×10^{8}	2.5×10^{4}
2-1	> 0 (hours)	0.52438	0.02730	0.9915	1.03×10^{17}	1.2×10^{13}
	> 24	0.54370	0.03622	0.9992	2.25×10^{13}	2.6×10^{9}
	> 120	0.54888	0.03839	0.9991	5.44×10^{12}	6.2×10^{8}
	> 240	0.55753	0.04187	0.9997	7.62×10^{11}	8.7×10^{7}
	> 300	0.55511	0.04093	0.9999	1.25×10^{12}	1.4×10^{8}

Table 3.8 Results of Curve Fitting and Extrapolated Times to Reach e = 0.06--Continued

ID Number[a]	Data Used for Curve Fitting	a	b	Coefficient of Correlation (R)	Extrapolated Time (hours)	Extrapolated Time (Years)
2-2	> 0 (hours)	0.44335	0.01515	0.9162	2.02×10^{25}	2.3×10^{21}
	> 24	0.47980	0.03247	0.9929	8.51×10^{12}	9.7×10^{8}
	> 120	0.49630	0.03955	0.9992	1.07×10^{11}	1.2×10^{7}
	> 240	0.49709	0.03988	0.9955	9.12×10^{10}	1.0×10^{7}
	> 300	0.50200	0.04186	0.9987	3.62×10^{10}	4.1×10^{6}
2-3	> 0 (hours)	0.39390	0.01674	0.8836	8.83×10^{19}	1.0×10^{16}
	> 24	0.45580	0.04390	0.9732	1.04×10^{9}	1.2×10^{5}
	> 120	0.49809	0.06126	0.9975	1.42×10^{7}	1.6×10^{3}
	> 240	0.51685	0.06864	0.9989	4.53×10^{6}	5.2×10^{2}
	> 300	0.51996	0.06984	0.9989	3.85×10^{6}	4.4×10^{2}
3-1	> 0 (hours)	0.47981	0.05112	0.9907	1.63×10^{8}	1.9×10^{4}
	> 24	0.52329	0.07106	0.9984	3.31×10^{6}	3.8×10^{2}
	> 120	0.53629	0.07651	0.9985	1.68×10^{6}	1.9×10^{2}
	> 240	0.54918	0.08174	0.9986	9.66×10^{5}	1.1×10^{2}
	> 300	0.52253	0.07138	0.9985	3.02×10^{6}	3.4×10^{2}
4-1	> 0 (hours)	0.38193	0.02868	0.9852	1.67×10^{11}	1.9×10^{7}
	> 24	0.39275	0.03398	0.9992	6.19×10^{9}	7.1×10^{5}
	> 120	0.39785	0.03615	0.9973	2.22×10^{9}	2.5×10^{5}
	> 240	0.41331	0.04238	0.9783	2.17×10^{8}	2.5×10^{4}
	> 300	0.46025	0.06105	0.9667	3.60×10^{6}	4.1×10^{2}

Table 3.8 Results of Curve Fitting and Extrapolated Times to Reach e = 0.06--Continued

ID Number[a]	Data Used for Curve Fitting	a	b	Coefficient of Correlation (R)	Extrapolated Time (hours)	Extrapolated Time (Years)
4-2	> 0 (hours)	0.30475	0.00795	0.9196	6.17×10^{30}	7.0×10^{26}
	> 24	0.32844	0.01849	0.9873	3.29×10^{14}	3.7×10^{10}
	> 120	0.33778	0.02240	0.9990	2.51×10^{12}	2.9×10^{8}
	> 240	0.34174	0.02399	0.9976	5.56×10^{11}	6.3×10^{7}
	> 300	0.34676	0.02596	0.9991	1.11×10^{11}	1.3×10^{7}
5-1	> 0 (hours)	0.45331	0.02851	0.9982	6.24×10^{13}	7.1×10^{9}
	> 24	0.45830	0.03094	0.9977	7.50×10^{12}	8.6×10^{8}
	> 120	0.46621	0.03434	0.9990	6.76×10^{11}	7.7×10^{7}
	> 240	0.45761	0.03085	0.9954	7.77×10^{12}	8.9×10^{8}
	> 300	0.44151	0.02443	0.9638	4.12×10^{15}	4.7×10^{11}
5-2	> 0 (hours)	0.37957	0.01453	0.9626	1.00×10^{22}	1.1×10^{18}
	> 24	0.40334	0.02510	0.9951	4.76×10^{13}	5.4×10^{9}
	> 120	0.41136	0.02847	0.9999	2.20×10^{12}	2.5×10^{8}
	> 240	0.41353	0.02933	0.9997	1.13×10^{12}	1.3×10^{8}
	> 300	0.41284	0.02906	0.9994	1.39×10^{12}	1.6×10^{8}

[a]The first number represents the test number, which is the last digit shown in the sample number in Table 3.7; the second digit indicates the pressure step.

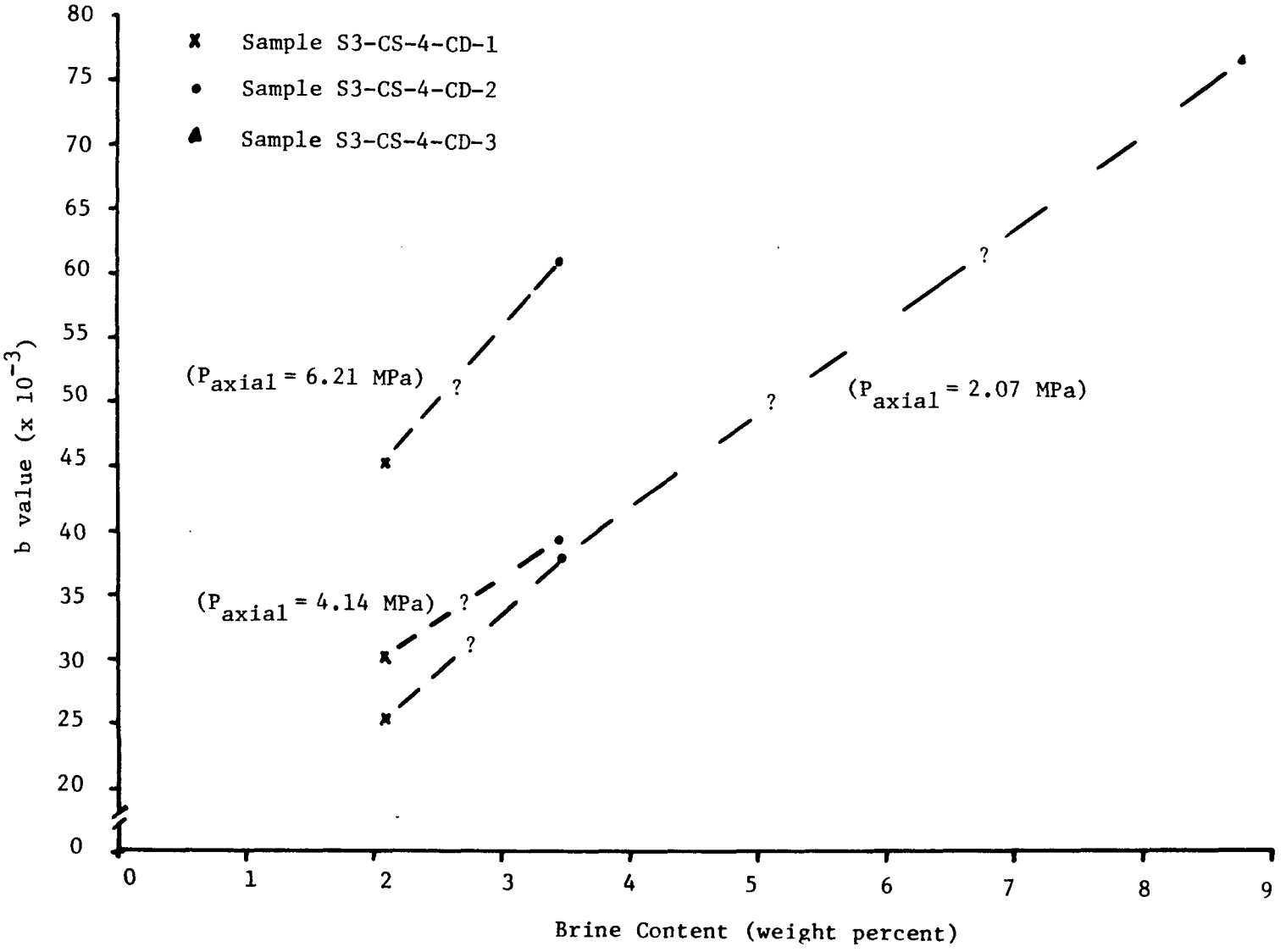

Figure 3.25 Consolidation rates (b) as a function of brine content.

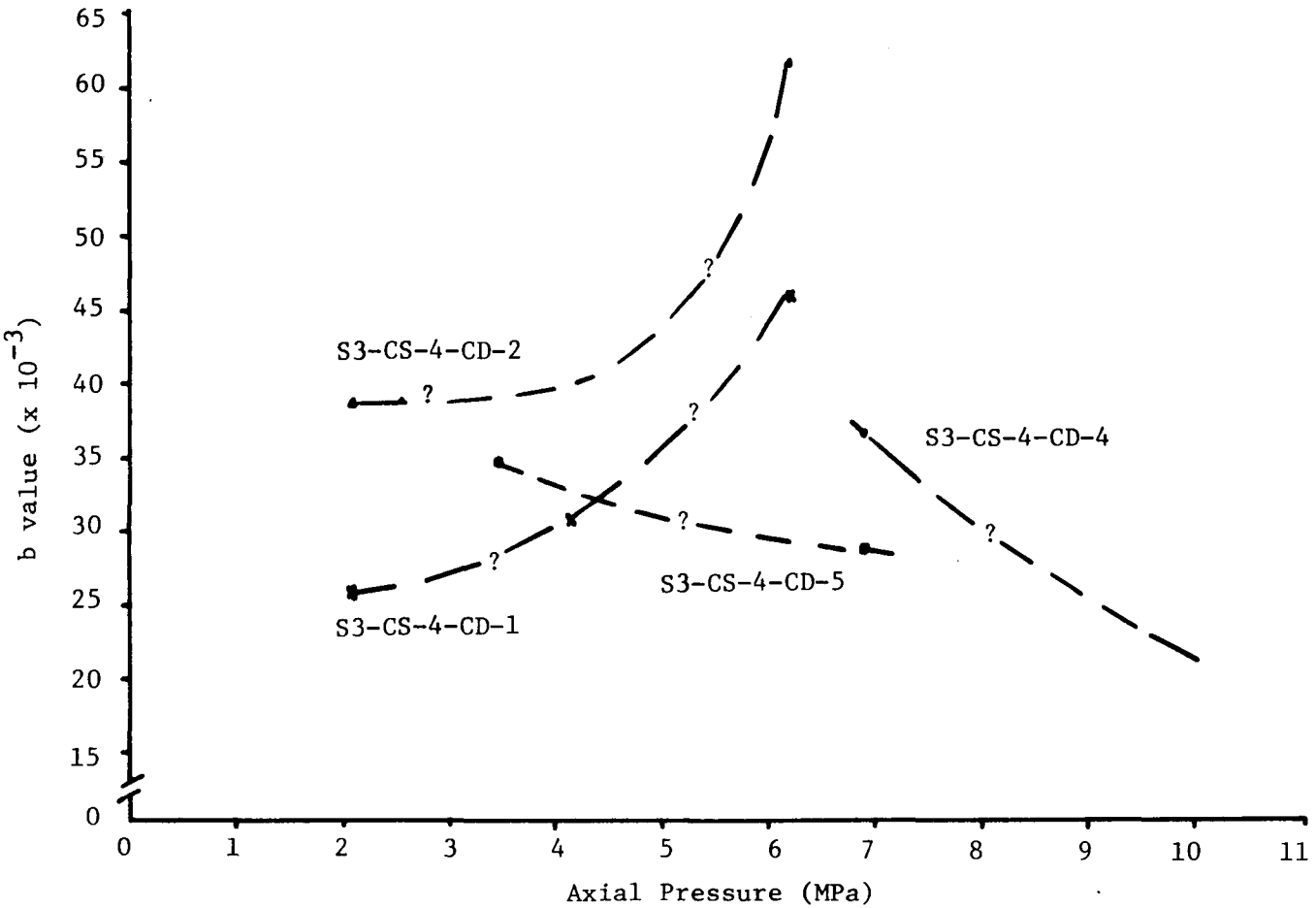

Figure 3.26 Consolidation rates (b) as a function of axial pressure.

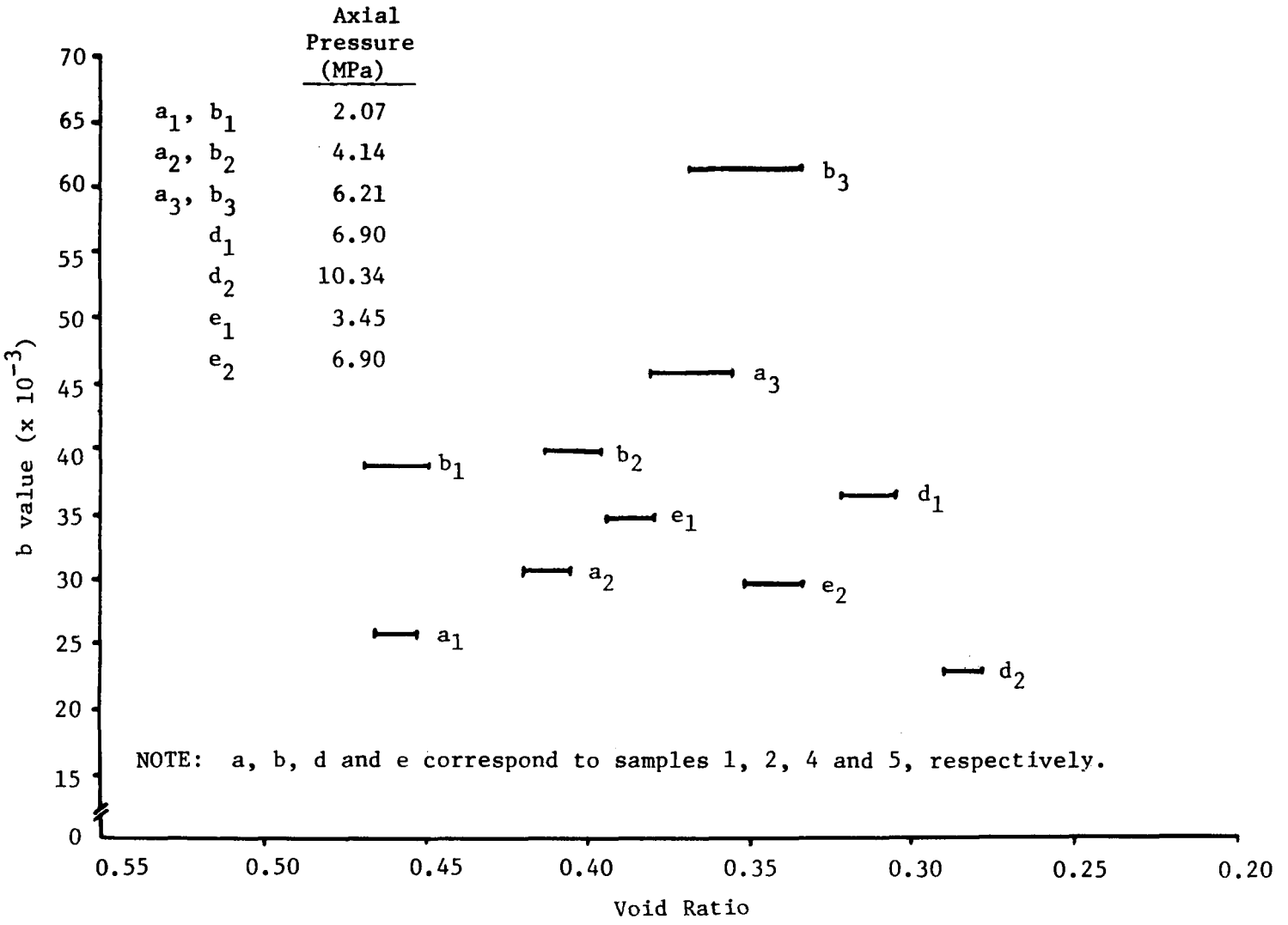

Figure 3.27 **Consolidation rates (b) as a function of void ratio. The line segments indicate the void ratio range from which the corresponding b value was obtained (i.e. after 120 hours and before the next pressure increment).**

behavior is found in the effect of consolidation stress on the compression index for clay samples (Mesri and Godlewski, 1977).

3.7.4 Discussion

The stress dependency of the creep rate is important in constitutive modeling of crushed salt consolidation. Intuitively, one would expect that the creep rate should increase with axial pressure. However, this dependency is often obscured and complicated by concurrent structural effects. Considering the steady-state and isothermal case, the creep rate (b) of crushed salt may be expressed as a simple function of the consolidation stress (p), i.e.:

$$b = c\ p^n \tag{3.1}$$

a form analogous to the reduced expression of potential laws for salt creep under the same conditions (Fuenkajorn and Daemen, 1988, Ch. 2, p. 45). Given two consolidation stresses and corresponding creep rates, Eq. (3.1) can be rewritten as:

$$b_1/b_2 = (p_1/p_2)^n \tag{3.2}$$

The stress exponent (n) can then be calculated if the stress ratio (p_1/p_2) and the creep ratio (b_1/b_2) are known. The stress ratio, the corresponding creep rate ratio (for data after 120 hours), and the resulting stress exponent are given in Table 3.9 for samples 1 and 2. The stress exponent varies from 0.1 to near 1. However, for both tests, the consolidation during the last two pressure steps only accounts for a void ratio reduction of 0.1, as compared to the total reduction of approximately 0.4 (see Table 3.7). If the structure collapse effect is assumed to be minimal for the last two consolidation pressure steps and can be neglected, the stress exponent near 1 may represent the real stress dependency of the crushed salt creep rate within the test conditions.

The creep rates obtained from the five uniaxial strain consolidation tests decrease more rapidly with time than those obtained from the hydrostatic consolidation tests by Holcomb and Shields (1987). Major differences exist in test configuration and the resulting boundary stress state. In the hydrostatic consolidation, the isotropic boundary stresses are three-dimensionally active. In the uniaxial strain consolidation, only the axial stress is active. The lateral stresses remain passive and are due to the semi-rigid confinement. It is postulated that pore reduction processes such as grain breakage, intergranular sliding, and intragranular gliding are more effective in three dimensions for the hydrostatic loading than for the laterally restrained, uniaxial loading. Pore reduction and creep rate are thus expected to be higher in hydrostatic consolidation than in uniaxial strain consolidation.

In the tests as performed here, frictional interaction between the pipe and the crushed salt may reduce consolidation.

Table 3.9 Results of Calculations of Stress Exponent for Samples 1 and 2

Sample Number	P_1 (MPa)	b_1	P_2 (MPa)	b_2	P_3 (MPa)	b_3
1	2.07	0.02560	4.14	0.03045	6.55	0.04563
2	2.07	0.03839	4.14	0.03955	6.55	0.06126

Sample Number	P_2/P_1	b_2/b_1	Stress Exponent	P_3/P_1	b_3/b_1	Stress Exponent	P_3/P_2	b_3/b_2	Stress Exponent
1	2	1.189	0.25	3.16	1.782	0.51	1.58	1.500	0.89
2	2	1.030	0.10	3.16	1.596	0.41	1.58	1.549	0.95

P is the axial consolidation pressure. b is the void ratio reduction rate obtained from the curve fitting for consolidation data collected after 120 hours. The subscript corresponds to the pressure step.

Differences in sample preparation and installation may contribute to the difference in creep rates. In Holcomb and Shields' tests, the crushed salt was first divided into eight portions and each fraction was poured individually into a cylindrical cell, each time followed by the addition of a small amount of distilled water. Our procedure requires that saturated brine be added to the crushed salt before installation. Based on our observations, it is considered likely that particle segregation occurs during pouring in dry conditions. Segregation would lead to more structural anisotropy for Holcomb and Shield's samples. There is evidence that clay samples of anisotropic structure deform faster than those of isotropic structure (Krizek et al., 1977). The same effect might occur in consolidating crushed salt samples of different structure.

The accelerated creep of wet salt samples has been linked to the theories of the Joffe effect and the enhanced pressure solution (Stokes et al., 1960; Varo and Passaris, 1977; De Boer, 1977; Holcomb and Shields, 1978; Jenyon, 1986; Yost and Aronson, 1987). If the stress exponent of nearly 1 (Table 3.9) is realistic, it implies that the enhanced pressure solution may be the dominant mechanism for the increased creep rate of wet crushed salt (Holcomb and Shields, 1987). The Joffe effect describes increased plastic behavior due to the change in fracture behavior of solids brought about by the elimination of surface defects in a solvent. It is postulated that adding saturated brine to a crushed salt sample would have little effect in terms of removing surface defects when compared to adding distilled water. Additionally, the slow creep rates obtained from our tests might have resulted from the overload hardening effect (Wawersik and Preece, 1984) as the intended "constant" applied axial stress actually fluctuates by about 7%. The measured creep rate thus would be lower than it should be if the pressure were kept truly constant.

There is a concern that crushed salt backfill could become brine-saturated during long-term consolidation (Nowak and Stormont, 1987). It is conceivable that once reconsolidating crushed salt saturates, further reductions in void ratio and thus in permeability are impeded by the low compressibility of entrapped brine. Assuming permeabilities of 10^{-6} to 10^{-8} darcy for mine-disturbed zones, Bredehoeft (1988) calculated that a brine-saturated condition in the unbackfilled WIPP salt repository may be expected within 50 to 30,000 years. This time would be much less if the repository were backfilled. Should this be true, studies on crushed salt consolidation under saturated conditions obviously may be warranted.

3.8 Unconfined Compressive Strength of Consolidated Crushed Salt

Strength of consolidated crushed salt is important as it is an indicator of the relative ease with which the backfill can be mined, should retrieval of the waste become necessary (Pfeifle et al., 1987). It also is a useful indicator of consolidation and healing. Strength is related to stiffness, and stiffness as a function of time, consolidation, or void ratio, will determine the reaction forces exerted by consolidating backfill on the converging excavation walls, and thus will influence excavation closure rates. Unconfined

compressive testing is employed as one characterization test for consolidated crushed salt.

Samples S4-CS2-SN3-WG-4-CD-1-D and S4-CS2-SW3-WG-4-CD-2-W remain solid after having been pushed out from the pipes. The former sample (air-dried) has an unconfined compressive strength of 4.5 MPa (650 psi). The latter sample (wet) is preserved for demonstrating a result of crushed-salt consolidation. Strength testing of samples S4-CS2-SN3-UG-1-CD-1-D and S4-CS2-SW3-UG-1-CD-2-D is not possible as they broke while they were pushed out of the pipes (Figure 3.13). Attempts to retrieve sample S4-CS2-SN2-WG-8-CD-1-D failed because the piston tilted and jammed inside the pipe.

3.9 Friction During Consolidation in Pipes

A concern about testing the consolidation of crushed salt in (steel) pipes by means of axial loading is the extent to which friction along the interface between the pipe wall and the salt might reduce the load acting on the salt, as compared to the load acting on the driving piston. This concern is further enhanced by the experimental arrangement. The driving force is maintained by air pressure on the piston, necessitating the installation of O-rings or seals around the piston, in order to minimize airflow through the crushed salt. Early on during testing the concern about friction was dismissed, based on the observation that the driving piston moved readily upon application of an air pressure of about 0.14 to 0.28 MPa (20 to 40 psi), a small fraction of the applied consolidation pressure. It is recognized that the bond strength between the seals and the pipe may increase with time, e.g. if the seals tend to freeze, given the long duraction of these tests. This suspicion may be confirmed by the last line in Table 3.10. The axial stress required to push the last sample listed in the table out of the cylinder dropped by nearly 1 MPa upon removal of the O-ring from the pipe. Table 3.10 also shows that samples for which the driving piston was sealed with metal seals (the first three samples) required significantly lower loads than those for which the piston was sealed with O-rings (last two samples).

The push-out strengths for the first three samples are relatively small compared to the consolidation stresses. During initial consolidation, when the consolidation stresses are lowest, the interface strength is essentially zero. As the crushed salt consolidates, and lateral stresses build up, the interface strength increases, and some of the applied axial load is transmitted in shear to the pipe itself. Hence, the measured axial load overestimates the true consolidation load. Given the small loads required for push-out testing, and the expected exponential load dissipation (Stormont and Daemen, 1983), it is reasonable to assume that most of the sample will be under a relatively uniform load. Clearly, it would be desirable to measure the true load acting on the sample, e.g. by means of strain gages on the pipe, or load cells underneath and within the plugs. Nevertheless, it would be desirable to minimize wall friction.

Table 3.10 Push-Out Loads on Consolidated Crushed Salt

Sample	Peak Axial Stress (MPa)
S4-CS2-SN3-WG-4-CD-1-D	1.19
S4-CS2-SN3-WG-4-CD-2-W	1.29
S3-CS-4-CD-3	0.4
S3-CS-4-CD-4	5.84
S3-CS-4-CD-5	2.8/1.94*

*Dropped from 2.8 to 1.94 MPa when O-ring slipped out of cylinder.

3.10 Summary and Conclusions

Series A tests include four quasi-static consolidation experiments of crushed salt aimed at studying the effects of particle size and brine content. The results of consolidating two air-dried crushed salt samples of different uniform particle size (2.36 - 2.00 mm vs. 0.841 - 0.419 mm) indicate that the sample with larger particle size consolidates more rapidly than the sample of smaller particle size. This is contrary to findings of crushed salt consolidated in brine. Although further testing is needed to resolve the uncertainty, it is possible that the dependency of crushed salt consolidation on particle size may not be significant if the test sample is dry. For two crushed salt samples with the same grain size distribution but different brine content, the wet sample consolidates more rapidly than does the air-dried sample. The consolidation rate of the wet sample decreases with consolidation and with time, but this rate decrease may have been due to inadequate prevention of loss of brine through evaporation. Conversely, the result may suggest the need to assure, for in-situ consolidation, that premature drying, e.g. as a result of thermally induced air convection, does not take place.

Multistage consolidation tests under uniaxial strain conditions are conducted on five wet crushed salt samples. The first three tests confirm that the creep rate of crushed salt appears to increase as the brine content or the axial pressure increases. Quantitative relationships are not developed due to the limited data base. The stress dependency of the crushed salt creep rate may have a stress exponent close to 1. This pressure dependency is obscured for Samples 4 and 5, most likely due to the counteracting structural effect resulting from comparatively large initial loading and subsequent pressure incrementing.

A curve fitting technique is used to fit the consolidation data to the empirical equation: $e(t) = a - b \log t$, where t is time in hours and e(t) is the void ratio. Excluding the first 120 hours data results in an excellent fit, with a coefficient of correlation greater than 0.995. The extrapolated times required for the crushed salt to form an effective barrier (e = 0.06) to ground water and radionuclide migration typically range from 10^6 to 10^{13} hours (i.e. 100 to 1 billion years). Uniaxially consolidating crushed salt in a pipe is a limiting condition, in which the biaxial effect of borehole or shaft closures is simulated by uniaxial creep. A faster creep rate may be expected in situ.

There are indications that the type of fluids added (e.g. whether distilled water or saturated brine) and the structural anisotropy of the sample should be considered in further studies of the consolidation behavior of crushed salt.

3.11 Recommendations

It is clear that more tests are necessary for a better understanding of the consolidation behavior of crushed salt. The following recommendations may be useful to further studies.

(1) The variation of the "constant" pressure applied to consolidate crushed salt should be reduced to minimize the overload hardening effect. Good control of environmental temperature is important.

(2) It is suggested that consolidation tests be conducted on crushed salt samples to which brine or water have been added. The results may help in resolving the uncertainty about the role of the Joffe effect in the enhanced consolidation of wet crushed salt.

(3) Crushed salt samples constructed using different installation methods should be used for studying the effect of structural anisotropy on the consolidation rate. The tests would be most beneficial if the laboratory installation methods closely follow likely field backfilling techniques. A small pressure increment up to the desired constant consolidation pressure should be adopted. This will avoid structural collapses and the resulting significant changes in structural anisotropy, which might be obtained otherwise.

(4) Consolidation and permeability testing of brine-saturated crushed salt samples is necessary for the case of a saturated salt repository.

(5) Study of the creep behavior of irregularly shaped particles subject to point loading is recommended. A crushed salt particle assembly, even when loaded uniformly externally, consists of a large number of particles of various shapes interacting at many discrete points. Optimizing the design of such a backfill, i.e. selecting the appropriate grain size distribution, particle shape, moisture content, etc., involves an exceedingly large range of variables. Similarly, assessing or predicting the consolidation of a given backfill design is difficult in the absence of experimental data for the specific design under consideration. For that reason it would seem desirable to study in more detail the interaction mechanics at the particle level. Such investigations should include experimental work as well as theoretical analyses. They would be aimed at understanding creep of interacting particles, i.e. creep in salt samples subjected to complex loading. Initial experiments and analyses could consist of creep loading of Brazilian (indirect tension) disk type samples, for which the elastic stress distribution is readily available. Performing such experiments would clarify the deformation of creeping salt under combined compression and tension. Results also could be used to assess the validity of salt constitutive models under fundamentally different sets of boundary conditions and test geometries, a basic validation requirement.

(6) Geometrical characterization of the pore space and of the particle contact configuration at various levels of consolidation should assist in identifying particle interaction mechanics. It could be performed by macroscopic and microscopic study of samples cut from a consolidating mass at a range of densities.

CHAPTER FOUR

PIPE FLOW TESTS

4.1 Introduction

Cement, bentonite and crushed salt are proposed sealing materials for salt repository penetrations (boreholes, shafts; e.g. Kelsall et al., 1985a,b,c). The performance (especially the hydraulic conductivity) of the sealing materials needs to be determined in order to allow repository performance assessments, in particular to permit inclusion and evaluation of the influence of seal parameters.

Pipe flow tests are used to study sealing performance. Plugs have a length to diameter ratio of one. This ratio might have to be reduced for large diameter plugs to obtain a measurable outflow in an acceptable time.

Gas permeability testing (nitrogen) is preferred to testing with brine. Advantages may be summarized as: (1) elimination of the likely difficulties resulting from plugging of porous stones and/or screens with salt (Baes et al., 1983), (2) elimination of laborious and always uncertain efforts required to remove air from the sample if a liquid permeant is used, (3) ability to obtain measurable flows without the use of excessive pressures (Muskat, 1946), and (4) minimization of the possible alterations of sample texture or fabrication resulting from dissolution and/or recrystallization.

Pipe flow permeameters of 20 cm (8 in), 10 cm (4 in) and 2.5 cm (1 in) diameter are used to study hydraulic conductivity. Stainless steel 304 has been chosen for construction of the permeameters, primarily due to the cost constraint, as opposed to more corrosion-resistant materials such as Mo, Ni, and Ti-base alloys (Griess, 1982; Short et al., 1981; Ladish Co., 1976, p. 87).

4.2 Pipe Flow Permeameter Design

A pipe flow permeameter consists of a cylindrical chamber, a disk piston, two circular end plates, and bolts and nuts for assemblage. O-rings or PolyPak seals are used wherever sealing is required. All pipe flow permeameters have a similar design except for the dimensions. An assemblage drawing is shown in Figure 4.1. The 20 cm (8 in) permeameter is designed to accept a 28 cm (11 in) long rock specimen. Shorter specimens require a spacing platen or cylinder at the bottom of the test chamber. A nominal axial stress of up to 10 MPa (1500 psi) (with a safety factor of 2.3) may be applied to the sample. Nominal fluid pressure provided by a gas-over-brine pump can go up to 10 MPa (1500 psi) with a F.S. of 3.7.

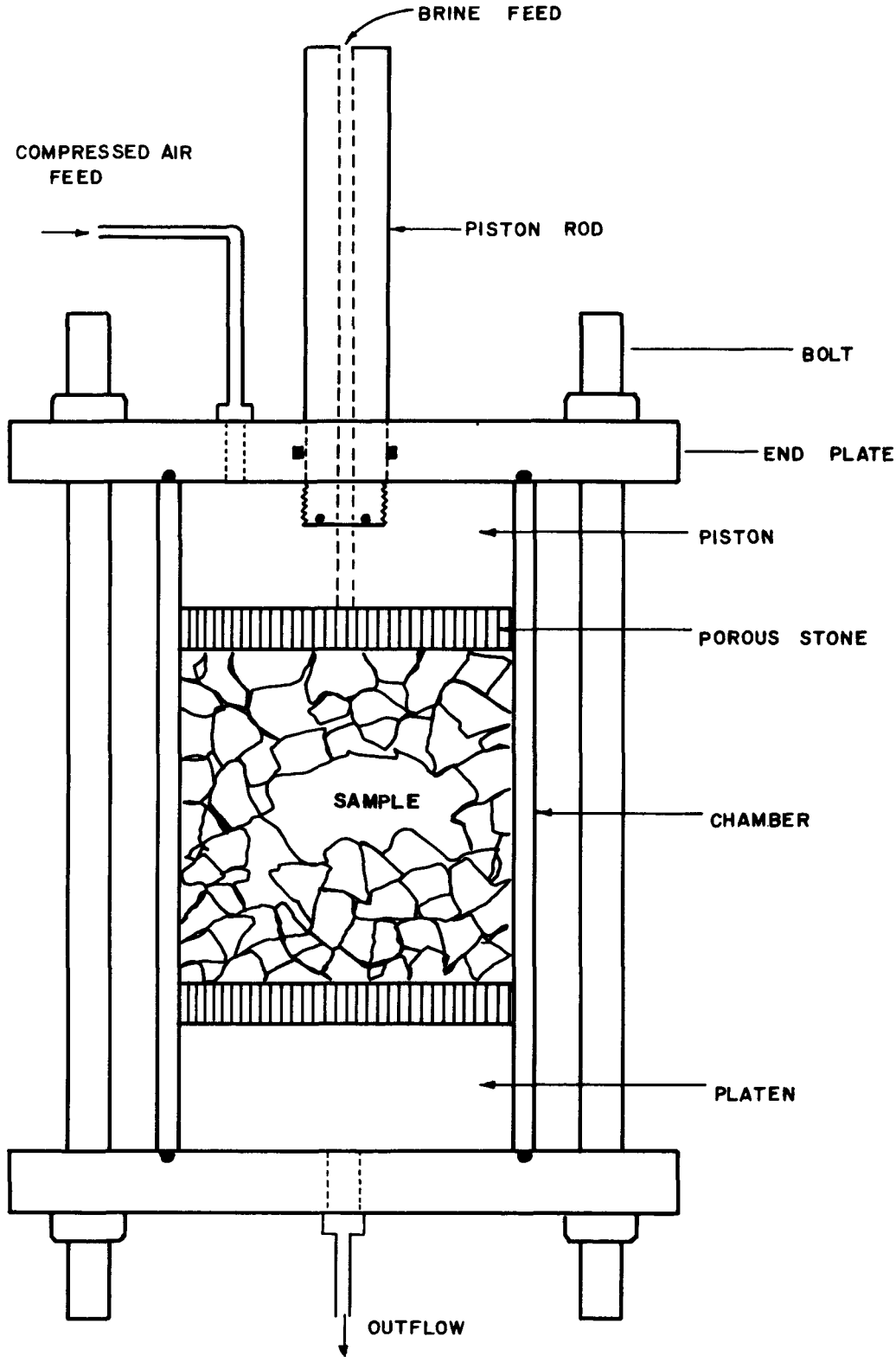

Figure 4.1 Assemblage drawing of a pipe flow permeameter.

4.3 Pipe Flow Permeability Testing on Consolidated Crushed Salt

A number of permeability measurements of crushed salt have been reported (Shor et al., 1981; Baes et al., 1983; Kelsall et al., 1984; Kappei and Gessler, 1984; Holcomb and Shields, 1987; IT Corporation, 1987; Case et al., 1987). In order to predict the effectiveness of crushed salt as a fluid barrier, the permeability associated with various stages of consolidation must be determined (Stormont, 1984).

A procedure to determine the permeability of a consolidated sample is given in Appendix D. This procedure largely follows ASTM D4525-85 practice . The following deviations from the standard are used. Only stainless steel pipe flow permeameters are used in this permeability testing, in order to allow application of higher stresses than would be permissible with the elastomer permeameters recommended in the ASTM standard. The pressure gage employed to monitor the pressure differential across the specimen has a resolution of 1380 Pa (0.2 psi), compared with a minimum resolution of 250 Pa (0.04 psi) recommended by the ASTM standard. The specimens are not oven-dried, nor is the nitrogen air (the permeant) dried with silica gel, especially for samples consolidated wet.

Preliminary permeability testing has been performed on sample S4-CS2-SN2-WG-8-CD-1-D (203 mm in diameter, air-dried) to test the applicability of Gilmont flowmeters (Gilmont Instruments, Inc., 1986). After consolidation, the porosity of the sample was reduced from the original 38.3 to 24.3%. The unloaded consolidated sample has a permeability of 1.22 darcy at a pressure differential of 13.8 kPa (2 psi). When an axial pressure of 1.9 MPa (275 psi) is applied to compress the sample against the confining pipe, the permeability reduces to 0.81 darcy. Both results fit very well the permeability-porosity relation obtained by IT Corporation (1987, Fig. 3-4; also Case et al., 1987) for dry consolidation of 0.9 mm mean particle size crushed salt. The initial value closely matches the permeability-porosity relation obtained by Kappei and Gessler (1984) for well-graded crushed salt. The second measurement gives a substantially higher permeability. Preferential flow paths along the sample-pipe interface are evident. Just prior to the latter permeability measurement, a flow rate of 200 cc/min was observed, before the introduction of permeant. This air flow was due to a leak of the piston seals. The flow rate due to the leak was subtracted from the final measurement since both readings were within the linear range of the flow rate scale shown on the Gilmont flowmeter No. 13.

CHAPTER FIVE

SUMMARY, CONCLUSIONS AND RECOMMENDATIONS

5.1 Summary and Conclusions

This report presents results from an experimental investigation of aspects of the behavior of crushed salt relevant to its eventual use as a sealant and backfill material for a HLW repository in salt. The work was terminated early in response to the implementation of the Nuclear Waste Policy Amendments Act.

Geometrical characterization of the tested crushed salt includes determination of grain size distribution and of particle shape parameters. Shape characterization shows, as expected, considerable cubic symmetry. A noticeable shift towards disk shapes is observed with increasing particle size. For the smallest size, well below the single grain size of salt crushed for sample preparation, a mix is found which includes disk-, blade-, and roller-shaped fragments.

Volume changes, pore volume changes, permeability changes and stiffness changes of crushed backfill under the influence of the convergence of the excavations within which the crushed salt is emplaced are likely to be critical behavior parameters describing the eventual sealing performance of crushed salt. For that reason, consolidation of crushed salt under controlled loading has been a high priority of this experimental program. Two series of crushed salt consolidation tests, referred to as series A and B, have been performed.

Crushed salt is emplaced in a steel cylinder, and the axial deformation is monitored during the application of sustained stepwise increased axial loads. The results of creep consolidation have been fitted to published semi-empirical laws. Consolidation creep testing has been performed on air-dried and on moistened samples. Crushed salt to which brine has been added consolidates faster than dry crushed salt. Possible explanations include increased dissolutioning at the (highly stressed) contact points, reduced sliding friction between grains, and increased creep rate of salt crystals (e.g. Varo and Passaris, 1977). Time-dependent void ratio reduction can be described reasonably well as a linear function of the logarithm of time, although noticeable temporary accelerations or rate fluctuations do occur. The latter are presumed to be associated with some localized creep rupture of salt grains, or fluctuations of residual shear strength at contact points (Fuenkajorn and Daemen, 1988, pp. 407-412), resulting in particle rearrangements. Although problems in the driving systems can not be excluded altogether, the rate fluctuations have been observed in several systems, and appear to be quite similar to those reported by Holcomb and Zeuch (1988, Fig. 12).

Extrapolating the results to calculate the time at which crushed salt consolidation might reduce the void ratio to that of intact in-situ

salt suggests a time requirement of many centuries. It is recognized that such a calculation extrapolates by many orders of magnitude beyond the time scale on which measurements have been made. Also, the experiments reported here and on which the time-dependent relations are based started out with an extremely loosely emplaced crushed salt, and the extrapolation was based on an average consolidation rate derived from experiments at relatively low consolidation pressures. Even so, the results clearly suggest that considerable benefits would be derived from relatively dense emplacement, in the limit, from the emplacement of preconsolidated or precompressed crushed salt bricks (Tyler et al., 1988; Tyler, 1989).

The void reduction rate reported here is considerably smaller than results published for isostatic consolidation. Neither triaxial (axial loading, confined sample) nor isostatic testing would appear to correspond very closely to the most likely actual in-situ loading configuration. These two load configurations might correspond to lower and upper bound type conditions. In isostatic testing, a three-dimensional active force is applied. In uniaxial testing, one active driving force is applied, while passive reaction forces develop perpendicular to the active force. In situ a biaxial active driving displacement will cause consolidation, with a passive confining reaction force developing normal to the plane in which convergence takes place (in addition to the reaction forces within the plane itself).

The consolidation rate is not clearly or simply related to applied stress. It is postulated that the lack of such a relation may be due to the overriding effect of other variables, such as sample history, initial emplacement density, differences in sample structure (grain size distribution, particle arrangement, etc.). As pointed out recently by Holcomb and Zeuch (1988, pp. 35-36), the apparent lack of stress-dependency of the results may be due to an inadequate analysis of the results, in which the correct reference density is not appropriately accounted for.

The predictability of crushed salt consolidation remains highly uncertain, as is further emphasized in the subsequent section on research needs. The considerable benefits derived from the emplacement of crushed salt are recognized, e.g. reduced rock mass deformation, reduced differential stress in excavation walls, eventual consolidation and rehealing to an essentially intact rock mass, equivalent in its waste isolation capability to that of a virgin rock salt mass. From a repository sealing point of view, however, considerably more evidence will be needed to demonstrate its eventual effectiveness as a seal. This in itself is a strong argument in favor of the emplacement of seal types (e.g. concrete, salt blocks) that avoid the large uncertainty associated with early performance of crushed salt. The complementary beneficial action of crushed salt backfill, particularly for the very long term repository performance and waste isolation, deserves recognition. Its numerical time-dependent integration in performance assessments will be difficult, given the considerable uncertainties in predicting the long-term mechanical and hydrological characteristics of the consolidating mass.

5.2 Recommendations for Future Research

The scope of the work completed is far too limited to allow drawing any firm conclusions. Sufficient results and experience have been gained to allow making a number of suggestions for follow-up studies. Recommendations for future investigations can conveniently be subdivided into those dealing with straightforward improvements of test procedures and instrumentation reported on here, and those dealing with fundamentally different or complementary investigations.

The most obvious recommendation for future work, beyond improving the test procedures to assure that correct results are obtained, is to perform a sufficient number of tests to allow statistical evaluation of the data significance. Test instrumentation aspects in need of improvement are first and foremost the loading system. Fluctuations in applied axial load need to be reduced, frictional losses need to be determined and minimized, and the load actually transmitted to the salt needs to be monitored.

One of the more serious limitations of the tests reported here, in addition to the small number of tests, is the severely limited number of test configurations. As pointed out for example by Sjaardema and Krieg (1987), in order to develop, quantify and validate a truly comprehensive constitutive model for salt consolidation, it would seem virtually essential to conduct polyaxial tests. The tests as performed here, in uniaxial strain, could be more fully instrumented, e.g. by emplacing strain gages on relatively thin wall pipe, thus allowing monitoring of the three-dimensional, albeit radially symmetric, stress and strain sample history. Complementary to constant load tests would be constant strain and constant strain rate tests. Tests with such applied displacement boundary conditions are likely to be required for validating constitutive models for crushed salt. It would be desirable to perform concurrent repeated permeability measurements during consolidation. Such measurements affect the humidity within the sample, and hence need to be designed with considerable care.

Given the statically indeterminate nature of in-situ salt consolidation, resulting as it does from the interaction between the consolidating salt and the converging excavation walls, it would be desirable to determine stiffness as a function of degree of consolidation. Test designs for this purpose involve serious difficulties, primarily due to the sensitivity of salt to the loading path and history. The simplest test might consist of determining stiffness as a function of density on samples subjected to fast consolidation, i.e. under high stress. Such an approach raises concerns about whether the results adequately provide the stiffness of crushed salt consolidated to the same density but at lower stress levels and for much longer durations (Fordham, 1988, p. 103).

The consolidation of crushed salt is largely governed by the interaction between particles, i.e. the deformations at particle contacts, and by particle deformations. The predominant deformations thus take place in highly nonuniform stressfields which are likely to include tensile stresses, and which certainly include steep stress and

strain gradients. Very limited experimental investigations have been published about salt behavior under such loading conditions. A logical recommendation aimed at developing an improved understanding of crushed salt consolidation is to perform tests and analyses under conditions that allow detailed observations on deformation of salt subjected to steep stress gradients, to nonuniform biaxial stressfields, and to (point) contact stresses. Examples of possible test geometries are illustrated in Figures 5.1 and 5.2. The suggested tests are aimed at investigating the behavior of single particles, and of the contact between particles. Tests would need to be instrumented comprehensively, notably with displacement monitoring at multiple points, in order to assure that discriminatory back analysis of the data is possible. For mechanistic model development purposes, it would be desirable to test with extreme controlled boundary conditions, e.g. constant load, constant strain rate, unconfined, and rigidly confined. Tests aimed at simulating more empirically the likely in-situ consolidation could be performed by applying a decreasing strain rate, or a decreasing load. All tests would require rigorous environmental control, particularly with regard to moisture content and temperature. The contact tests especially need to be performed for different moisture conditions at the interface. It would be highly desirable to identify the mechanisms that contribute to crushed salt consolidation. This is likely to include short duration mechanisms, such as particle splitting, contact crushing, and plastic flow, as well as transient and steady-state creep. Presumably, as consolidation progresses, the changes in particle contacts will decrease and fewer and fewer short duraction events are likely to affect consolidation trends. Mechanism characterization could be accomplished in part by microscopic investigation of salt behavior around contacts and within particles. Complementary determinations based on detailed intrepretation of comprehensive test results would be highly desirable (Wawersik and Zeuch, 1986).

Selection of particle sizes is a significant parameter in test design. Contradictory desiderata are likely to be encountered, depending on whether one wishes to emphasize the desirability of simulating as closely as possible expected in-situ conditions, or whether one wishes to investigate fundamental aspects of salt consolidation. To the extent that expected particle sizes that will be used in practice are known, it clearly would be desirable to test representative size ranges. In addition, it almost certainly would be desirable to test "particles" (e.g. disks, spheres, cylinders, cubes) prepared from single crystals, as well as particles that contain grain boundaries. Equally important test variables are size distribution, possibly shape and shape distribution, and installation procedures, notably as they affect initial installed density. Similar questions arise as for the study of size effects, e.g. should these variables be selected primarily to simulate expected practical emplacement conditions, aimed at quantifying semi-empirical approaches, or should the principal objective be to obtain a fundamental understanding of the behavior?

Most contacts are likely to be of a point to surface type (Figure 5.3). Most contacts illustrated in Figures 5.1 and 5.2 are of a point to point type. It is postulated that symmetry in the test

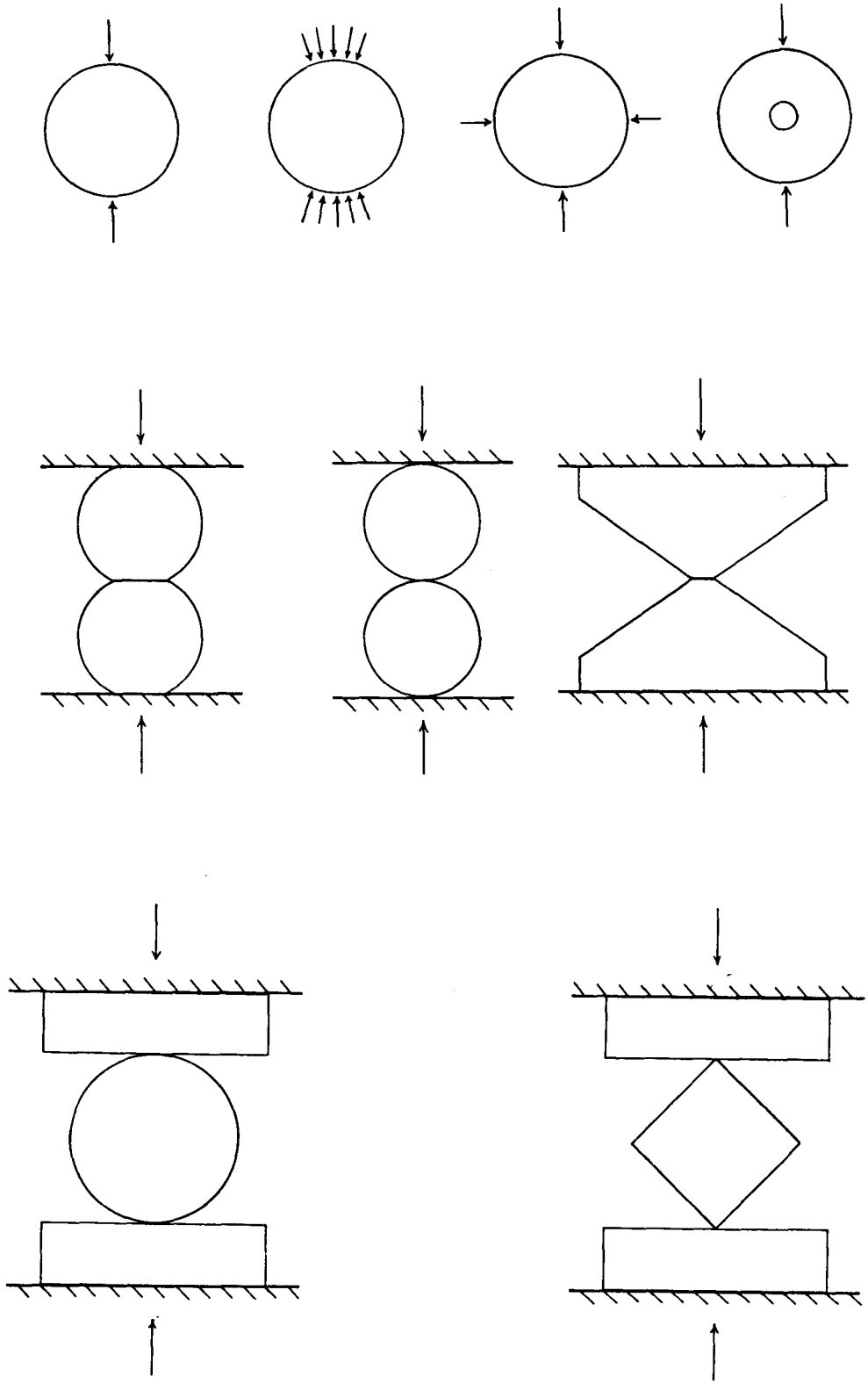

Figure 5.1 Suggested test configurations for studying single particle, and particle contact mechanical behavior.

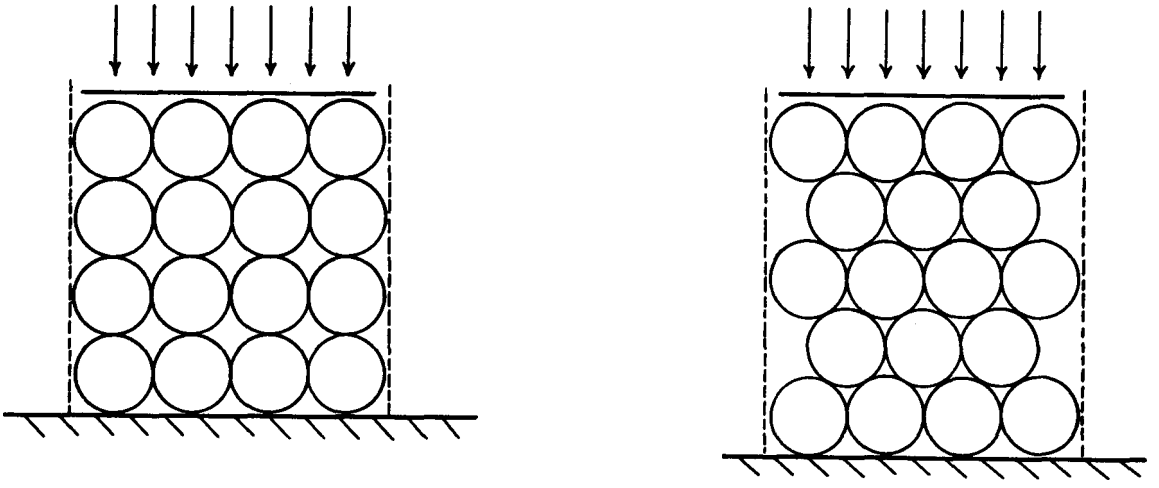

Figure 5.2 Ordered packings of identical spherical or cylindrical salt particles.

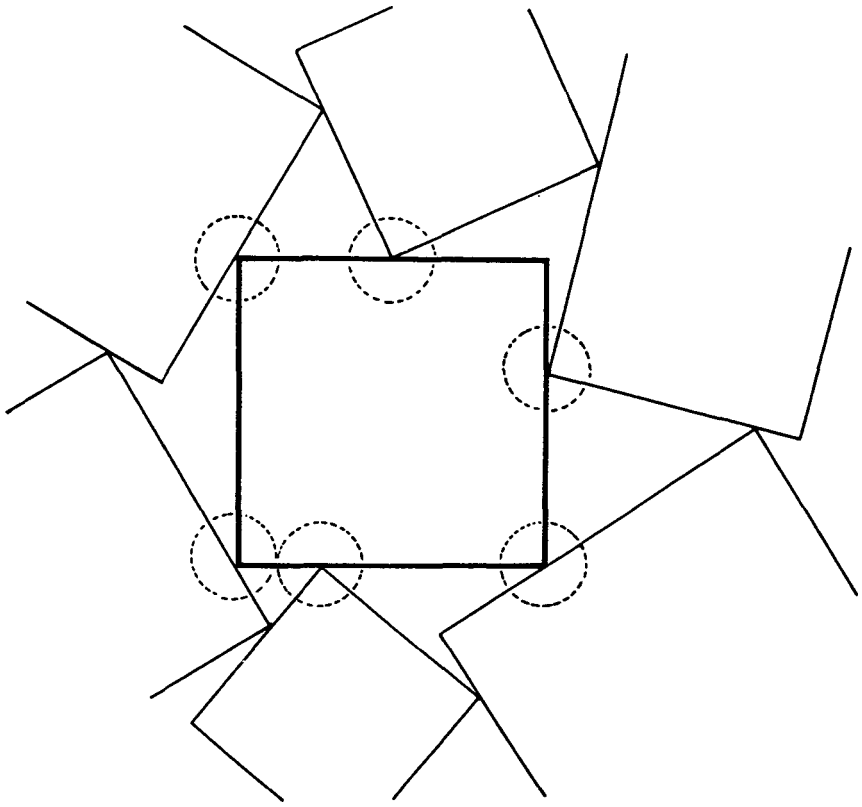

Figure 5.3 Contacts between salt particles likely to be of a point to surface type.

configuration may simplify interpretation and enhance understanding of participating mechanisms. Nevertheless, an argument certainly could be made that it might be more immediately productive to focus directly on point to surface contact studies. Experimental variables, e.g. boundary conditions, environmental conditions, particle shapes and sizes, would be subject to the same considerations as for point-to-point contact tests.

Several potential test matrices or lists of variables to be considered for salt consolidation studies have been published (IT Corporation, 1984, Section 5.2; Myers, 1986; Pfeifle et al., 1987). A reevaluation of these recommendations, in light of available test results and analyses, would be desirable to establish priorities for future investigations. Complementary to the definition of test parameters based on judgment and experience is the development of test plans based on consolidation modeling, on fundamental mechanics governing consolidation, and on constitutive models. A number of models have been applied or developed for the description of crushed salt consolidation (Shor et al., 1981; Zeuch et al, 1985; Yost and Aronson, 1987; Sjaardema and Krieg, 1987; Holcomb and Zeuch, 1988; Fordham, 1988). Design of tests based specifically on analyses of this type and aimed at determining essential discriminating variables would be highly desirable. Finally, because the ultimate objecting of understanding and predicting crushed salt consolidation is to predict its interaction with converging excavations in salt rooms, future experimental designs could benefit from an evaluation of interaction analyses (Wagner, 1980; IT Corporation, 1984; Kelsall et al., 1984; Nowak and Stormont, 1987; Niou and Pietz, 1987; Korthaus, 1984; Liedtke and Bleich, 1984).

A topic that deserves explicit attention is the uniformity, or lack thereof, within a consolidating crushed salt mass. Field observations have shown pronounced nonuniform consolidation across a sixty year old backfill in a mine room (Kappei and Gersler, 1984). Similar nonuniformities have been observed in pipe consolidation testing (Holcomb and Zeuch, 1988, p. 6 discuss several examples, and examples are discussed in Section 3.6 of this report). The gross disturbance caused by a relatively small change in pipe internal diameter is illustrated in Figure 3.13. In sum, ample indications suggest that consolidation is likely to be a highly nonuniform process. For laboratory testing, boundary conditions can be selected to enhance uniformity. This has advantages for interpretational and modeling purposes. An approach focused exclusively on uniform conditions run the risk of underestimating the potential significance of inhomogeneous consolidation. Particularly because of the statically indeterminate rock-backfill interaction, detailed modeling of such nonuniform consolidation is likely to require a true constitutive model, i.e. a model integrating relations between stress, strain, density, time stress and strain deviations, etc. Such a comprehensive mechanistic model development would be desirable, especially for long-term predictions. It will require a major modeling and testing program. A preliminary semi-empirical program aimed at directly investigating nonuniformity may well be productive by identifying general trends and influencing variables. Post-consolidation pore space and contact point geometry characterization across pipe consolidation samples of a range

of diameters may assist in clarifying the extent of the inhomogeneity, and may assist in identifying whether a real need exists for the development of a truly complete constitutive formulation.

One interesting option that deserves consideration would be to consolidate crushed salt within hollow salt cylinders by applying lateral stresses to the cylinders. Such an experiment would allow simultaneously the study of the predictability of salt borehole closure and of crushed salt consolidation. As such, it could constitute a useful although severe validation experiment for constitutive models for both interacting components of the system. It is recognized that arguments have been made that the presence of crushed salt within a creeping shaft (or borehole) should not significantly impact hole closure (Sjaardema and Krieg, 1987, p. 36). As pointed out by IT Corporation (1987, p. 26), the bulk modulus of crushed salt starts increasing rapidly once the porosity drops below 25%. Similarly, Fordham (1988, p. 104) observed substantial stiffness changes at about 30% porosity. Beyond that range, therefore, one would expect the development of potentially significant interaction forces, as the stiffnesses of the two components of the interacting system become of the same order of magnitude. A changing stiffness approach has been implemented by Liedtke and Bleich (1984), who show the rapid reduction in excavation convergence as a result of the reaction force buildup in the consolidating and stiffening crushed salt backfill.

Many uncertainties would affect the design of such an interactive experiment, and most notably the selection of the external boundary conditions, e.g. whether the cylinder should be pressurized at constant pressures, or loaded to some controlled external strain, displacement or rate. Similarly, decisions would be required about axial loading or confinement of salt cylinders and emplaced crushed salt. Finally, the fluid conditions inside the cylinder need to be selected, e.g. with or without liquid or gas, drained, vented, or closed, etc. Given the complexity of this experiment, it clearly would be desirable to perform a careful analytical test design, even recognizing the present uncertainty about the feasibility of detailed descriptions of the mechanical behavior of the two interacting components.

CHAPTER SIX

REFERENCES

Allen, A.S. and J. Paone, 1982, "Surface Subsidence Control by Backfilling," Ch. 4, Section 1.9, pp. 210-226, Underground Mining Methods Handbook, W.A. Hustrulid, ed., Society of Mining Engineers of AIME, New York, 1982.

ASTM C136-84a, "Standard Method for Sieve Analysis of Fine and Coarse Aggregates," Annual Book of ASTM Standards, Section 4, Construction, Vol. 04.02, Concrete and Mineral Aggregates, American Society for Testing and Materials, Philadelphia.

ASTM C702-80, "Standard Method for Reducing Field Samples of Aggregates to Testing Size," Annual Book of ASTM Standards, Section 4, Construction, Vol. 04.02, Concrete and Mineral Aggregates, American Society for Testing and Materials, Philadelphia.

ASTM D2216-80, "Standard Test Method for Laboratory Determination of Water (Moisture) Content of Soil, Rock, and Soil-Aggregate Mixtures," Annual Book of ASTM Standards, Section 4, Construction, Vol. 04.08, Soil and Rock; Building Stones, American Society for Testing and Materials, Philadelphia.

ASTM D4525-85, "Standard Test Method for Permeability of Rocks by Flowing Air," Annual Book of ASTM Standards, Section 4, Construction, Vol. 04.08, Soil and Rock; Building Stones, American Society for Testing and Materials, Philadelphia.

Baes, C.F., Jr., L.O. Gilpatrick, F.G. Kitts, H.R. Bronstein, and A.J. Shor, 1983, "The Effect of Water in Salt Repositories: Final Report," ORNL-5950, prepared by the Oak Ridge National Laboratory for the U.S. Department of Energy, Oak Ridge, TN.

Blanks, R.F., 1952, "Good Concrete Depends on Good Aggregate," Civil Engineering, Vol. 122, no. 9, September, pp. 651-655.

Bredehoeft, J.D., 1988, "Will Salt Repositories Be Dry?," EOS Transactions, American Geophysical Union, Vol. 69, No. 9, March 1.

Bredehoeft, J.D., A.W. England, D.B. Stewart, N.J. Trask, and I.J. Winograd, 1978, "Geological Disposal of High-Level Radioactive Wastes - Earth Science Perspectives," Geological Survey Circular 779, U.S. Geological Survey, 15 pp.

Brezovec, D., 1983, "Pneumatic Stowing Seals Mines," Coal Age, Vol. 88 No. 11, pp. 56-57.

Brezovec, D. and D.N. Hedges, 1986, "With Careful Planning, a Mine Closes Economically and Efficiently," Coal Age, Vol. 91, No. 11, pp. 42-45.

Carman, 1939, "Permeability of Saturated Sands, Soils and Clays," Journal of Agricultural Science, Vol. XXIX, part 2, pp. 262-273.

Case, J.B., P.C. Kelsall, and J.L. Withiam, 1987, "Laboratory Investigation of Crushed Salt Consolidation," pp. 189-196, 28th U.S. Symposium on Rock Mechanics, Tucson, AZ, June-July, A.A. Balkema, Rotterdam.

Christensen, C.L., C.W. Gulick, and S.J. Lambert, 1983, "Sealing Concepts for the Waste Isolation Pilot Plant (WIPP) Site," SAND81-2195, prepared by Sandia National Laboratories, Albuquerque, NM, for the U.S. Department of Energy.

Crawford, C.B. and J.G. Sutherland, 1971, "The Empress Hotel, Victoria, British Columbia. Sixty-Five Years of Foundation Settlements," Canadian Geotechnical Journal, Vol. 8, No. 1, pp. 77-93.

Daemen, J.J.K., W.B. Greer, K. Fuenkajorn, A. Yazdandoos, H. Akgun, A. Schaffer, A.F. Kimbrell, T.S. Avery, J.R. Williams, B. Kousari, and R.O. Roko, 1986, "Rock Mass Sealing - Experimental Assessmen of Borehole Plug Performance, Annual Report, June 1984 - May 1985," NUREG/CR-4642, prepared for the U.S. Nuclear Regulatory Commission, Office of Nuclear Regulatory Research, Division of Radiation Programs and Earth Sciences, by the Department of Mining and Geological Engineering, University of Arizona, Tucson.

De Boer, R.B., 1977, "On the Thermodynamics of Pressure Solution - Interaction Between Chemical and Mechanical Forces," Geochimica et Cosmochimica Acta, Vol. 41, pp. 249-256.

Feda, J., 1982, Mechanics of Particulate Materials - The Principles, Elsevier Scientific Publishing Co., New York, 447 pp.

Fordham, C.J., 1988, "Behavior of Granulate Halite for Use a a Backfill in Potash Mines," Ph.D. Thesis, University of Waterloo, Ontario.

Fowkes, R.S. and J.F. Fritz, 1974, "Theoretical and Experimental Studies on the Packing of Solid Particles: A Survey," IC-8623, Bureau of Mines, U.S. Department of the Interior.

Fuenkajorn, K. and J.J.K. Daemen, 1988, "Borehole Closure in Salt," NUREG/CR-5243, prepared for Division of Engineering, Office of Nuclear Regulatory Research, U.S. Nuclear Regulatory Commission, Washington, DC, by the Department of Mining and Geological Engineering, University of Arizona, Tucson.

Gilmont Instruments, Inc., 1986, Gilmont Catalog G86-87, Great Neck, NY, 66 pp.

Giuffre, M.S., C.M. Koplik, R.L. Plum, and R. Talbot, 1979, "Information Base for Waste Repository Design: Volume 5. Decommissioning of Underground Facilities," NUREG/CR-0495, prepared for U.S. Nuclear Regulatory Commission, by the Analytic Sciences Corporation, Reading, MA.

Griess, J.C., 1982, "Evaluation of Corrosion Damage to Materials After Three Years in the Avery Island Salt Mine," ORNL/TM-8351, prepared by the Oak Ridge National Laboratory for the U.S. Department of Energy, Oak Ridge, TN.

Grim, W., 1968, Kali-und Steinsalzbergau (Potash and rock salt mining), VEB Deutscher Verlag fuer Grundstoffindustrie, Leipzig.

Gureghian, A.B., L.A. Scott, and G.E. Raines, 1983, "Performance Assessment of a Shaft Seals System in a HLW Repository in the Gibson Dome Area," ONWI-494, Office of Nuclear Waste Isolation, Battelle Memorial Institute, Columbus, OH.

Hansen, F.D., 1976, "Experimental Consolidation of Granulated Rock Salt with Application to Sleeve Buckling," ORNL/sub-4269/21, prepared by the Oak Ridge National Laboratory, Oak Ridge, TN, for the U.S. Department of Energy.

Harr, M.E., 1977, Mechanics of Particulate Media, McGraw-Hill, Inc., New York, 543 pp.

Herdan, G., 1960, Small Particle Statistics, Butterworths Co., London, 418 pp.

Heywood, H., 1947, "The Scope of Particle Size Analysis and Standardization," Symposium on Particle Size Analysis, Institution of Chemical Engineers, Vol. 25, London.

Holcomb, D.J. and D.W. Hannum, 1982, "Consolidation of Crushed Salt Backfill Under Conditions Appropriate to the WIPP Facility," SAND82-0630, prepared by Sandia National Laboratories, Albuquerque, NM, for the U.S. Department of Energy.

Holcomb, D.J. and M. Shields, 1987, "Hydrostatic Creep Consolidation of Crushed Salt with Added Water," SAND87-1990, prepared by the Sandia National Laboratories, Albuquerque, NM, for the U.S. Department of Energy.

Holcomb, D.J. and D.H. Zeuch, 1988, "Consolidation of Crushed Rock Salt, Part I: Experimental Results for Dry Salt Analyzed Using a Hot-Pressing Model," Sandia Report SAND88-1469, prepared by Sandia National Laboratories, Albuquerque.

Holtz, R.D. and W.D. Kovacs, 1981, An Introduction to Geotechnical Engineering, Prentice-Hall, Inc., Englewood Cliffs, NJ, 733 pp.

Hunter, T.O., 1980, "Role of Borehole Plugging in the Evaluation of the Waste Isolation Pilot Plant," SAND80-0502C, prepared by Sandia

National Laboratories for the U.S. Department of Energy, Albuquerque, NM.

IT Corporation, 1984, "Assessment of Crushed Salt Consolidation and Fracture Healing Processes in a Nuclear Waste Repository in Salt," BMI/ONWI-546, prepared for Office of Nuclear Waste Isolation, Battelle Memorial Institute, Columbus, Ohio.

IT Corporation, 1987, "Laboratory Investigation of Crushed Salt Consolidation and Fracture Healing," BMI/ONWI-631, prepared for Office of Nuclear Waste Isolation, Battelle Memorial Institute, Columbus, Ohio.

Jaeger, J.C. and N.G.W. Cook, 1979, Fundamentals of Rock Mechanics 3rd Edition, Chapman and Hall, Co., London.

Jenyon, M.K., 1986, "Salt with a Pinch of Water," Nature, Vol. 324, pp. 515-516, 11 December.

Jezierski, H., 1984, "Dam Construction in Salt Formations," pp. 261-7, Vol. 1, Waste Management '84, Tucson, AZ.

Kappei, G. and K. Gessler, 1984, "In Situ Tests on the Behavior of Backfill Materials," pp. 311-328, Second Conference on the Mechanical Behavior of Salt, Hanover, Sept. 24-28, H.R. Hardy, Jr., and M. Langer, eds., Trans Tech Publications, 1988.

Kelsall, P.C., J.B. Case, D. Meyer, and W.E. Coons, 1982, "Schematic Designs for Penetration Seals for a Reference Repository in Bedded Salt," ONWI-405, prepared by D'Appolonia Consulting Engineers, Inc., for Office of Nuclear Waste Isolation, Battelle Memorial Institute, Columbus, Ohio.

Kelsall, P.C., W.E. Coons, and D. Meyer, 1983, "Repository Sealing Program Plan: Repository in Salt," ONWI-414, prepared by D'Appolonia Consulting Engineers, Inc., for Office of Nuclear Waste Isolation, Battelle Memorial Institute, Columbus, OH.

Kelsall, P.C., J.B. Case, J.W. Nelson, and J.G. Franzone, 1984, "Assessment of Crushed Salt Consolidation and Fracture Healing in a Nuclear Waste Repository in Salt," Waste Management '84, Tucson, AZ, Vol. 1, pp. 457-463.

Kelsall, P.C., J.B. Case, W.E. Coons, J.G. Franzone, and D. Meyer, 1985a, "Schematic Designs for Penetration Seals for a Repository in the Permian Basin," BMI/ONWI-564, prepared by IT Corporation for Office of Nuclear Waste Isolation, Battelle Memorial Institute, Columbus, Ohio, December.

Kelsall, P.C., J.B. Case, D. Meyer, J.G. Franzone, and W.E. Coons, 1985b, "Schematic Designs for Penetration Seals for a Repository in Richton Dome," BMI/ONWI-562, prepared by IT Corporation for Office of Nuclear Waste Isolation, Battelle Memorial Institute, Columbus, Ohio, December.

Kelsall, P.C., D. Meyer, J.B. Case, and W.E. Coons, 1985c, "Schematic Designs for Penetration Seals for a Repository in the Paradox Basin," BMI/ONWI-563, prepared by IT Corporation for Office of Nuclear Waste Isolation, Battelle Memorial Institute, Columbus, Ohio, December.

Korthaus, E., 1984, "Effect of Backfill Materials on Cavity Closure," pp. 521-532, Second Conference on the Mechanical Behavior of Salt, Hanover, Sept. 24-28, H.R. Hardy, Jr., and M. Langer, eds., Trans Tech Publications, 1988.

Kozeny, J., 1927, "Ueber kapillare Leitung des Wassers in Boden," Sitz. Ber. Akad. Wiss. Wien, Mathem-Natuwiss. Abt. 136, p. 271.

Krizek, R.J., K.S. Chawla, and T.B. Edil, 1977, "Directional Creep Response of Anisotropic Clays," Geotechnique, Vol. 27, No. 1, pp. 37-51.

Krumbein, W.C. and L.L. Sloss, 1963, Stratigraphy and Sedimentation, 2nd Edition, Freeman Co., San Francisco, 660 pp.

Ladd, C.C., R. Foott, K. Ishihara, F. Schlosser, and H.G. Poulos, 1977, "Stress-Deformation and Strength Characteristics," Proceedings of 9th International Conference on Soil Mechanics and Foundation Engineering, Tokyo, Japanese Society of Soil Mechanics and Foundation Engineering, Vol. 2, pp. 421-494.

Ladish Co., 1976, "Stainless Steel Fittings," Ladish Co. Catalogue, Cudahy, WI.

Le Comte, P., 1965, "Creep in Rock Salt," Journal of Geology, Vol. 73, no. 3, pp. 469-484.

Liedtke, L. and W. Bleich, 1984, "Convergence Calculations for Back-Filled Tunnels in Rock Salt," pp, 551-580, Second Conference on the Mechanical Behavior of Salt, Hanover, Sept. 24-28, H.R. Hardy, Jr., and M. Langer, eds., Trans Tech Publications, 1988.

Lindner, E.N. and B.H.G. Brady, 1983, "Memory Aspects of Salt Creep," Proceedings: First Conference on the Mechanical Behavior of Salt, Pennsylvania State University, November, 1981, Trans Tech Publications, Clausthal, Germany, pp. 241-273.

Lo, K.Y., 1961, "Secondary Compression of Clays," Journal of the Soil Mechanics and Foundations Division, ASCE, Vol. 87, No. 4, pp. 61-87.

Loudon, A.G., 1952, "The Computation of Permeability from Simple Soil Tests," Geotechnique, Vol. III, no. 4, pp. 165-183.

Lowry, W.D., 1956, "Factors in Loss of Porosity by Quartzose Sandstones of Virginia," Bulletin of American Association of Petroleum Geologists, Vol. 40, pp. 489-500.

Malewski, J., 1984, "A Comparison of Particle Shape Characteristics of Crushed Basalt and Granite Rocks," International Symposium on Aggregates, Nice, France, May 21-23, Theme III, Bulletin of the International Association of Engineering Geology, no. 29, pp. 401-405.

Martin, G., 1928, "Researches on the Theory of Fine Grinding," Transactions British Ceramic Society, 27, pp. 247-259.

Mather, B., 1955, "Shape, Surface Texture, and Coatings," Significance of Tests and Properties of Concrete and Concrete Aggregates, ASTM, STP No. 169, American Society for Testing Materials, pp. 284-296.

Mesri, G. and P.M. Godlewski, 1977, "Time and Stress-Compressibility Interrelationship," Journal of the Geotechnical Engineering Division, ASCE, Vol. 103, No. GT5, May, pp. 417-430.

Meyer, D., R.H. Goodwin, and J.C. Wright, 1980, "Repository Sealing: Evaluation of Materials Research Requirements," pp. 43-63, Borehole and Shaft Plugging Proceedings, Columbus, OH, May 1980 Workshop. Published by OECD, Paris.

Miller, H.D.S., 1983, "Use of Rocksalt as Backfill," pp. 341-345, Potash Technology, R.M. McKercher, ed., Pergamon Press, Toronto.

Mraz Project Consultants Ltd., 1987, "Use of Backfill in New Brunswick Potash Mines," Final Report by Denison-Potacan Potash Company, Sussex, New Brunswick, for the Canada Centre for Mineral and Energy Technology, Energy, Mines and Resources Canada.

Muskat, M., 1946, The Flow of Homogeneous Fluids through Porous Media Edwards Brothers, Inc., Ann Arbor.

Nelson, J.W. and P.C. Kelsall, 1984, "Prediction of Long-Term Creep Closure in Salt," Proceedings of the 25th Symposium on Rock Mechanics, Northwestern University, Evanston, Illinois, June 25-27, pp. 1115-1125.

Nowak, E.J. and J.C. Stormont, 1987, "Scoping Model Calculations of the Reconsolidation of Crushed Salt in WIPP Shafts," SAND87-0879, prepared by the Sandia National Laboratories, Albuquerque, NM, for the U.S. Department of Energy.

Niou, S. and J.M. Pietz, 1987, "Coupled Brine Migration and Stress Analysis for Repository Room Saturation in Bedded Salt," pp. 601-608, Rock Mechanics, Proceedings of the 28th U.S. Symposium I.W. Farmer et al., eds., A.A. Balkema, Rotterdam.

Orr, C., Jr., 1966, Particulate Technology, MacMillan Co., New York.

Pfeifle, T.W., 1987a, "Mechanical Properties and Consolidation of Potential DHLW Backfill Materials: Crushed Salt and 70/30

Bentonite/Sand," Contractor Report SAND85-7208, RE/SPEC Inc., Rapid City, SD; Sandia National Laboratories, ALbuquerque, NM.

Pfeifle, T.W., 1987b, "Backfill Material Specifications and Requirements for the WIPP Simulated DHLW and TRU Waste Technology Experiments," Contractor Report SAND85-7209, RE/SPEC Inc., Rapid City, SD; Sandia National Laboratories, ALbuquerque, NM.

Pfeifle, T.W., P.E. Senseny, and K.D. Mellegard, 1987, "Influence of Variables on the Consolidation and Unconfined Compressive Strength of Crushed Salt," BMI/ONWI-627, prepared by RE/SPEC Inc. for Office of Nuclear Waste Isolation, Battelle Memorial Institute, Columbus, Ohio.

Ratigan, J.L. and R.A. Wagner, 1978, "Thermomechanical Analysis of Crushed-Salt Backfilled Disposal Rooms in a Conceptual Radioactive Waste Repository in Dome Salt," in Conceptual Design Report, National Waste Terminal Storage Repository for Storing Reprocessing Wastes in Dome Salt Formation, Special Study No. 2, Vol. XVIII, Stearns-Roger Services, Denver, CO.

Rausch, D.O. and R.C. Stitzer, 1973, "Filled Stopes and Combination Methods," Section 12.16, pp. 12-233/253, Vol. 1, SME Mining Engineering Handbook, Society of Mining Engineers of AIME, New York.

Rockwood, N.C., 1948, "Production and Manufacture of Fine and Coarse Aggregates," Symposium on Mineral Aggregates, ASTM STP 83, American Society for Testing Materials, Philadelphia, PA, pp. 88-116.

Schwartz, C.E. and J.M. Smith, 1953, "Flow Distribution in Packed Beds," Industrial and Engineering Chemistry, Vol. 45, pp. 1214-1215.

Shor, A.J., C.F. Baes, and C.M. Canonico, 1981, "Consolidation and Permeability of Salt in Brine," ORNL-5774, prepared by the Oak Ridge National Laboratory for the U.S. Department of Energy, Oak Ridge, TN.

Sjaardema, G.D. and R.D. Krieg, 1987, "A Constitutive Model for the Consolidation of WIPP Crushed Salt and Its Use in Analyses of Backfilled Shaft and Drift Configurations," SAND87-1977, prepared by Sandia National Laboratories, Albuquerque, NM, for the U.S. Department of Energy.

South, D.L. and J.J.K. Daemen, 1986, "Permeameter Studies of Water Flow Through Cement and Clay Borehole Seals in Granite, Basalt and Tuff," NUREG/CR-4748, prepared by the Department of Mining and Geological Engineering, University of Arizona, for the U.S. Nuclear Regulatory Commission.

Stinebaugh, R.E., 1979, "Compressibility of Granulated Rock Salt," SAND79-1119, prepared by Sandia National Laboratories, for the U.S. Department of Energy, Albuquerque, NM.

Stokes, R.J., T.L. Johnston, and C.H. Li, 1960, "Environmental Effects on the Mechanical Properties of Ionic Solids with Particular Reference to the Joffe Effect," Transactions of the Metallurgical Society of AIME, Vol. 218, August, pp. 655-662.

Stormont, J.C., 1984, "Plugging and Sealing Program for the Waste Isolation Pilot Plant (WIPP)," SAND84-1057, prepared by Sandia National Laboratories, for the U.S. Department of Energy, Albuquerque, NM.

Stormont, J.C. and J.J.K. Daemen, 1983, "Axial Strength of Cement Borehole Plugs in Granite and Basalt," NUREG/CR-3594, Topical Report to U.S. Nuclear Regulatory Commission, by the Department of Mining and Geological Engineering, University of Arizona, Tucson.

Suklje, L., 1969, Rheological Aspects of Soil Mechanics, Wiley-Interscience Co., New York, 571 pp.

Tyler, L.D., 1989, "WIPP In Situ Tests in Support of Performance Assessment," Waste Management '89, Tucson, AZ.

Tyler, L.D., R.V. Matalucci, M.A. Molecke, D.E. Munson, E.J. Nowak, and J.C. Stormont, 1988, "Summary Report for the WIPP Technology Development Program for Isolation of Radioactive Waste," SAND88-0844, prepared by Sandia National Laboratories, Albuquerque, NM, for the U.S. Department of Energy.

Urai, J.L., J.S. Christopher, H.J. Zwart, and G.S. Lister, 1986, "Weakening of Rock Salt by Water During Long-Term Creep," Nature, Vol. 324, 11, December, pp. 554-557.

Varo, L. and E.K.S. Passaris, 1977, "The Role of Water in the Creep Properties of Halite," Proceedings of Conference on Rock Engineering, University of Newcastle upon Tyne, England, April 4-7, pp. 85-100.

Wagner, R.A., 1980, "Preliminary Investigation of the Thermal and Structural Influence of Crushed Salt Backfill on Repository Disposal Rooms," ONWI-138, prepared by RE/SPEC, Inc., for Battelle Office of Nuclear Waste Isolation, Columbus, OH.

Waldschmidt, W.A., 1941, "Cementing Material in Sandstones and Their Probable Influence on Migration and Accumulation of Oil and Gas," Bulletin of American Association of Petroleum Geologists, Vol. 25, pp. 1839-1879.

Wawersik, W.R., 1983, "Determination of Steady State Creep Rates and Activation Parameters for Rock Salt," pp. 72-92, Measurement of Rock Properties at Elevated Pressures and Temperatures, ASTM

STP 869, H.J. Pincus and E.R. Hoskins, eds., ASTM, Philadelphia, PA.

Wawersik, W.R. and D.S. Preece, 1984, "Creep Testing of Salt - Procedures, Problems and Suggestions," Mechanical Behavior of Salt I, Proceedings of the First Conference on the Mechanical Behavior of Salt, The Pennsylvania State University, November 9-11, 1981, Trans Tech Publications, Clausthal-Zellerfeld, Federal Republic of Germany, pp. 421-449.

Wawersik, W.R. and D.H. Zeuch, 1986, "Modeling and Mechanistic Interpretation of Creep of Rock Salt Below 200°C," Tectonophysics, 121, 125-152.

Weyl, P.K., 1959, "Pressure Solution and the Force of Crystallization - A Phenomenological Theory," Journal of Geophysical Research, Vol. 64, pp. 2001-2025.

Williams, J.R. and J.J.K. Daemen, 1987, "The Sealing Performance of Bentonite/Crushed Basalt Borehole Plugs," NUREG/CR-4983, Technical Report to the U.S. Nuclear Regulatory Commission, Office of Nuclear Regulatory Research, Division of Engineering Safety, by the Department of Mining and Geological Engineering, University of Arizona, Tucson.

Winterkorn, H.F. and H.-Y. Fang, 1975, "Soil Technology and Engineering Properties of Soils," Ch. 2 in Foundation Engineering Handbook, H.F. Winterkorn and H.-Y. Fang, eds. Van Nostrand Reinhold Company, New York.

Yost, F.G. and E.A. Aronson, 1987, "Crushed Salt Consolidation Kinetics," SAND87-0264, prepared by Sandia National Laboratories, for the U.S. Department of Energy, Albuquerque, NM.

Zeuch, D.H., 1989, "Isostatic Hot-Pressing Mechanism Maps for Pure and Natural Sodium Chloride: Applications to Nuclear Waste Isolation in Bedded and Domal Salt Formations," SAND88-2207, prepared by Sandia National Laboratories, Albuquerque, NM, for the U.S. Department of Energy.

Zeuch, D.H., D.J. Holcomb, and H.S. Lauson, 1985, "Analysis of Consolidation of Granulated Rocksalt Using a Plastic Flow Model for Isostatic Hot-Pressing," SAND84-1106, prepared by Sandia National Laboratories, Albuquerque, NM, for the U.S. Department of Energy.

Zingg, T., 1935, "Beitrag zur Schotteranalyze" (Contribution to pebble analysis), Schweizerische Mineralogische und Petrographische Mitteilungen, Vol. 15, pp. 39-140.

APPENDIX A

Salt Crushing Procedure

Apparatus:

1) Hammer and/or sledge hammer
2) Shovel
3) Jaw crusher (model no. FW 32786, manufactured by Denver Equipment Co., Denver, CO)
4) Adjustable roller crusher (model no. 771, manufactured by Sturtevant Mill Co., Boston, MA)
5) Haulage Cart (2)
6) Heavy-duty plastic bags
7) Safety glasses
8) Metal brush
9) Air gun

Procedure:

1) Put on safety glasses. Use hammer or sledge hammer to break a salt block into pieces of suitable size for the jaw crusher.

2) Use metal brush and air gun to clean jaw crusher, roll crusher, and haulage carts.

3) Put haulage cart 1 underneath the jaw crusher. Turn on the machine. Feed the broken pieces into the jaw crusher. The haulage cart below collects the crushed aggregates. After crushing is finished, turn the machine off.

4) Adjust the roll crusher such that the opening is close to the maximum grain size desired. Put haulage cart 2 underneath the roller crusher and then turn on the machine. Shovel the salt aggregates from cart 1 to the roller crusher.

5) The crushed salt falls into cart 2. Turn off the machine.

6) Shovel the crushed salt into a plastic bag.

7) Use metal brush to remove any salt particles remaining on the machines. Use air gun to clean places that the metal brush can not reach. Clean the haulage carts with the brush and air gun. Clean the floor thoroughly.

APPENDIX B

Sieve Analysis of Crushed Salt

Test Procedure

Objective

The purpose of this procedure is to determine the particle size and the size distribution of crushed salt. Salt is crushed in accordance with the procedure in Appendix A. Reduce the crushed salt to a convenient sample for sieve analysis following ASTM C702-80.

Apparatus

(1) Ohaus scale for coarse aggregates; readable to 1 g (max. capacity = 20 kg)
(2) Mettler P1200 electric balance for fine aggregates, readable to 0.01 g (max. capacity = 1200 g)
(3) U.S. Standard sieves: in descending order, 12.70 mm (0.5 in), 9.423 mm (0.371 in), 6.68 mm (0.263 in), 4.74 mm (0.187 in, No. 4), 2.36 mm (0.0937 in, No. 8), 2.00 mm (0.0787 in, No. 10), 0.841 mm (0.0331 in, No. 20), 0.419 mm (0.0165 in, No. 40), 0.249 mm (0.0098 in, No. 60), 0.178 mm (0.007 in, No. 80), 0.106 mm (0.0042 in, No. 100), 0.075 mm (0.0029 in, No. 200)
(4) Fisher wheeler sieve shaker (max. load capacity 9 kg).

Procedure

Test procedure for particle size analysis of crushed salt follows the standard practice ASTM C136-84a. Oven-drying is not necessary for an air-dried crushed salt sample, unless it is required for a specific purpose. If drying is necessary, follow the procedure in Appendix E.

A cumulative curve of crushed salt particle size is produced from the sieve analysis results. The cumulative percentage passing by weight is plotted against grain size (in mm), with the smaller grain sizes going toward the right. The effective size (D_{10}), average grain size (D_{50}), and coefficient of uniformity (Cu, i.e. D_{60}/D_{10}) are determined and recorded. They are defined as follows:

D_{10} = grain size (in mm) corresponding to 10% passing by weight, generally referred to as the effective size

D_{50} = grain size (in mm) corresponding to 50% passing by weight, generally referred to as the average grain size

D_{60} = grain size (in mm) corresponding to 60% passing by weight

Cu = coefficient of uniformity (D_{60}/D_{10}).

Report the weight percentage retained on each sieve.

References

ASTM C136-84a, "Standard Method for Sieve Analysis of Fine and Coarse Aggregates," Annual Book of ASTM Standards, Section 4, Vol. 04.02, Concrete and Mineral Aggregates, American Society for Testing and Materials, Philadelphia.

ASTM C702-80, "Standard Method for Reducing Field SAmples of Aggregates to Testing Size," Annual Book of ASTM Standards, Section 4, Vol. 04.02, Concrete and Mineral Aggregates, American Society for Testing and Materials, Philadelphia.

APPENDIX C

Particle Shape Analysis of Crushed Salt

Procedure

Objective

The purpose of this procedure is to characterize the shapes of crushed salt particles. Three methods are described. Method A provides a general description of particle shape in terms of sphericity and roundness (angularity). Method B, based on particle intercepts, provides a means for classifying particles according to their shape. Shape-related parameters such as the volume-shape factor, surface-shape factor, and specific surface can be obtained with Method C. This method is based on the assumption that the particles are rectangular, which is a reasonable assumption for crushed salt.

Apparatus

Magnifying glass or microscope
Caliper or micrometer (readable to 0.1 mm)

Sampling

Perform a sieve analysis on the crushed salt sample to be analyzed following the procedure given in Appendix B. At least 100 particles from each sieve used in the sieve analysis are required for Method A. At least 100 particles from each of the sieves larger than 0.42 mm mesh (U.S. Standard No. 40) are required for Method B and Method C. If the number of particles retained by a sieve is less than 100, use all the particles. Whenever a reduction of sample size is desired, follow ASTM C702-80, to insure representative sampling.

Procedure

I. Method A

Visually compare the shape of a sampled particle to the standard particle images on the chart (Figure 4.10, Krumbein and Sloss, 1963, p. 111; Figure 3.16, Williams and Daemen, 1987), and locate the one most like it. (For fine or very fine particles, use magnifying glass or microscope.) Record the corresponding numerical values for sphericity and roundness (angularity). Repeat for each sampled particle. Calculate and record the average (mean) sphericity and roundness and their standard deviations. Repeat for each size fraction.

II. Method B

(1) Visually examine a sampled particle. Find three perpendicular intercept axes a, b and c, i.e. the longest, the intermediate, and the shortest axis, respectively.

(2) Use caliper or micrometer to measure the lengths of a, b and c axes to 0.1 mm accuracy. Record the measurements.

(3) Compute and record the b/a and c/b ratios. Plot b/a (vertical) vs. c/b (horizontal) on an arithmetic scale.

(4) Use Zingg's classification scheme (Figure 4.8, Krumbein and Sloss, 1963, p. 107; Figure 3.19, Williams and Daemen, 1987) to classify the particle into one of the following shape classes: disk, blade, roller, or spheroid. Obtain the intercept sphericity of the particle from the plot.

(5) Repeat Steps (1) through (4) for each sampled particle.

(6) Compute the means and standard deviations for the a, b and c intercepts.

(7) Calculate the ratios of the means: $\bar{b}/\bar{a}$ and $\bar{c}/\bar{b}$.

(8) Following Step (4), obtain the average shape classification and intercept sphericity for the size fraction.

(9) Repeat Steps (1) through (8) for each size fraction.

III. Method C

This method is an integration of particle shape characterizations proposed by Heywood (1947), Herdan (1960), and Harr (1977).

(1) Follow steps (1) and (2) of Method B.

(2) Calculate:

Flakiness (f) = b/c

Elongation (e) = a/b

Projected diameter (d_p) = $(4ab/\pi)^{1/2}$

Volume of particle (v) = abc

Surface area of particle (s) = 2(ab + bc + ca)

Equivalent diameter (d_e) = $(6v/\pi)^{1/3}$

Sieve aperture (A) = $(d_p/1.38)/[ef^2/(1 + f^2)]^{1/2}$

(3) Repeat steps (1) and (2) for all sampled particles of a size fraction. Compute the means and standard deviations for a, b, c, f, e, d_p, v, s, d_e and A.

(4) Calculate the specific surface (S_{si}), angularity factor (f_{ai}, volume-shape factor (α_{vi}), and surface-shape factor (α_{si}) for the size fraction i:

$$\text{Specific surface } (S_{si}) = \sum_{j=1}^{n} S_i \Big/ \sum_{j=1}^{n} v_i \,, \qquad \text{(C.1)}$$

where n = number of particles

$$\text{Angularity factor } (f_{ai}) = S_s/(\pi \bar{A}^2) \,, \qquad \text{(C.2)}$$

where $\bar{A}$ = average sieve aperture

$$\text{Volume-shape factor } (\alpha_{vi}) = \bar{V}\, \bar{d}_p^{1/3} \,, \qquad \text{(C.3)}$$

where $\bar{V}$ = average volume of particles

$\bar{d}_p$ = mean projected diameter of particles

$$\text{Surface-shape factor } (\alpha_{si}) = \bar{s}\, \bar{d}_p^{1/2} \qquad \text{(C.4)}$$

where $\bar{s}$ = average surface of particles

(5) Repeat Steps 1 through 4 for all size fractions.

(6) Plot the calculated specific surface (S_s) against the mean particle size for each size fraction. Extrapolate the curve to obtain estimated specific surface for the finer size fractions, which are not being analyzed directly.

(7) Compute the specific surface of a graded crushed salt sample:

$$S_s = \sum_{i=1}^{N} S_{si}\, W_i \,, \qquad \text{(C.5)}$$

where N = total number of size fractions
W_i = weight percent of size fraction i

References

ASTM C702-80, "Standard Method for Reducing Field Samples of Aggregates to Testing Size," Annual Book of ASTM Standards, Section 4, Vol. 04.02, Concrete and Mineral Aggregates, American Society for Testing and Materials, Philadelphia.

Harr, M.E., 1977, Mechanics of Particulate Media, McGraw-Hill, Inc., New York.

Herdan, G., 1960, Small Particle Statistics, Butterworths Co., London.

Heywood, H., 1947, "The Scope of Particle Size Analysis and Standardization," Symposium on Particle Size Analysis, Institution of Chemical Engineers, Vol. 25, London.

Krumbein, W.C. and L.L. Sloss, 1963, Stratigraphy and Sedimentation, 2nd Edition, Freeman Co., San Francisco.

Williams, J.R. and J.J.K. Daemen, 1987, "The Sealing Performance of Bentonite/Crushed Basalt Borehole Plugs," NUREG/CR-4983, prepared for the U.S. Nuclear Regulatory Commission, Office of Nuclear Regulatory Research, Division of Engineering, by the Department of Mining and Geological Engineering, University of Arizona, Tucson.

APPENDIX D

Installation of Crushed Salt Plugs

Procedure

D.1 Objective

The purpose of this procedure is to prepare and install crushed salt plugs for radial permeameter tests, pipe flow tests, and push-out tests. The plug diameter ranges from 25 mm to 200 mm. The plug length to diameter ratio is initially selected as between 1 and 4.

D.2 Crushed Salt Characterization

1. Sample Identification

   The origin of the salt (block number) must be identified. Each sample or plug must be labeled, and the label must remain associated with the sample, i.e. included within and on logs and containers, and attached to any vessel (e.g. pipe, permeameter) in which the plugs are tested.

2. Size Analysis

   Performed in accordance with size analysis procedure (Appendix B).

3. Shape Analysis

   Shape analysis is performed only for specific purposes. It is performed in accordance with the procedure in Appendix C.

4. Moisture Content Determination

   Moisture content determination is required for all installations except for plugs immediately filled with brine. It is performed in accordance with the procedure in Appendix E.

D.3 Installation Procedure

Crushed salt plugs are installed according to one of the following methods:

D.3.1 Method A: Compressed Crushed Salt Plugs

The weight of crushed salt to be installed is calculated from the plug volume and the density of crushed salt. A tightly fitting porous

stone or steel plate is placed at the bottom of the hole or pipe. Crushed salt is poured into the hole or pipe. The salt poured in the hole is weighed, either by differential weighing of the pipe, sample or container into which it is poured, or by weighing the remainder in the container from which salt is poured into the hole, pipe, or sample. A porous stone is placed on the crushed salt. A steel platen is placed on the porous stone. A compressive load is applied to the top steel platen. The compressive stress, axial displacement, room temperature and time are recorded.

D.3.2 Method B: Compacted Crushed Salt Plugs

A crushed salt sample is split into small subsamples using a mechanical splitter (ASTM C702-80, Section 6.1). The bulk volume of crushed salt in each subsample is equivalent to the required thickness of each compaction layer in the plug. The thickness for each layer is the same, and ranges from 0.25 to 0.50 of the hole diameter. The number of layers depends upon the required plug length. To obtain uniformity along the entire plug length, each layer is subjected to the same compactive effort and energy. Compaction can be performed using a needle compactor (Daemen et al., 1986, Fig. 3.1) or another compaction device that is identified in the test report and described in a cited reference. The compactive effort, energy input, temperature, bulk density, and moisture content are recorded.

D.3.3 Method C: Crushed Salt Plugs without Compaction or Compression

Salt particles of known size distribution are poured into the borehole. The volume of salt particles is approximately equal to the required plug volume. Neither compression nor compaction is applied to the crushed salt plug. This method has been used in consolidation testing of crushed salt (Chapter 3). A porous stone is placed at each end of the plug for vented tests. A steel plate is used for the unvented tests. Temperature and moisture content are recorded.

D.4 Reference

ASTM C702-80, "Standard Method for Reducing Field Samples of Aggregate to Testing Size," Annual Book of ASTM Standards, Section 4, Vol. 04.02, Concrete and Mineral Aggregates, American Society for Testing and Materials, Philadelphia.

APPENDIX E

Determination of Moisture Content of Crushed Salt

Objective

The objective of this procedure is to determine the moisture content of crushed salt. Moisture content refers to the amount of water or moisture on the surface of the salt particles, in the form of pore water or free water (ASTM D 2216-80,3.4). No attempt is made to remove fluid inclusions (brine or water trapped inside salt crystals or along unbroken crystal boundaries).

Procedure

Determination of the moisture content of crushed salt follows an allowed alternate in ASTM D2216-80 (Note 5) with respect to temperature. The drying is done by placing the crushed salt in an oven at 60 $\pm$ 5C, or by using a vacuum desiccator at a vacuum of 133 Pa (910 mm Hg) and at a temperature between 23 and 60C. The crushed salt is distributed evenly in a flat container (e.g. pan) such that the thickness of the bed does not exceed twice the maximum grain size.

Reference

ASTM D2216-80, "Standard Method for Laboratory Determination of Water (Moisture) Content of Soil, Rock, and Soil-Aggregate Mixtures," Annual Book of ASTM Standards, Section 4, Vol. 04.08, Concrete and Mineral Aggregates, American Society for Testing and Materials, Philadelphia.

APPENDIX F

Pipe Flow Test Procedure

Apparatus:

1) Plastic mixing pan
2) Plastic shovel and rod
3) Balance (readable to 1 g)
4) Precision tape or ruler (readable to 0.254 mm (0.01 inch)
5) Pipe flow permeameter
6) Nitrogen tank (2)
7) Pressure gage (2)
8) Gas-over-brine pump
9) Dial gage
10) Neogene bottle or glass container
11) High precision pipette
12) Porous stone (2)
13) Perforated platen
14) Rubber hammer.

Sample Installation:

1) Sieve the crushed salt to the desired size range. Place the crushed salt in a plastic mixing pan. Put the crushed salt and the pan in an oven at 110°C (230°F). Weigh at regular intervals until a constant weight is obtained. Alternatively, the air-dried sample can be used without additional oven-drying if the moisture content is predetermined. (The amount of crushed salt should be more than required for the testing.)

2) Use plastic scoop to mix the crushed salt thoroughly by turning the entire sample over three times. Stir the sample with plastic rod until it appears to be homogeneous.

3) Adjust the permeameter to a level position. Place a porous stone and/or a perforated platen (depending on the desired length of the sample) at the bottom of the test chamber. Measure the distance from the top of the porous stone (or the platen) to the top of the test chamber. Three such measurements, approximately 120° apart, are necessary to get a good average value (d_1).

4) Measure the distance d_3 required from the top of the chamber such that the difference between d_1 and d_3 gives the desired sample length. Mark the inner surface of the chamber at depth d_3.

5) Use a plastic scoop to transfer the crushed salt from the mixing pan to the test chamber. Pour the crushed salt quickly by turning the shovel over. Spread the crushed salt evenly over the area of the chamber.

6) Repeat Step 5 until the top surface of the sample reaches the mark made in Step 4. A porous stone and/or a perforated platen is then placed on top of the sample. Follow the same measurement procedure as in Step 3 to obtain an average value d_2, the distance from the top of the test chamber to the upper porous stone. Subtract d_2 and the thickness of the porous stone and/or the platen from d_1. This gives the final length of the sample.

7) Weigh the plastic pan with the remaining crushed salt. The difference with the weight measurement of Step 1 gives the weight of the crushed salt installed.

8) Place a second porous stone on the sample. Place piston in the test chamber. A rubber hammer may be used to force the piston into the chamber. Bolt the top plate onto the permeameter, tightly tightening the nuts, to complete the assemblage of the permeameter. Connect the brine feed and the air feed to the permeameter.

Testing Procedure:

A schematic illustration of the pipe flow testing system is shown in Figure F.1.

1) Close bleeder valve 1. Open nitrogen tank 1. Adjust the regulating valve to apply a low pressure (e.g. 207 kPa (30 psi)) to the piston to bring the piston into contact with the top porous stone. Shut off the nitrogen tank and open the bleeder valve.

2) Introduce pre-saturated brine from the bottom of the permeameter to fill the confined test chamber until excess brine is present at bleeder 2 (bleeder valve open). Clip off the supply of brine. Allow air to escape from bleeder 2.

3) Open valve 3. Introduce a small amount of brine from the gas-over-brine pump through the brine feed to the test chamber by applying pressure (e.g. 138 kPa (20 psi)) to the piston in the pump. The air trapped in the brine feed should be forced to escape through bleeder 2. When no more air bubbles come out of bleeder 2, close the bleed valve.

4) Set up the dial gage to monitor the movement of the piston rod of the permeameter. Record the initial position of the dial gage needle.

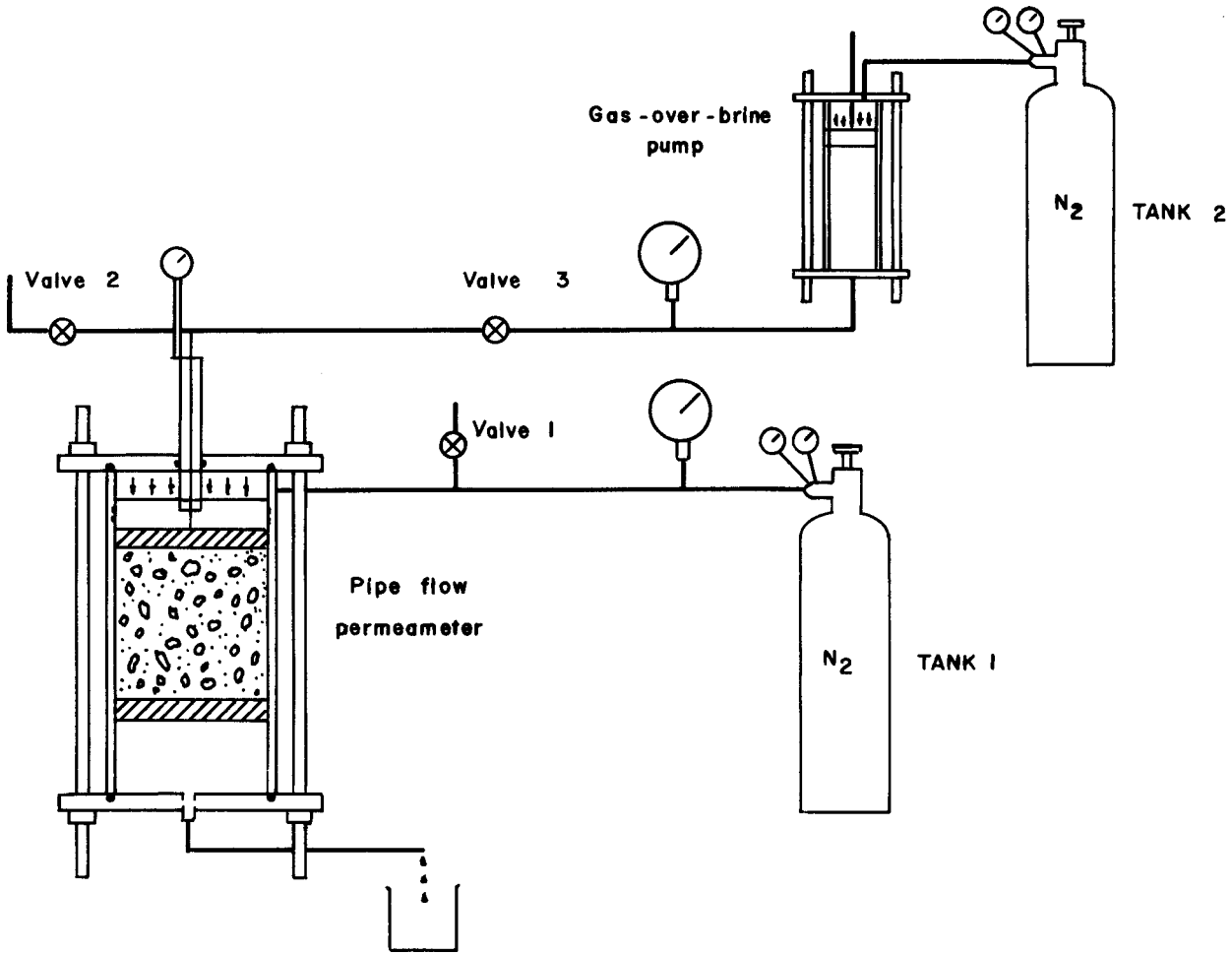

Figure F.1 Schematic illustration of the pipe flow testing system.

5) Adjust the regulating valve of nitrogen tank 1 to apply the desired pressure (pressure gage reading) to the permeameter piston. Adjust the regulating valve of nitrogen tank 2 to pressurize the gas-over-brine pump so that a desired hydraulic pressure is obtained (read from the pump pressure gage). Valves 1 and 3 must be opened, while valve 2 remains closed, before applying pressure to the system.

6) Record the displacement of the piston rods of the permeameter and of the gas-over-brine pump at regular recorded times. Calculate and record the length of the sample, the inflow and the outflow. The length of the sample is calculated from the movement of the piston rod of the flow permeameter. The inflow is calculated from the displacement of the piston rod of the gas-over-brine pump. The outflow collected in a neogene bottle or a glass container is weighed. The outflow can be measured using high precision pipettes, provided the flow rate is small.

7) The void fraction is calculated from the weight of the sample and the volume it occupies. The permeability is calculated from the hydraulic pressure drop and the flow rate using Darcy's law.

8) Follow Step 5 to change the loading stress and the hydraulic pressure. Repeat Steps 6 and 7 for measurements and calculations.

NRC FORM 335 (6 83) U.S. NUCLEAR REGULATORY COMMISSION

BIBLIOGRAPHIC DATA SHEET

1 REPORT NUMBER (Assigned by TIDC, add Vol. No., if any)
NUREG/CR- 5402

2 Leave blank

3 TITLE AND SUBTITLE
Crushed Salt Consolidation

4 RECIPIENT'S ACCESSION NUMBER

5 DATE REPORT COMPLETED
MONTH May YEAR 1989

6 AUTHOR(S)
S. Ouyang, J. J. K. Daemen

7 DATE REPORT ISSUED
MONTH July YEAR 1989

9 PROJECT/TASK/WORK UNIT NUMBER

8 PERFORMING ORGANIZATION NAME AND MAILING ADDRESS (Include Zip Code)
Department of Mining and Geological Engineering
University of Arizona
Tucson, AZ 85721

10 FIN NUMBER
NRC-04-86-113
FIN D1192

11 SPONSORING ORGANIZATION NAME AND MAILING ADDRESS (Include Zip Code)
Division of Engineering
Office of Nuclear Regulatory Research
U.S. Nuclear Regulatory Commission
Washington, DC 20555

12a TYPE OF REPORT
Technical (Formal)

12b PERIOD COVERED (Inclusive dates)
1986-1988

13 SUPPLEMENTARY NOTES

14 ABSTRACT (200 words or less)
The objective of this study is to investigate the time-dependent consolidation of confined crushed salt under axial loading. The crushed salt is geometrically characterized in terms of its grain size distribution and by means of particle shape determinations. Crushed salt of a selected grain size distribution is emplaced in a steel cylinder, and an axial load is applied to the salt. The deformation is monitored. The axial load is increased in steps. Results are presented as void ratio vs. time curves, for the various applied stresses. Air dried samples have a brine content of 0.2%; moistened samples have a brine content ranging from 1.75 to 8.8%. The general consolidation trend can be represented as a linear function of the logarithm of time, but with noticeable temporary accelerations. Consolidation time calculations, predicted from the results of fitted curve parameters, admittedly extrapolated far beyond the measurement range, indicate that reconsolidation of the materials as emplaced and tested here would require many centuries. It deserves emphasis that these experiments were initiated on an extremely loose crushed salt fill. Consolidation rate increases with brine content. The dependency upon applied stress remains ambiguous. The obtained void reduction rates are significantly lower than published results determined from isostatic consolidation. Given the small number of tests completed, all results and conclusions must be considered preliminary. Tests in configurations that may be more representative for expected in-situ consolidation conditions are recommended.

15a KEY WORDS AND DOCUMENT ANALYSIS

Creep
Void ratio
Grain size distribution
Particle shape

15b DESCRIPTORS

Permeability
Backfill
Repository
Sealing

16 AVAILABILITY STATEMENT
Unlimited

17 SECURITY CLASSIFICATION (This report) Unclassified

18 NUMBER OF PAGES

19 SECURITY CLASSIFICATION (This page) Unclassified

20 PRICE
$

*U.S. GOVERNMENT PRINTING OFFICE:1989-241-590:00145